University of Alberta

Characterisation of Asphaltene Monolayers using a Langmuir Trough and an Atomic Force Microscope at Air-Water and n-Heptane-Water Interfaces

by

Steven Andrew Lawrence

A thesis submitted to the Faculty of Graduate Studies and Research in partial fulfillment of the requirements for the degree of Master of Science

in

Chemical Engineering

Department of Chemical and Materials Engineering

Edmonton, Alberta

Spring 2003

National Library of Canada
Acquisitions and Bibliographic Services
395 Wellington Street
Ottawa ON K1A 0N4
Canada

Bibliothèque nationale du Canada
Acquisitions et services bibliographiques
395, rue Wellington
Ottawa ON K1A 0N4
Canada

Your file Votre référence

Our file Notre référence

The author has granted a non-exclusive licence allowing the National Library of Canada to reproduce, loan, distribute or sell copies of this thesis in microform, paper or electronic formats.

L'auteur a accordé une licence non exclusive permettant à la Bibliothèque nationale du Canada de reproduire, prêter, distribuer ou vendre des copies de cette thèse sous la forme de microfiche/film, de reproduction sur papier ou sur format électronique.

The author retains ownership of the copyright in this thesis. Neither the thesis nor substantial extracts from it may be printed or otherwise reproduced without the author's permission.

L'auteur conserve la propriété du droit d'auteur qui protège cette thèse. Ni la thèse ni des extraits substantiels de celle-ci ne doivent être imprimés ou autrement reproduits sans son autorisation.

0-612-82300-8

Canada

University of Alberta

Library Release From

Name of Author: Steven Andrew Lawrence

Title of Thesis: Characterisation of Asphaltene Monolayers using a Langmuir Trough and an Atomic Force Microscope at Air-Water and n-Heptane-Water Interfaces

Degree: Master of Science

Year this Degree Granted: 2003

Permission is herby granted to the University of Alberta Library to reproduce single copies of this thesis and to lend or sell such copies for private, scholarly or scientific research purposes only.

The author reserves all other publication and other rights in association with the copyright in the thesis, and except as herein before provided, neither the thesis nor any substantial portion thereof may be printed or otherwise reproduced in any material form whatever without the author's prior written permission.

Steven Lawrence

Steven Andrew Lawrence
3495 Fraser Road
Prince George, B.C.
V2N 6E6

Date: Dec 16, 2002

University of Alberta

Faculty of Graduate Studies and Research

The undersigned certify that they have read, and recommend to the Faculty of Graduate Studies and Research for acceptance, a thesis entitled *Characterisation of Asphaltene Monolayers using a Langmuir Trough and an Atomic Force Microscope at Air-Water and n-Heptane-Water Interfaces* submitted by Steven Andrew Lawrence in partial fulfillment of the requirements for the degree of Master of Science in Chemical Engineering.

Dr. Jacob Masliyah
(supervisor)

Dr. Zhenghe Xu
(supervisor)

Dr. Chongqing Ru
(committee member)

Dr. Alan Nelson
(committee chair)

Date: Dec 11, 2002

Abstract

The Langmuir trough is a useful tool for studying surfactant behaviour at interfaces and interfacial phenomena in emulsions. The behaviour of different asphaltene fractions at air-water and n-heptane-water interfaces have been characterised by pressure-area isotherms, monolayer compression-expansion hysteresis, and relaxation characteristics.

Asphaltene monolayers were transferred to silicon wafer and mica substrates using the Langmuir-Blodgett and Langmuir-Schaefer method at a number of surface pressures. The topography of the Langmuir-Blodgett films was analysed using an atomic force microscope and the contact angle of the deposited films was measured by a drop shape analyser.

When comparing Langmuir-Blodgett films at different interfaces, asphaltene molecules were found to be more closely packed at the n-heptane-water interface than at the air-water interface.

The effects of two commercial demulsifiers on asphaltene monolayers at n-heptane-water interfaces were also analysed with regard to reduction of film rigidity.

Acknowledgements

I would like to take this opportunity to thank my supervisors, Dr. Jacob Masliyah and Dr. Zhenghe Xu, for their guidance and counsel throughout this thesis. Their enthusiasm and knowledge in the area of surface chemistry has been invaluable. I would also like to thank Dr. Li Yan Zhang for his assistance on the Langmuir trough and atomic force microscope. Without his experience, this project would have taken far longer to complete. Finally, I would like to thank all my colleagues at the University of Alberta, who were often willing to lend a hand, and have also contributed in many small ways to this thesis.

Financial support for this research was provided through the NSERC Industrial Research Chair in Oil Sands Engineering, held by Dr. Jacob Masliyah.

Table of Contents

1. Introduction to Asphaltenes and their Role at Interfacial Boundaries.....1

1.1. Introduction.....1

1.2. Overview of Thesis.....2

1.3. Literature Review.....4

1.3.1. Asphaltene Structure and Classification.....4

1.3.2. Asphaltenes and Emulsion Stabilisation.....7

1.3.3. Monolayers and the Langmuir Trough.....10

1.3.3.1. History.....10

1.3.3.2. Langmuir Trough.....11

1.3.3.3. Wilhelmy Plate and Electrobalance.....12

1.3.3.4. Langmuir-Blodgett Films.....14

1.3.3.5. Air-Water Interface.....16

1.3.3.6. Asphaltene Langmuir Monolayers at Air-Water Interfaces.....18

1.3.3.7. Oil-Water Interfaces.....20

1.3.3.8. Asphaltene Langmuir Monolayers at Oil-Water Interfaces.....23

1.3.4. Atomic Force Microscope (AFM).....23

2. Experimental.....27

2.1. Materials.....27

2.2. Equipment.....27

2.2.1. Langmuir Trough.....27

2.2.1.1. Air-Water Interface Trough.....29

2.2.1.2. Oil-Water Interface Trough.....29

2.3. Procedures.....30
2.3.1. Asphaltene Extraction.....30
2.3.2. Asphaltene Fractionation.....31
2.3.3. Asphaltene Solution Preparation Procedure.....33
2.3.4. Molecular Weight Analysis by Vapour Pressure Osmometry (VPO).....34
2.3.5. Asphaltene Density Analysis (Vibrating U-Tube).....34
2.3.6. Elemental Analysis.....35
2.3.7. FTIR Spectral Analysis of Asphaltene Powders.....35
2.3.8. Langmuir Trough (Air-Water Interface).....35
2.3.8.1. Pressure Area Isotherms.....36
2.3.8.2. Compression-Expansion Experiments.....37
2.3.8.3. Relaxation.....37
2.3.8.4. Langmuir Blodgett Deposition.....38
2.3.9. Langmuir Trough (Oil-Water Interface).....39
2.3.9.1. Pressure Area Isotherms.....40
2.3.9.2. Compression Expansion Experiments.....41
2.3.9.3. Relaxation Experiments.....41
2.3.9.4. Langmuir Blodgett Deposition.....41
2.3.9.5. Demulsifier Addition.....42
2.3.10. Contact Angle Measurements.....42
2.3.11. Atomic Force Microscopy (AFM).....43
3. Asphaltene Properties.....44
3.1. General Asphaltene Appearance.....44
3.2. Asphaltene Molecular Weight Analysis.....44
3.3. Density Analysis.....45

3.4. Elemental Analysis.....46
3.5. FTIR Spectral Analysis.....46
4. Air-Water Interface.....48
4.1. Pressure Area Isotherms.....48
4.2. Hysteresis Isotherms.....57
4.3. Relaxation Isotherms.....62
4.4. Effect of pH on Π-A Isotherms.....65
4.5. Effect of Temperature on Π-A Isotherms.....66
4.6. Deposition of Langmuir-Blodgett (LB) Films.....69
4.6.1. Atomic Force Microscope (AFM) Images.....71
4.6.2. Contact Angle Measurements.....80
4.7. Summary.....82
5. n-Heptane-Water Interface.....84
5.1. Π-A Isotherms at n-Heptane-Water Interface.....84
5.2. Hysteresis Effects at n-Heptane-Water Interface.....89
5.3. Relaxation Isotherms at n-Heptane-Water Interface.....94
5.4. AFM Images of LB Films at n-Heptane-Water Interface.....99
5.5. Contact Angle Measurements.....104
5.6. Summary.....107
6. Effects of Demulsifiers at n-Heptane-Water Interface.....109
6.1. Demulsifier Chemical Properties.....109
6.2. Demulsifiers at n-Heptane-Water Interface.....109
6.3. Demulsifier Effect on Asphaltenes at n-Heptane-Water Interface.....112
6.4. Summary.....114
7. Conclusions and Recommendations for Future Work.....115

7.1. General Summary.....115

7.2. Summary of Experimental Results.....115

7.2.1. Asphaltene Properties.....115

7.2.2. Air-Water Interface.....116

7.2.3. n-Heptane-Water Interface.....117

7.3. Summary of Contributions.....117

7.4. Recommendations for Future Work.....118

Bibliography.....120

List of Tables

Table 1.1: Building Blocks in Oil Sand Asphaltene.....5

Table 3.1: Asphaltene Molecular Weights.....44

Table 3.2: Asphaltene Density.....45

Table 3.3: Elemental Analysis of Asphaltene Powders.....46

Table 3.4: Structural Features of Infrared Spectral Bands of Asphaltene Powders.....47

Table 4.1: Extrapolated Critical Area, Critical Surface Pressure and Zero Surface Pressure of Asphaltene Monolayers at Air-Water Interface at 20°C.....57

Table 4.2: Extrapolated Critical Area, Critical Surface Pressure and Zero Surface Pressure of Asphaltene Monolayers at Air-Water Interface at 49°C.....69

Table 4.3: Transfer Ratio of Various Samples of Asphaltene at Different Surface Pressures at 20°C.....70

Table 5.1: Extrapolated Critical Area, Critical Surface Pressure and Zero Surface Pressure of Asphaltene Monolayers at n-Heptane-Water Interface.....88

Table 5.2: Static Contact Angle and Error for Asphaltene Fractions at Different Surface Pressures.....107

Table 6.1: Properties of Commercial Demulsifiers from Champion Technologies Inc.....109

List of Figures

Figure 1.1: Macrostructure of asphaltics.....6

Figure 1.2: Water-in-oil emulsion stabilised by surfactants.....8

Figure 1.3: Schematic representation of a Langmuir trough.....11

Figure 1.4: Wilhelmy plate partially submerged.....12

Figure 1.5: Formation of LB films using hydrophilic and hydrophobic substrates.....15

Figure 1.6: Pressure-area isotherm of stearic acid with different phases of molecular packing.....17

Figure 1.7: KSV liquid-liquid interfacial trough.....21

Figure 1.8: Principles behind and atomic force microscope.....24

Figure 2.1: A photograph of the KSV Minitrough assembly.....28

Figure 2.2: A photograph of the air/water trough with barriers.....29

Figure 2.3: A close up photograph of the oil-water trough and barrier.....30

Figure 2.4: Asphaltene fractionation procedure.....33

Figure 3.1: FTIR spectral analysis of asphaltene powders.....47

Figure 4.1a: Pressure area isotherm of arachidic acid at air-water interface.....48

Figure 4.1b: Pressure-area isotherm for arachidic acid in the presence of 1mM of $CdCl_2$ at pH 6.0 (modified from Yazdanian et al., 1990).....49

Figure 4.1c: Pressure-area isotherms of arachidic acid at 20°C. Solid line is the isotherm on pure water, and the dotted line is on an aqueous subphase containing $3X10^{-4}M$ $CdCl_2$ and $5X10^{-5}M$ $NaHCO_3$ at pH 6.6 (Claesson and Berg, 1989).....49

Figure 4.2: Pressure-area isotherms of high molecular weight asphaltene at the air-water interface.....50

Figure 4.3: Pressure-area isotherms of three fractions of asphaltenes.....52

Figure 4.4: Pressure-area isotherm of the whole asphaltene with phases indicated.....54

Figure 4.5a: Calculation of A_c, A_0 and π_c of the whole asphaltene from the pressure-area isotherm.....55

Figure 4.5b: Calculation of A_c, A_0 and π_c of the high molecular weight asphaltene from the pressure-area isotherm.....56

Figure 4.5c: Calculation of A_c, A_0 and π_c of the low molecular weight asphaltene from the pressure-area isotherm.....56

Figure 4.6: High molecular weight hysteresis isotherm; first and third compression-expansion cycles shown.....58

Figure 4.7a: Hysteresis of the high molecular weight asphaltene, three compression-expansion cycles shown.....58

Figure 4.7b: Hysteresis of the low molecular weight asphaltene, three compression-expansion cycles shown.....59

Figure 4.7c: Hysteresis of the whole asphaltene, three compression-expansion cycles shown.....59

Figure 4.8: High molecular weight asphaltene hysteresis isotherm; comparison of compression to 20 mN/m and 60 mN/m.....61

Figure 4.8a: Normalised relaxation isotherms for low molecular weight fraction at various compression pressures.....63

Figure 4.8b: Normalised relaxation isotherms for high molecular weight fraction at various compression pressures.....63

Figure 4.8c: Normalised relaxation isotherms for the whole asphaltene at various compression pressures.....64

Figure 4.9: Normalised relaxation isotherms of high and low molecular weight fractions initially compressed to 25 mN/m.....65

Figure 4.10: High molecular weight asphaltene fraction at different pH values in the aqueous subphase.....66

Figure 4.11a: Pressure-area isotherms of high molecular weight fraction of asphaltene at 20 and 49.2°C.....67

Figure 4.11b: Pressure-area isotherms of low molecular weight fraction of asphaltene at 20 and 49.2°C.....68

Figure 4.11c: Pressure-area isotherms of the whole asphaltene at 20 and 49.6°C.....68

Figure 4.12: Freshly cleaned mica slide with no monolayer on surface.....72

Figure 4.13a: AFM image of low molecular weight fraction on mica at 30 mN/m, TR=1.018.....73

Figure 4.13b: AFM image of high molecular weight fraction on mica at 30 mN/m, TR=0.814.....73

Figure 4.13c: AFM image of whole asphaltene on mica at 30 mN/m, TR=0.487.....74

Figure 4.14a: AFM image of low molecular weight fraction on mica at 0 mN/m, TR=0.493.....75

Figure 4.14b: AFM image of low molecular weight fraction on mica at 5 mN/m, TR=0.934.....75

Figure 4.14c: AFM image of low molecular weight fraction on mica at 30 mN/m, TR=1.018.....76

Figure 4.14d: AFM image of low molecular weight asphaltene fraction on glass (LS deposition) at 65 mN/m.....76

Figure 4.15a: AFM image of high molecular weight fraction on mica at 0 mN/m TR=1.056.....77

Figure 4.15b: AFM image of high molecular weight fraction on mica at 5 mN/m TR=1.066.....77

Figure 4.15c: AFM image of high molecular weight fraction on mica at 30 mN/m TR=0.814.....78

Figure 4.15d: AFM image of high molecular weight asphaltene fraction on mica (LS deposition) at 70 mN/m.....78

Figure 4.16: Water droplet on silicon wafer coated with whole asphaltene at 30 mN/m, TR=0.478.....80

Figure 4.17a: Static contact angle of a water droplet on high and low molecular weight fraction LB films at different surface pressures.....81

Figure 4.17b: Static contact angle of a water droplet on whole asphaltene LB films at different surface pressures.....81

Figure 5.1a: Pressure-area isotherm of DPPC at water-hexadecane interface (20°C).....85

Figure 5.1b: Pressure-area isotherm of DPPC at water-hexadecane interface (20°C) (modified from Thoma and Möhwald, 1995).....85

Figure 5.2a: Pressure-area isotherm of DSPC at water-heptane interface with 0.01 M NaCl in aqueous phase (20°C).....86

Figure 5.2b: Pressure-area isotherm of DSPC at water-heptane interface with 0.01 M NaCl in aqueous phase (20°C) (modified from Yue et al., 1976)...86

Figure 5.3: Pressure-area isotherms of three asphaltene samples at an n-heptane-water interface at 20°C.....87

Figure 5.4a: High molecular weight fraction asphaltene, hysteresis isotherm at n-heptane-water interface (20°C). First and second compression-expansion cycles are shown.....89

Figure 5.4b: Low molecular weight fraction asphaltene, hysteresis isotherm at n-heptane-water interface. First and second compression-expansion cycles are shown.....90

Figure 5.4c: Whole asphaltene, hysteresis isotherm at n-heptane-water interface (20°C). First and second compression-expansion cycles are shown.....90

Figure 5.5a: High molecular weight asphaltene, hysteresis isotherm at n-heptane-water Interface (20°C). First and second cycles are shown.....92

Figure 5.5b: Low molecular weight fraction asphaltene, hysteresis isotherm at n-heptane-water interface. First and second compression-expansion cycles are shown.....93

Figure 5.5c: Whole asphaltene, hysteresis isotherm at n-heptane-water interface (20°C). First and second compression-expansion cycles are shown.....93

Figure 5.6a: Normalised whole asphaltene relaxation curves at n-heptane-water water interface, compressed to various surface pressures (20°C).....94

Figure 5.6b: Normalised high molecular weight asphaltene relaxation curves at n-heptane-water interface, compressed to various surface pressures (20°C).....95

Figure 5.6c: Normalised low molecular weight asphaltene relaxation curves at n-heptane-water interface, compressed to various surface pressures (20°C).....95

Figure 5.7: Normalised relaxation curves of three fractions of asphaltenes compressed to similar surface pressures at n-heptane-water interface (20°C).....97

Figure 5.8a: Relaxation of high molecular weight asphaltene at air-water and n-heptane-water interfaces (20°C).....98

Figure 5.8b: Relaxation of low molecular weight asphaltene at air-water and n-heptane-water interfaces (20°C).....98

Figure 5.9: AFM image of bare silicon wafer with no monolayer on the surface.....100

Figure 5.10a: AFM image of low molecular weight asphaltene LB film on silicon wafer compressed to 5 mN/m, transfer ratio 1.404, at an n-heptane-water interface (20°C).....101

Figure 5.10b: AFM image of high molecular weight asphaltene LB film on silicon wafer compressed to 5 mN/m, transfer ratio 1.331, at an n-heptane-water interface (20°C).....101

Figure 5.10c: AFM image of whole asphaltene LB film on silicon wafer compressed to 5 mN/m, transfer ratio 1.259, at an n-heptane-water interface (20°C).....102

Figure 5.11a: AFM image of high molecular weight asphaltene LB film on silicon wafer compressed to 5 mN/m, transfer ratio 1.331 at n-heptane-water interface (20°C).....102

Figure 5.11b: AFM image of high molecular weight asphaltene LB film on silicon wafer compressed to 20 mN/m, transfer ratio 1.176 at n-heptane-water interface (20°C).....103

Figure 5.11c: AFM image of high molecular weight asphaltene compressed to 40 mN/m, transferred by LS deposition onto hydrophobic glass slide at n-heptane-water interface.....103

Figure 5.12: Contact angles of high molecular weight asphaltene deposited at various surface pressures from an n-heptane-water interface at 20°C.....105

Figure 5.13: Contact angles of high and low molecular weight asphaltenes deposited at various surface pressures from an n-heptane-water interface at 20°C.....106

Figure 6.1: Effect of demulsifier A on n-heptane-water interface at 20°C.....110

Figure 6.2: Effect of demulsifier B on n-heptane-water interface at 20°C.....111

Figure 6.3: Isotherms of high molecular weight asphaltene at n-heptane-water interface with varying concentrations of demulsifier A.....113

Figure 6.4: Isotherms of high molecular weight asphaltene at n-heptane-water interface with varying concentrations of demulsifier B.....113

Nomenclature

Abbreviations

AFM	Atomic Force Microscope
FTIR	Fourier Transform Infrared
LB	Langmuir-Blodgett
LS	Langmuir-Schaefer
DC	Direct Current
Π-A	Pressure-Area
G	Gaseous (Phase)
LE	Liquid Expanded (Phase)
LC	Liquid Condensed (Phase)
S	Solid (Phase)
DPPC	Dipalmitoylphosphatidycholine
PC	Phosphatidylcholine
VPO	Vapour Pressure Osmometry
DPPE	Dipalmitoylphosphatidylethanoamine
DSPC	Distearoylphosphatidylcholine
NPOE	Nitrophenyl octyl ether
NaCl	Sodium Chloride
PA	Palmitic Acid
H:T:B	Ratios of Heptane, Toluene, Bitumen
KBr	Potassium Bromide
GPC	Gel Permeation Chromatography

$CdCl_2$	Cadmium Chloride
PPM	Parts per Million

Symbols

L_p	Length (m)
W_p	Width (m)
T_p	Thickness (m)
$\rho_p, \rho_l, \rho_a, \rho_m, \rho_t$	Density (kg/m^3)
H_p	Depth (m)
g	Gravitational Acceleration Constant (9.81 m/s^2)
Π, π	Surface Pressure (mN/m)
γ, γ_0	Interfacial (Surface) Tension (mN/m)
F	Force (N)
X_a	Mass Fraction (of Asphaltene)
A_c	Critical Area (nm^2)
π_C	Critical Pressue (mN/m)
A_0	Zero Surface Area (nm^2)
TR	Transfer Ratio
θ_0	Static Contact Angle (degrees)

1 Introduction to Asphaltenes and their Role at Interfacial Boundaries

1.1 Introduction

An emulsion is a dispersion of one immiscible liquid into another. The dispersed phase exists in the continuous phase in the form of small droplets or globules. Emulsions are thermodynamically unstable due to their large interfacial surface area. As a result, under normal conditions, the dispersed phase droplets will attempt to coalesce, eventually leading to phase separation of the two liquids. However, emulsions can be stabilised by the presence of amphiphilic molecules in the system. Amphiphilic molecules have both a polar functional group attached to a non-polar hydrocarbon chain. As a result, these types of surface active molecules tend to migrate to interfaces and can significantly alter the properties of an interface. Often surfactants can prevent coalescence by acting as a steric boundary or by resisting drainage of the continuous film between two droplets of the same phase.

Emulsions are present in a number of industrial processes and can be found in fields ranging from the petrochemical to pharmaceutical industry. Emulsions can be desirable or undesirable in a particular field, depending on the application. In the petrochemical industry, undesirable water-in-oil emulsions often form during the production of crude oil. The stability of the emulsions is mainly due to the presence of natural surface active components found in crude oil and bitumen. These surfactants accumulate at the oil-water interfaces and give rise to a mechanically stable layer that enables the water to remain dispersed in the continuous oil phase (Puskás et al, 1996).

Asphaltenes represent the heaviest and most polar components in crude oil and bitumen (Andersen and Speight, 2001). As a result, the presence of asphaltenes is known to be a factor responsible for the stabilisation of water-in-oil emulsions (Mullins and Sheu, 1998). Most asphaltene research has focused on studying the role that asphaltenes have in stabilising emulsions or attempting to identify the surface active molecules that stabilise emulsions. A need to study the behaviour of asphaltenes at interfaces has motivated this study.

1.2 Overview of Thesis

The purpose of this research is to study the behaviour of asphaltenes at various interfaces. The Langmuir trough is an apparatus that can allow the study of films at air-liquid and liquid-liquid interfaces. The trough is also capable of transferring interfacial material onto a solid substrate, enabling one to study the film in a variety of other analytical methods such as, atomic force microscopy and contact angle measurements.

Chapter one of this thesis details the definition of asphaltenes and their role as surfactants. An understanding of the role asphaltenes play as amphiphilic molecules is necessary in understanding how a Langmuir trough operates. Chapter one also briefly reviews the historical study of interfacial films, and then reviews the design and operation of a Langmuir trough. Another apparatus used in the study of asphaltenes was the atomic force microscope (AFM). An AFM is capable of studying the topography of a surface at sub-nanometre scales. The theory and operation of an AFM are also reviewed in Chapter one.

Chapter two details the materials and equipment used to conduct experiments. Most experiments were conducted on asphaltenes precipitated from bitumen. This

chapter also provides detailed procedures of all the experiments performed. A variety of tests were performed to characterise the asphaltene samples, such as; molecular weight, density, elemental analysis and FTIR. Other tests using the Langmuir trough, AFM and contact angle measurements were performed to study asphaltene films.

Chapter three provides an analysis of a number of chemical and physical properties of asphaltenes such as: molecular weight, density, FTIR spectral analysis and elemental analysis.

Chapter four focuses on asphaltene monolayers at air-water interfaces. Some tests were compared with previously published literature to ensure that the Langmuir trough was operating correctly. The behaviour of the asphaltene films at air-water interfaces was analysed with respect to the mechanical properties of the films. The effects of temperature, pH and compression speed and a number of other factors on the asphaltene monolayers were also analysed. AFM images indicating the film topography are also analysed with regard to monolayer compressibility. Static contact angle measurements are correlated to compression of the asphaltene film and the effect of molecular weight of the asphaltene.

Chapter five focuses on asphaltene monolayers at n-heptane-water interfaces. The mechanical properties of the films were studied with regards to compression-expansion behaviours and relaxation mechanisms. A comparison between the differences in properties at the air-water and n-heptane-water interfaces was also detailed. AFM images indicating film topography were also analysed at a variety of surface pressures. Static contact angle measurements of asphaltene films deposited onto solid substrates were also studied.

The effects of two commercial demulsifiers from Champion Technologies Inc. on asphaltene monolayers at n-heptane-water interfaces were reported in Chapter six. The demulsifiers were heptane soluble and were introduced to the system in the organic phase.

Finally, the experimental conclusions and suggestions for future work are detailed in Chapter seven.

1.3 Literature Review

1.3.1 Asphaltene Structure and Classification

Asphaltenes are a solubility class that is precipitated from crude oil or bitumen by the addition of an alkane such as n-heptane. In general, asphaltenes are classified as large polar compounds of polyaromatic hydrocarbons consisting of mainly aliphatic and aromatic groups (Yarranton and Masliyah, 1996). Asphaltenes are particularly abundant in bitumen and comprise the highest molecular weight fraction with an average molecular weight ranging from the low hundreds to tens of thousands (Cyr et al., 1987). Through extensive studies, a number of major structural elements of asphaltenes have recently been identified. Asphaltenes are now thought of as assemblies of small and medium sized alkyl and napthenoaromatic hydrocarbons combined with sulphur and nitrogen derivatives (Strausz, 1999). Building blocks that form over 50% of the asphaltene are identified in Table 1.1, in which alkyl compounds are thought to comprise approximately 27% of the total carbon and form bridges, side chains, and ester-bound fatty acids that connect to ring structures (Peng et al., 1997).

Table 1.1: Building Blocks in Oil Sand Asphaltene (modified from Peng et al., 1997)

Thiophenes:

C_{12} to C_{25} Max. C_{14} | C_{10} to C_{28} Max. C_{13} | C_{12} to C_{26} Max. C_{15}

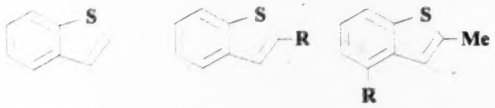

C_9 to C_{24} Max. C_{10} | C_9 to C_{24} Max. C_{10} | C_{11} to C_{25} Max. C_{11}

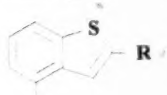

C_{11} to C_{24} Max. C_{11}

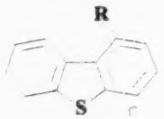

C_{13} to C_{25} Max. C_{13}

Fluorenes:

C_{14} to C_{25+} Max. C_{14} | C_{14} to C_{23}

n-Alkyl chains and bridges:

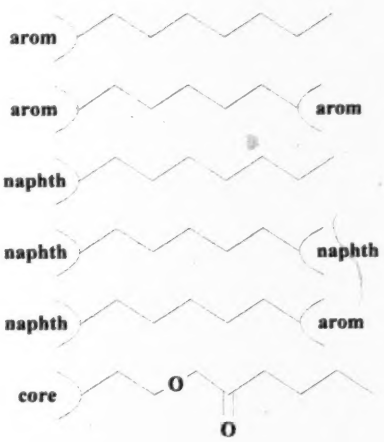

*R = n-alkyl

Cyclic sulfides:

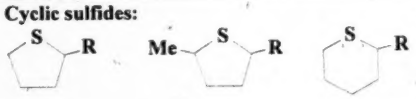

C_9 to C_{28} Max. C_{13} | C_{10} to C_{29} Max. C_{15} | C_{10} to C_{29} Max. C_{15}

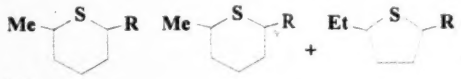

C_{10} to C_{29} Max. C_{13-14} | C_{10} to C_{29} Max. C_{17}

Alkanes:

C_{12} to C_{26}; Max. $C_{15,16}$

Alkylbenzenes:

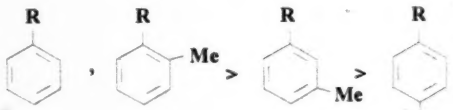

C_{12} to C_{28}

Alkylnaphthalenes and biphenyls:

Alkylanthracenes and phenanthrenes:

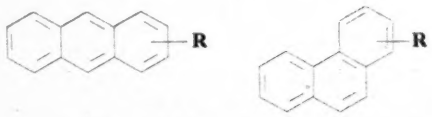

Naphthenocondensed benzo- and dibenzo-thiophenes, polybenzothiophenes, n-alcohols, carboxylic acids, etc.

A number of molecular models have been proposed to describe the physical and chemical properties of asphaltenes. A generally accepted model is identified in Figure 1.1, where an asphaltene particle is composed of individual sheets. These sheets are believed to form unit cells and larger associated micelles. The asphaltene structure is pictured as repeating units consisting of condensed aromatic rings, short aliphatic chains, and napthenic ring structures combined to form a complicated network (Dickie and Yen, 1967). Iron, vanadium, nickel and other metals are often present as heteroatoms attached to the network by aliphatic chains (Bouhadda et al., 2000).

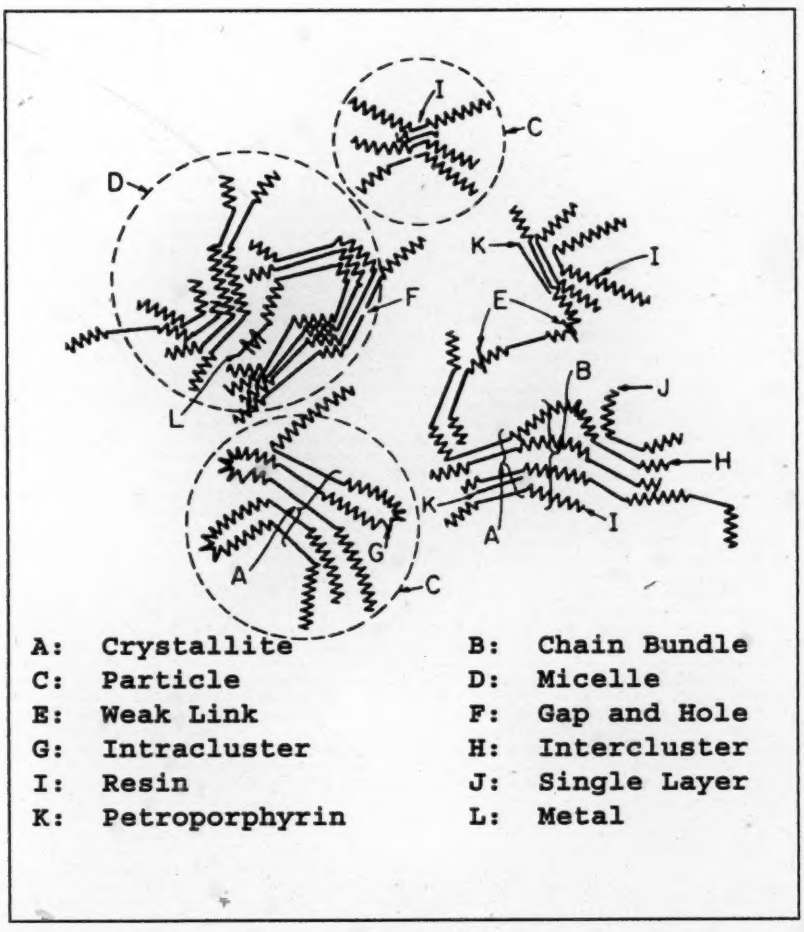

Figure 1.1 Macrostructure of asphaltics (modified from Dickie and Yen, 1967).

Asphaltenes can cause several difficulties during the production and processing of crude oil and bitumen. Asphaltenes are responsible for increasing the viscosity of crude oil, have a high tendency to form coke, and often precipitate in undesirable locations such as pipelines, wells and reaction vessels, causing declines in oil flow or even well blockages (Calemma, et al. 1998). Due to the difficulty that asphaltenes can cause during processing and the increased production of heavier crude oils, elucidation of the molecular structure of asphaltenes is of increased importance (Su, et al. 1998).

1.3.2 Asphaltenes and Emulsion Stabilisation

Stable emulsions are formed by the adsorption of surfactants to the oil-water interface. Asphaltenes found in crude oils or bitumen contain a sufficient number of polar functional groups. These polar ends accumulate at the interface with their hydrophobic ends remaining in the oil phase. Figure 1.2 shows a water droplet in oil stabilised by the presence of surfactants. In a stable emulsion, individual water droplets become encapsulated by a surfactant layer which prevents droplet coalescence. Studies by Lee (1999) indicated that strong emulsifying surfactants should have a large hydrophobic region to form a stable barrier around the water droplet, accompanied by a sufficient number of smaller hydrophilic sites necessary for adsorption at the oil-water interface. Lee also concluded that compounds with a higher solubility in the oil phase over the aqueous phase produce more stable water-in-oil emulsions.

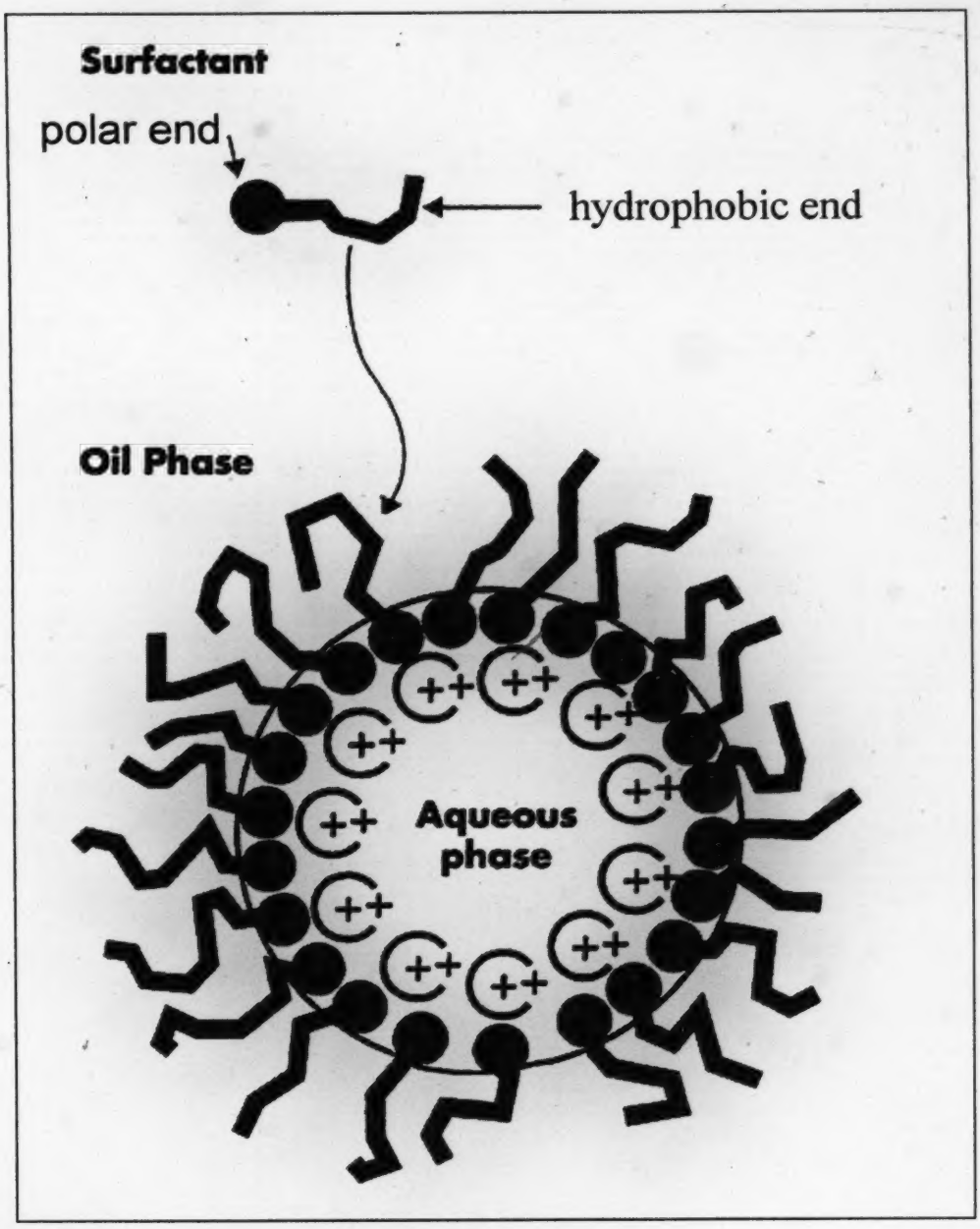

Figure 1.2 Water-in-oil emulsion stabilised by surfactants (Modified from Lee 1999).

Due to their polar nature, asphaltenes in crude oil and bitumen contribute to the stabilization of water-in-oil emulsions. Asphaltenes have been observed to gather at an

oil-water interface and form a stable skin which prevents the coalescence of water droplets (MacKay, 1987). McLean and Kilpatrick (1997) precipitated asphaltenes from a variety of crude oils using n-heptane and produced a number of stable water-in-oil emulsions. In some cases, the water-in-oil emulsions stabilised with asphaltenes were more stable than those generated by the crude oil itself. They concluded that asphaltenes have a key role in stabilizing emulsions and are most effective when they are near the point of incipient precipitation. Asphaltenes are an effective stabiliser of emulsions due to their solubility in crude oil, their high molecular weight, and by having sufficient numbers of polar compounds. McLean and Kilpatrick (1997) also analysed the synergistic effects of asphaltenes and resins on emulsion stability. They concluded that while resins may contribute to emulsion stability when combined with asphaltenes, resins are not essential in forming stable emulsions. Menon et al. (1988) conducted a number of studies on emulsions stabilised by mineral solids. They found that while emulsion formation was possible with solids alone, emulsions formed with asphaltenes were much more stable.

Water-in-oil emulsions contribute to several technical difficulties in the oil processing industry for a number of reasons. Stable emulsions increase both the volume and viscosity of the material to be transported and in the case of oil spills, can convert oil into a heavy, semi-solid material that is extremely difficult to clean up (Fingas, 1995). The emulsified water often contains high levels of salts. The high chloride presence from water soluble salts causes corrosion in many of the downstream reaction vessels and leads to increased maintenance costs (Kotlyar et al. 1998).

1.3.3 Monolayers and the Langmuir Trough

Amphiphilic molecules are molecules containing both a polar functional group and a non-polar tail. Asphaltenes are amphiphilic, and form monomolecular interfacial layers that straddle the polar (water) phase from the non-polar (oil or gas) phase. Through the use of a Langmuir trough, such monolayers have been extensively studied (Stokes and Evans, 1996).

1.3.3.1 History

In the late 1800's, Agnes Pockels systematically studied soap layers on water surfaces and discovered that the surface pressure would rapidly increase when the layers were compressed below a certain surface area (Kuhn, 1989). In 1917, Irving Langmuir pioneered methods for studying floating monolayers through the use of a film balance. The study of floating monolayers has greatly expanded our knowledge of the amphiphilic molecule behaviour at interfaces. In 1934, Katherine Blodgett successfully demonstrated that monolayers can be transferred onto solid substrates and can build up sequentially to produce multi-layer films (Gaines, 1983). Langmuir and Blodgett studied the structure of fatty acid multi-layer films by transferring monolayers into glass slides (Kuhn, 1989). Floating monolayers are generally referred to as Langmuir films, while mono or multilayers deposited on solid substrates are referred to as Langmuir-Blodgett (LB) films (KSV Instruments Ltd.).

The study of amphiphilic molecules, both as a Langmuir monolayer and LB films, has been very extensive in the past 70 years. Langmuir monolayer and LB film research are currently used in a variety of applications ranging from modelling systems in physics, biology and chemistry to investigating phenomena such as emulsions and bio-processes

to creating planned molecular assemblies organised with specific surface properties in mind (Kuhn, 1989).

1.3.3.2 Langmuir Trough

Langmuir monolayers and LB films are produced in a Langmuir trough. The trough is generally composed of Derlin or Teflon, with movable barriers that can compress an air/liquid or liquid/liquid interface. A sensitive electro-balance with a Wilhelmy plate is used to measure changes in surface pressure and a dipping mechanism is necessary to produce LB films on solid substrates (Constantino, 1999). A typical air-water interface Langmuir trough with a dipping well and substrate is shown in Figure 1.3.

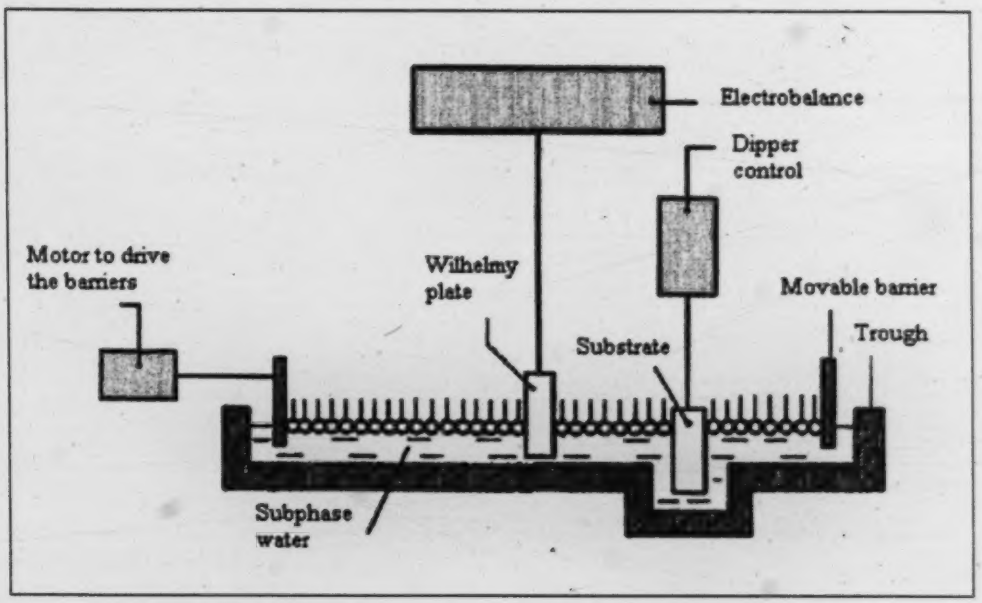

Figure 1.3 Schematic representation of a Langmuir trough (modified from Dynarowicz et al., 2001).

1.3.3.3 Wilhelmy Plate and Electrobalance

The surface pressure of the monolayer is measured by the Wilhelmy plate and the electrobalance. Surface pressure is the difference between the surface (or interfacial) tension of an interface without and with amphiphilic material present.

The following principles for the Wilhelmy plate and electrobalance are based on the description in, "KSV Minitrough: Instruction Manual for Windows 95/98/NT/2000." In this method, a thin non-reactive, hydrophilic plate (generally made of platinum, although other material such as glass or filter paper can be used) is partially immersed in the subphase. Figure 1.4 details a Wilhelmy plate partially submerged in a liquid.

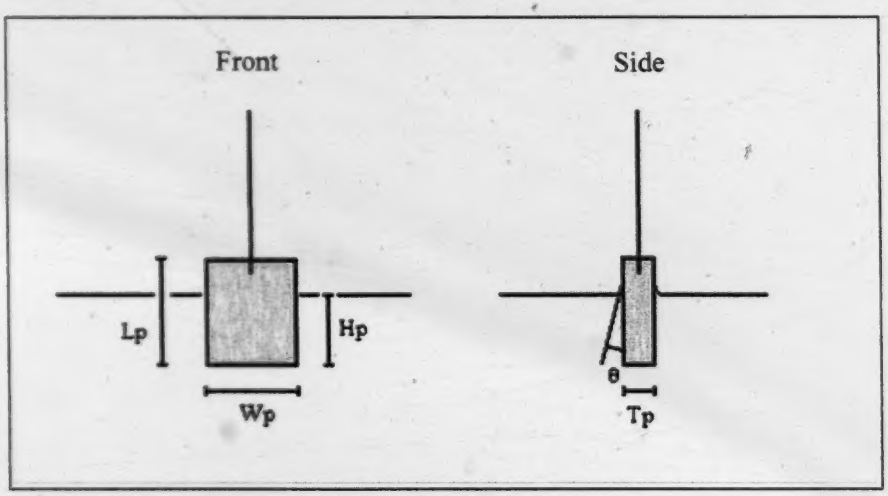

Figure 1.4 Wilhelmy plate partially submerged.

The following calculations use a rectangular plate of length (L_p), width (W_p), and thickness (T_p) with a density (ρ_p). The plate is submerged to a depth (H_p) in a liquid with a density (ρ_l). The net force on the plate is given by:

F = Gravity (down) + Surface Tension (down) + Buoyancy (up) [1.1]

Using γ as the interfacial tension (or surface tension in the case of a liquid/air interface), θ as the contact angle of the liquid on the plate, and g as the gravitational constant, this equation can be written as:

$$F = (\rho_p g L_p W_p T_p) + 2\gamma (T_p + W_p)(\cos\theta) - (\rho_l g W_p T_p H_p) \qquad [1.2]$$

Surface pressure (Π) is defined as the difference between the surface tension of a clean surface without a monolayer present (γ_0) and the surface tension with a monolayer present (γ):

$$\Pi = \gamma_0 - \gamma = -\Delta\gamma \qquad [1.3]$$

Surface pressure can be measured using the Wilhelmy plate to measure the change in the net force (ΔF) on the plate. Assuming that the plate is completely wetted by the liquid $\theta = 0$ (there is no deflection of the plate), along with a reference point of $\gamma_0 = 0$, then:

$$\Pi = -\Delta\gamma = -\left[\frac{\Delta F}{2(T_p + W_p)}\right] \qquad [1.4]$$

For a very thin plate, the width is far greater than the thickness ($W_p >> T_p$). Thus, for a thin, completely wetted plate, the surface pressure can be calculated as:

$$\Pi = -\frac{\Delta F}{2W_p} \qquad [1.5]$$

The change in force (ΔF) on the Wilhelmy plate is detected by coupling the plate to a sensitive electrobalance. In this way, the surface pressure for a known surface area can be readily calculated. By combining the surface pressure per unit area and the quantity of amphiphilic material present at the surface, a number of important monolayer properties can be analysed.

1.3.3.4 Langmuir-Blodgett Films

Langmuir-Blodgett films are produced by passing a substrate though an amphiphilic film at a desired surface pressure (Izumi et al. 1998). A variety of substrates can be used for deposition; glass and mica are among the most commonly used (Müller, et. al 1997). Repeated deposition of monolayers onto a solid substrate results in multilayered LB films (Tsukruk, 1997). Rigid monolayers can be transferred horizontally to solid substrates by bringing a substrate in contact with the Langmuir monolayer. Deposition in this manner is called the Schaefer method (Arslanov, 1992). This horizontal lifting method is very useful for rigid films in the solid region of the pressure-area isotherm and is called a Langmuir-Schaefer (LS) deposition (Ulman, 1991). With the transfer of monolayers onto solid substrates, more detailed analyses of amphiphilic molecules and their interfacial behaviour can be performed (Dynarowicz et al., 2001). LB films are routinely characterised by a variety of analytical methods such as: Fourier Transform Infrared Spectroscopy (FTIR), Atomic Force Microscopy (AFM) (Kurihara 1997), DC Conductivity, and infrared absorption (Izumi et al. 1998). Tsukruk (1997) conducted an extensive review of characterisation techniques and apparatuses used to evaluate LB films including contact angle, optical and electron microscopes, ellipsometry, and scanning probe microscope. Figure 1.5 shows several different

methods of producing LB mono and multilayer films on both hydrophobic and hydrophilic substrates.

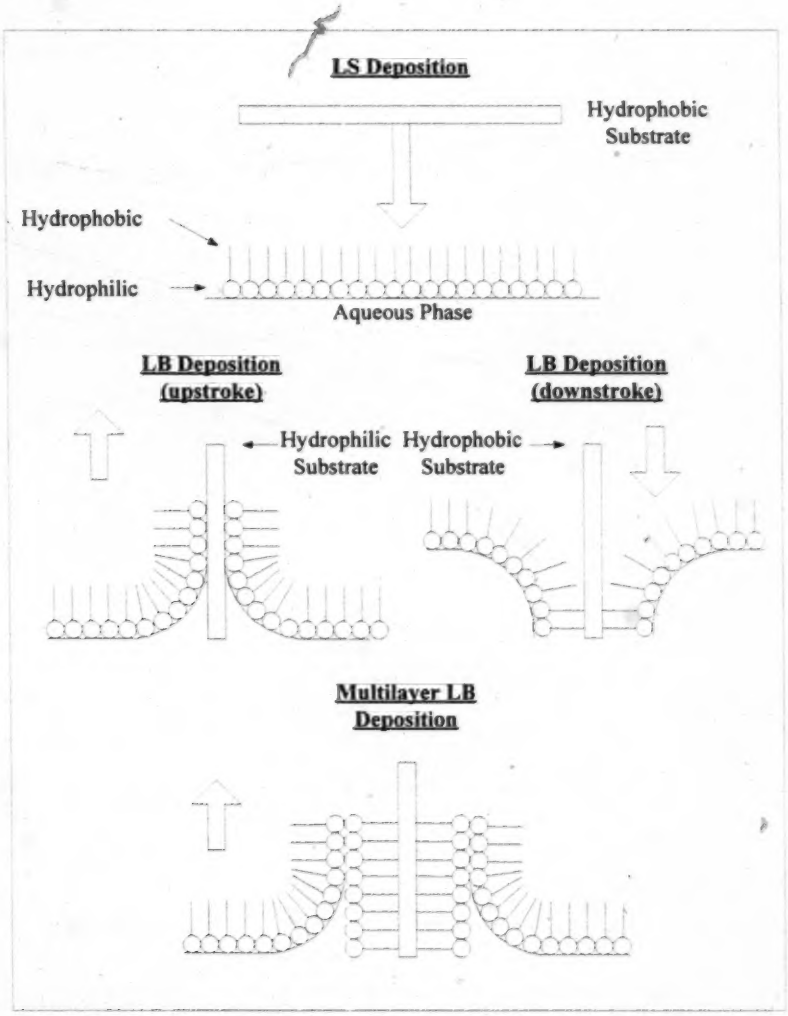

Figure 1.5 Formation of LB films using hydrophilic and hydrophobic substrates.

1.3.3.5 Air-Water Interface

The most common Langmuir monolayers are studied at air-water interfaces by floating the surfactant on the water surface and monitoring their surface pressure as a function of mean molecular area. When these studies are conducted at a constant temperature, they are referred to as Π-A isotherms. A Π-A isotherm of stearic acid is shown in Figure 1.6 along with the different phases of molecular packing (Tsukruk, 1997). Typically, a Π-A isotherm can be divided into four distinct regions: the gaseous phase (G), the liquid expanded phase (LE), the liquid condensed phase (LC), and the solid phase (S). However, with long-chained and more complex compounds, the assignment of only four regions is often an oversimplification of the real system, which can have complex transitions between phases (Peng et al., 2001). The gaseous phase refers to the state in which the surfactants are uniformly dispersed over the interface and are not directly interacting with each other. In the liquid expanded phase, the surface is compressed and the hydrophobic chains of the amphiphilic molecules begin to interact with each other. In the liquid condensed phase the surface is compressed to the point where the hydrophobic groups are forced to align on the surface. In the solid phase, the molecules are closely packed and further compression causes the monolayer to collapse.

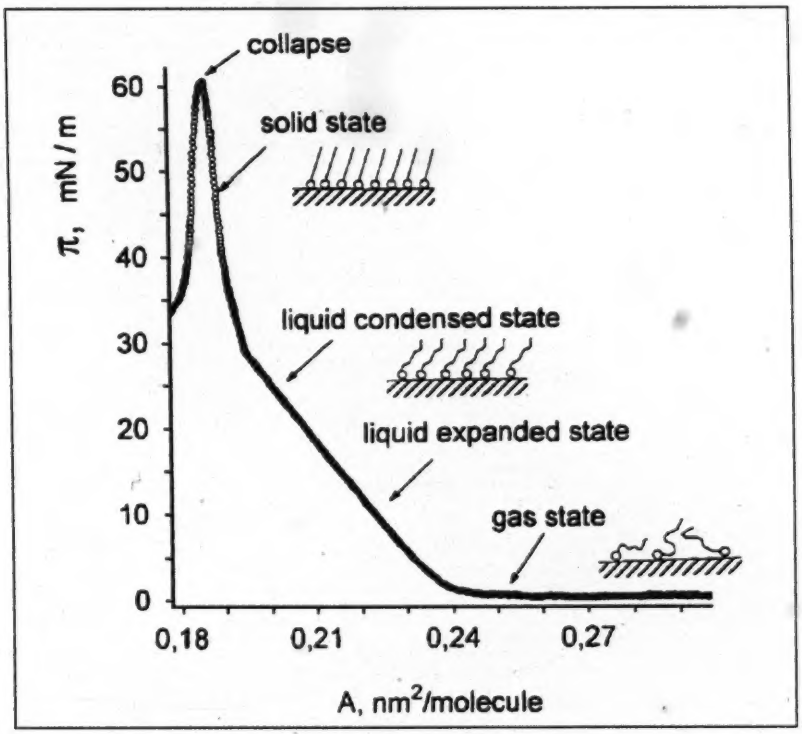

Figure 1.6 Pressure-area isotherm of stearic acid with different phases of molecular packing (modified from Tsukruk, 1997).

By measuring the surface pressure and trough area, it is also possible to gain a number of different perspectives into monolayer stability. The shape of the pressure-area isotherm can indicate a number of monolayer properties such as the mean molecular size of the individual surfactant molecules, the film rigidity and the critical pressure at which the monolayer collapses. The monolayer can also be compressed to a particular surface pressure and the relaxation in pressure can be measured as a function of time (Yang, 2001). While the barriers remain stationary, the individual molecules forming the monolayer reorganise to lower energy states through a number of mechanisms such as dissolution into the subphase and a variety of molecular reorganisations possibly due to adjustments in the distribution of charges and chain tilting (Viseu et al., 2001). A

Langmuir trough is also capable of obtaining information regarding the re-spreading capability or hysteresis of a monolayer by monitoring the surface pressure during successive compression/expansion cycles. Banerjee and Bellare (2001) studied the re-spreading capabilities of commercial surfactant mixtures used in treating respiratory distress syndrome combined with eucalyptus oil, by monitoring surface pressure when repeatedly compressing and expanding the monolayer. Possmayer et al. (2001) studied the "squeeze out" process of a number of commercial pulmonary surfactants mixed with phospholipids, such as dipalmitoylphosphatidycholine (DPPC) and unsaturated phosphatidylcholine (PC), by monitoring the monolayer through sequential compression/expansion cycles and measuring the reversibility of the pressure-area isotherms. Baker (1983) compressed solutions of phathalocyanine multiple times to observe the "locking together" of molecules over several compressions. Constantino et al. (1999) studied the hysteresis of the surface pressure-area isotherm of sugar cane baggase lignin monolayers on water, in order to characterise the stability of the monolayer with regard to dissolution of material into the bulk phase and molecular repacking during expansion.

1.3.3.6 Asphaltene Langmuir Monolayers at Air-Water Interfaces

Some groups have investigated Langmuir monolayers of bitumen and crude oil surface active components. Leblanc and Thyrion (1989) studied asphaltene monolayers from Venezuelan crude oil precipitated by pentane or heptane, and monolayers of deasphalted oil. Their studies attempted to determine the molecular weight of asphaltenes by extrapolating the Π-A vs. Π curves, as Π approaches zero and comparing the results to the molecular weights obtained using vapour pressure osmometry (VPO).

Nordli et al. (1991) studied Langmuir monolayers at air-water interfaces of the surface active fractions of some North Sea crude oils. In their studies, the surface active material was separated from the crude oil using functionalised silica as an absorbent. Their work analysed the effects of electrolytes, pH, temperature, and chemical additives in the aqueous subphase on the pressure-area isotherms and relaxation curves of the surfactants. Yang et al. (2001) studied the film properties of asphaltenes and resins. In their work, they investigated the effects of asphaltene and resin concentration on observed pressure-area isotherms, Π-A isotherms of asphaltene and resin mixtures, and Π-time (relaxation) curves of asphaltenes and resins. They also detailed the influence of asphaltene aggregation on monolayers, and on oil emulsion stabilisation. Ese et al. (1998) conducted a comparative study of several asphaltenes and resins from North Sea, European continent, and Venezuela crude oils by using a Langmuir trough at an air-water interface. The asphaltene fractions were precipitated from the crude oils using n-pentane. Their work studied the pressure-area isotherms of asphaltene and resin mixtures ranging from pure asphaltenes to pure resins. They concluded that asphaltenes appear to pack closer to the water surface and form a more rigid film than resins. Several studies of asphaltenes at air-water interfaces have been conducted by Marit-Helen Ese in papers such as, "Langmuir-Film Properties of Indigenous Crude Oil Components. Influence of Demulsifiers" (1999a) and "Compressibilities and excess surface area of mixed asphaltene/resin monolayers. Influence of demulsifiers." (1999b).

Ese (1999a) examined Π-A isotherms of asphaltene and resin mixtures and measured the effects of demulsifiers on monolayer stability. Ese found that an increased resin concentration in the asphaltene monolayer had a tendency to reduce film rigidity.

However, with the addition of demulsifiers to asphaltenes, Ese found that their tendency to reduce film rigidity was more pronounced and occurred at a much lower concentration than that of resins.

Ese, (1999b) compared the compressibility of monolayer films of asphaltenes and resins mixed with various demulsifiers. Ese, (1999b) concluded that compressibility calculations showed that addition of demulsifiers to high molecular weight asphaltene films yields an increased film compressibility and increased attraction between film components.

1.3.3.7 Oil-Water Interfaces

Modification of the traditional air-water Langmuir trough has led to the development of an interfacial Langmuir trough, enabling the study of amphiphilic molecules at the interface of two immiscible liquids such as oil and water. As surfactants in water and oil emulsions adsorb at oil-water interfaces in the interfacial Langmuir trough, amphiphilic molecules can be studied more effectively than in the traditional air-water trough. Most interfacial troughs are custom made or prototypes of various designs. Figure 1.7 shows a prototype interfacial trough developed by KSV Chemicals. The trough is made of Derlin and contains a small inside compartment for the denser aqueous phase and an outer compartment to contain the lighter oil phase. The barriers contain holes to allow the lighter phase to flow through while compression is occurring (Galet et al., 1999).

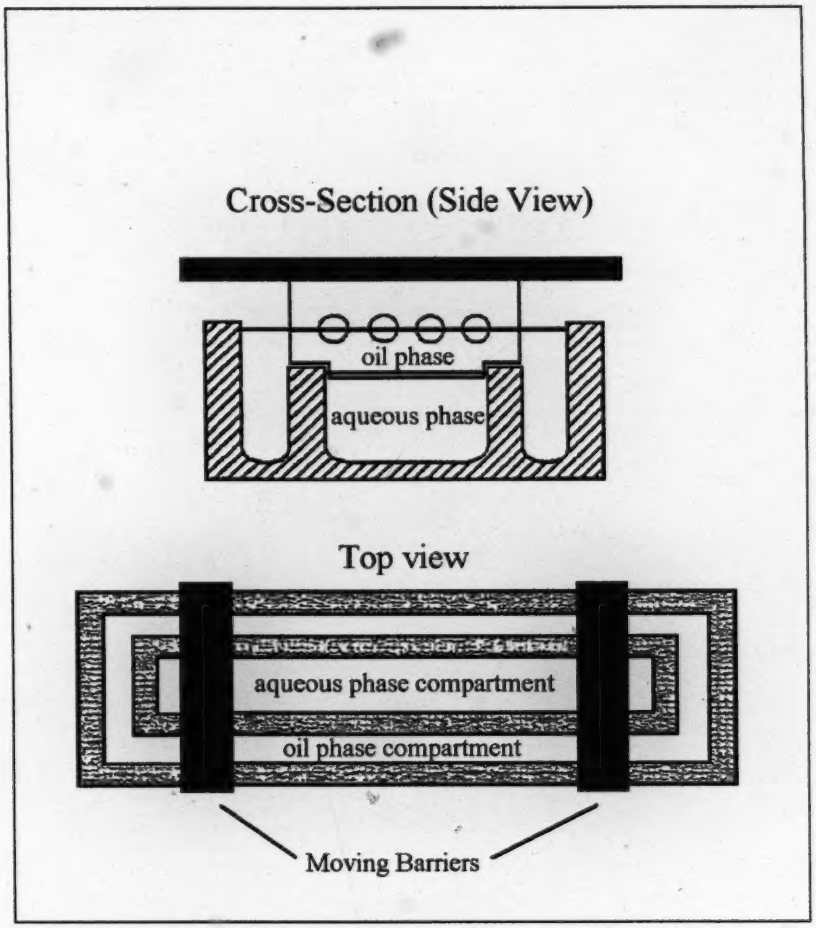

Figure 1.7 KSV liquid-liquid interfacial trough (modified from Galet et al, 1999).

Studies of amphiphilic molecules have recently been conducted using an interfacial trough to characterise a variety of fluid microstructures. Thoma and Möhwald (1994) extensively studied the pressure-area isotherms of phospholipid dipalmitoylphosphatidylethanoamine (DPPE) at the interface of water and hydrocarbons such as n-dodecane, n-hexadecane, and bicyclohexyl. Their work attempted to characterise the effect of hydrocarbon chain length and the type of hydrocarbon in the oil phase on the phospholipid monolayer. Thoma and Möhwald (1995) continued their work

by studying monolayers of dipalmitoylphosphatidylcholine (DPPC) at the interface of water and other hydrocarbons. This work investigated the ability of larger head groups of DPPC to affect the liquid condensed (LC) phase of the pressure area isotherms. Other studies of phospholipid monolayers at oil-water interfaces have been conducted by Grandell and Lasse (1998), who investigated the control of surface pressure of phosphatidylcholines (DPPC and DSPC) at water/1,2-dichloroethane interfaces, and by Liljeroth et. al. (2000), who investigated LB films of DSPC produced at water and nitrophenyl octyl ether (NPOE) interfaces.

Other amphiphilic material has been studied at oil-water interfaces in recent years. Murray and Nelson (1996) studied the pressure area isotherms of bovine serum albumin and β-lactoglobulin at interfaces using a prototype interfacial Langmuir trough. Aveyard et al. (2000) studied monolayer structure of charged latex particles at water (with NaCl) and octane using a modified Langmuir trough. Watanabe et al. (1990) studied the ion-binding behaviour of crown ether ((Octadecyloxy)methyl-18-crown-6) using an interfacial Langmuir trough at water and liquid paraffin interfaces.

Interfacial Langmuir troughs have also been used to investigate surfactants that affect the stability of water-in-oil emulsions. Ghaicha et al. (1995) used an interfacial Langmuir trough to study the packing efficiency of surfactants such as sorbitan mono-oleate and diethanolamine derivatives of polyisobutylene succinic anhydride at various molecular weights at water/heptane and water/paraffin oil interfaces. Their work compared the difference in molecular packing and hydrocarbon chain length to the surfactant effectiveness in producing stable water-in-oil emulsions.

1.3.3.8 Asphaltene Langmuir Monolayers at Oil-Water Interfaces

Due to the relatively recent development of the interfacial Langmuir trough, very little literature has been published on asphaltenes at oil-water interfaces. Ese et al. (1999) studied asphaltene and resin monolayers at air-water and water-decane interfaces using an interfacial trough from KSV Chemicals (see Figure 1.7) and examined the effect of adding various demulsifiers on monolayer stability. Ese et al. found that asphaltenes and resins had the ability to form relatively rigid monolayers at a water-decane interface. They also found that chemical additives of high molecular weights have a much larger effect on monolayer compressibility than additives of lower molecular weights. Their results indicated that higher molecular weight additives made the monolayers highly compressible and restrictive in the formation of rigid asphaltene monolayers, due to extensive adsorption of the additives at the interface. Ese et al. (1999) also concluded that the demulsifiers may play a role in destabilising the monolayers by dispersing the asphaltenes into the oil phase.

1.3.4 Atomic Force Microscope (AFM)

Atomic force microscopy is a high resolution method capable of investigating LB film structures and defects at length scales from 0.1nm to 10μm (Zasadzinski et al., 1994). The AFM can be used to study the topographical structure of surfaces at the nanometric dimension. This is a significant improvement over conventional optical microscopy, which has inherent lower resolution constraints (Hollars and Dunn, 1998). The AFM is capable of producing high-resolution images yielding information about surface topography, symmetry of local molecular packing, presence of molecular defects and molecular scale ordering (Tsukruk, 1997).

The atomic force microscope (AFM) is an important tool for imaging surfaces at a sub-microscopic level. The AFM used, a sharp tip on a cantilever to scan over a surface. During scanning, surface structures deflect the tip and cantilever (Miller et al. 1996), and by measuring the tip deflection using a laser and photodiode, a topographic image of the surface is obtained (Balashev et al. 2001). Figure 1.8 shows a simplified schematic of an AFM.

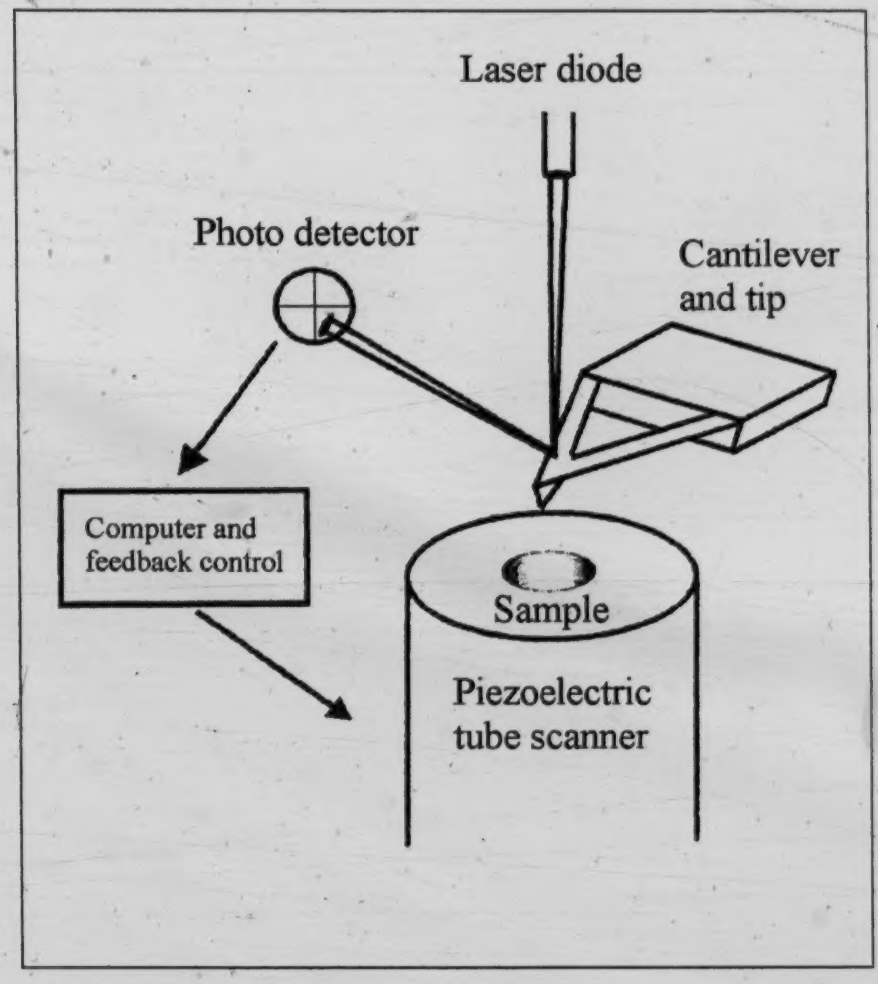

Figure 1.8 Principles behind an atomic force microscope (modified from Balashev et al, 2001).

In order to study a Langmuir monolayer with the AFM, the film must be transferred to a solid substrate. A number of different materials are used as a surface support for films studied using an AFM. Müller et al. (1997) indicated that surfaces of mica, glass, silicon and gold are commonly used as solid supports for AFM imaging and by using the Langmuir-Blodgett (LB) technique, a Langmuir monolayer can be transferred to the necessary solid substrate for investigation.

In a number of reports on fatty acids and their salts, an atomic force microscope was used to study film structure. Kurnaz and Schwartz (1996) used an AFM to characterise the surface morphology of multi-layers of arachidic acid/cadmium arachidate mixtures deposited on mica substrates. Their work characterised the phase separation of the LB films at small length scales (50-100 nm) as a function of pH. Sigiyama et al. (1998) investigated the structure of various arachidic acid salts at different pH values, on hydrogen-terminated silicon wafers. Vickery and Dunn (2001) studied the topography of palmitic acid (PA) monolayers on mica in order to characterise the bulk diffusion of the PA onto the mica surface.

Due to the relatively recent development of the AFM and the small body of literature studying asphaltenes using a Langmuir trough, there are currently few studies available on asphaltene LB films using an AFM. Toulhoat et al. (1994) studied asphaltenes adsorbed onto cleaved mica using an atomic force microscope. Mica slides were dipped into toluene solutions containing dissolved asphaltenes and were allowed to dry. The study focused on the evolution of asphaltene aggregates on the mica as a function of immersion time, and on a comparison of the structures formed by filtered and unfiltered asphaltenes. They concluded through observation, that an unfiltered asphaltene

solution contains material that is poorly solvated in toluene. Ese et al. (2000) used an AFM to study asphaltene LB films on mica surfaces. This was a continuation of their previous work in which they studied the influence of resins and demulsifiers on asphaltene Langmuir monolayers (Ese et al., 1998). They used an AFM to directly visualise the film properties that were indirectly observed (by a Langmuir trough) and found that addition of resins disturbed the rigid structure of the asphaltene film. Increasing resin concentration builds up a monolayer with a more open network. The observed open network monolayers were found to have a higher compressibility as compared to the closed network films formed by asphaltenes alone. The addition of demulsifiers was found to form a monolayer that contained both a more open network structure and a substantial increase in size of the structural units. The rigidity of these monolayers was found to be greatly reduced. The degree of openness of the film and the increase in size of the structural units could be directly related to the compressibility of the monolayer.

2 Experimental

2.1 Materials

Coker feed bitumen was supplied by Syncrude Canada Ltd. Toluene (99.8%), acetone (99.8%), n-heptane, (99.6%), sulphuric acid (98%), and Nochromix were supplied by Fisher Scientific. Hydrochloric acid (99.999%), sodium hydroxide (99.99%), chloroform (99.9%), arachidic (eicosanoic) acid (99%), cadmium chloride (99.99%), and dichlorodimethylsilane (99%) were purchased from Aldrich Chemical Co. Inc. Ethanol (99.8%) was supplied by Fluka Chemika. Dodecane (99%), n-hexadecane (99%) and L-α-dipalmitoyl phosphatidycholine (98%) were supplied by Acros Organics. L-α-phosphatidylcholine distearol (99%) was provided by Sigma Chemical Co. Demulsifiers A and B were supplied by Champion Technologies. All the water used was passed through a Millipore filter system that produces ultra-high purity water with a resistivity of 18.2 MΩ-cm.

2.2 Equipment

2.2.1 Langmuir Trough

All measurements relating to Langmuir monolayers and Langmuir-Blodgett films were performed on a KSV Minitrough from KSV Instruments Ltd. (Finland). A photograph of the KSV Minitrough with an air-water interface trough is shown in Figure 2.1.

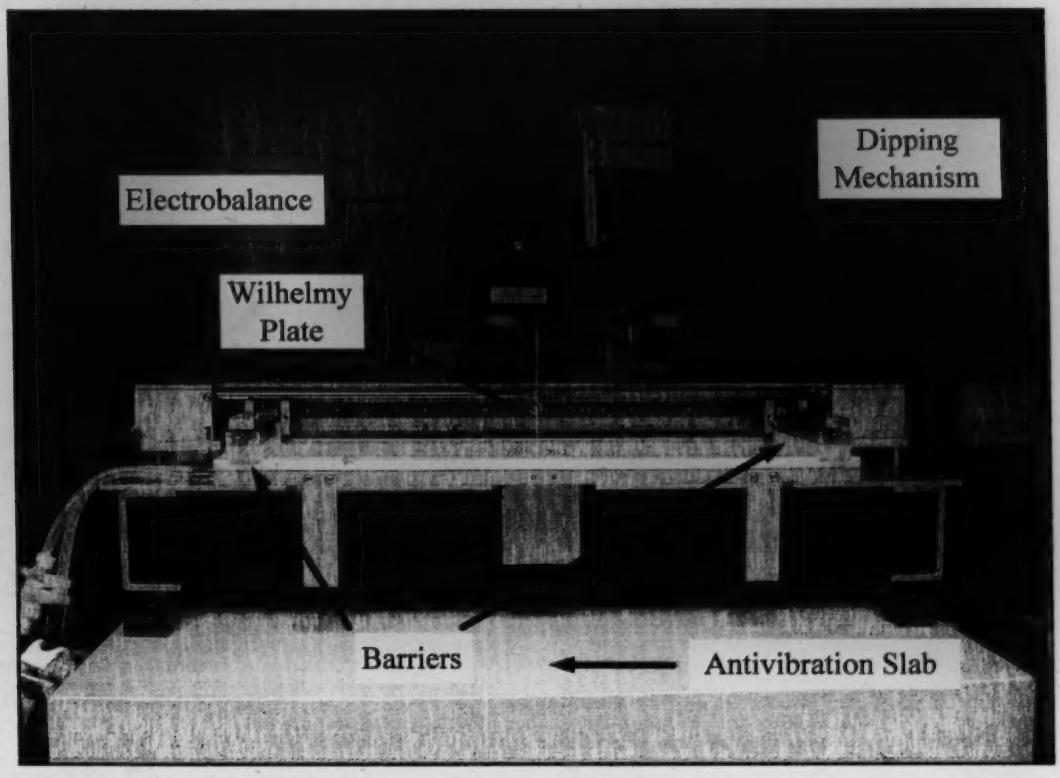

Figure 2.1 A photograph of the KSV Minitrough assembly.

The trough was placed on four foam pads which rested on a 25 kg epoxy anti-vibration slab. Two pieces of grooved rubber pads were stacked under each of the four corners of the epoxy slab. The trough was located inside a ventilated enclosure to minimize contamination. The temperature was controlled by a circulating water bath (Fisher Scientific, Isotemp 3006) with a built-in jacket in the trough. The Wilhelmy plate consisted of a strip of filter paper (Whatman #5) for all air-water interface measurements and a platinum strip for all oil-water interface measurements.

2.2.1.1 Air-Water Interface Trough

All measurements at the air-water interface were conducted using an air-water trough composed of Teflon with a maximum surface area of 24225.0 mm^2. The barriers were composed of Derlin and compressed the monolayer by riding along the surface of the trough. A photograph of the air-water trough with the barriers is shown in Figure 2.2.

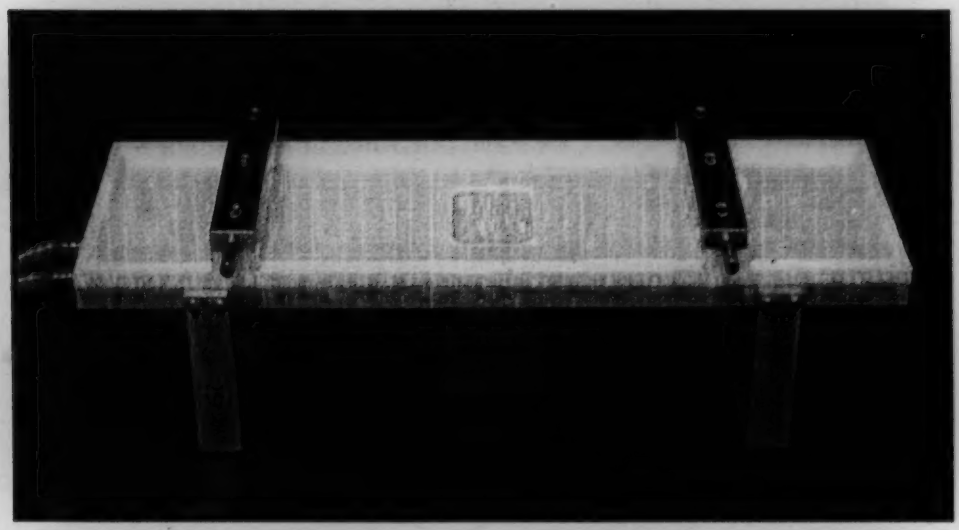

Figure 2.2 A photograph of the air-water trough with barriers.

2.2.1.2 Oil-Water Interface Trough

All oil-water interface measurements were conducted using an oil-water interface trough composed of Derlin with a maximum interfacial area of 17010 mm^2. The trough had an inside compartment for the higher density aqueous phase on which the lighter phase was poured. The two barriers were also made of Derlin and contained eight holes

each to allow the lighter phase liquid to pass through during compression. An image of one oil-water barrier on the trough is shown in Figure 2.3.

Figure 2.3 A close up photograph of the oil-water trough and barrier.

2.3 Procedures

2.3.1 Asphaltene Extraction

The bitumen was initially dissolved in toluene and centrifuged at 20,000 rpm for 30 minutes to remove any solids present in the sample. The bitumen/toluene mixture was then decanted and dried until the toluene was fully evaporated. The dry bitumen was then recovered. Asphaltenes were precipitated from the bitumen by mixing the bitumen at a volume ratio of 40 parts heptane to 1 part bitumen. The bitumen/n-heptane mixture was shaken for two hours on a laboratory shaker and left overnight to allow the asphaltenes to precipitate. The supernatant was decanted and the precipitated asphaltenes were washed

repeatedly with n-heptane until the supernatant was colourless. The asphaltenes were dried until the n-heptane was completely evaporated. This asphaltene sample was named "whole asphaltene" and the sample was not further fractionated. The whole asphaltene is approximately 11.9% of the original coker feed bitumen.

2.3.2 Asphaltene Fractionation

Figure 2.4 shows graphically detailed procedures used to yield different fractions of asphaltenes. The coker feed bitumen was initially mixed with n-heptane and toluene at a ratio of 5H:5T:1B, where H stands for n-heptane, T for toluene, and B for bitumen (this notation will be used for the remainder of the thesis). The mixture was shaken for two hours on a laboratory shaker and then centrifuged for 30 minutes to remove any precipitated solids in the sample. The supernatant was recovered and additional n-heptane was added to the mixture to create a supernatant with a volume concentration of 20H:5T:1B. The mixture was shaken for two hours, left overnight to allow the asphaltenes to precipitate, and then centrifuged for 30 minutes. The precipitated solids were recovered by decanting the supernatant and this fraction was named the "high molecular weight asphaltene fraction". Additional n-heptane was added to the supernatant to create a volume concentration of 40H:5T:1B. The precipitation procedure was repeated and the solid precipitates removed are named "the middle molecular weight asphaltene fraction". Additional n-heptane was added to the supernatant to obtain a volume concentration of 60H:5T:1B. The precipitation procedure was repeated one final time and the precipitates collected here are named "the low molecular weight asphaltene fraction". Further addition of n-heptane did not result in additional precipitation of asphaltenes. After fractionation, the asphaltene solid fractions were crushed into smaller

pieces using a glass-stirring rod. The fractionated asphaltenes were then washed with large quantities of n-heptane to dissolve maltenes that may have been co-precipitated with the asphaltenes. The mixture was shaken for two hours then allowed to settle overnight. After settling, the supernatant was decanted. This process was repeated until the solution of n-heptane became colourless. It was important to break the large pieces of precipitated asphaltenes to completely remove the maltene fraction during washing. The mass distribution of the fractionated asphaltenes is: 45% high molecular weight, 47% middle molecular weight, 8% low molecular weight. The total mass of the fractionated asphaltenes is approximately 7.3% of the original coker feed bitumen. Of the fractionated asphaltenes, only the low and high molecular weight fractions were extensively studied. This was done in order to observe any major differences in surface behaviour caused by asphaltene molecules of different molecular weight.

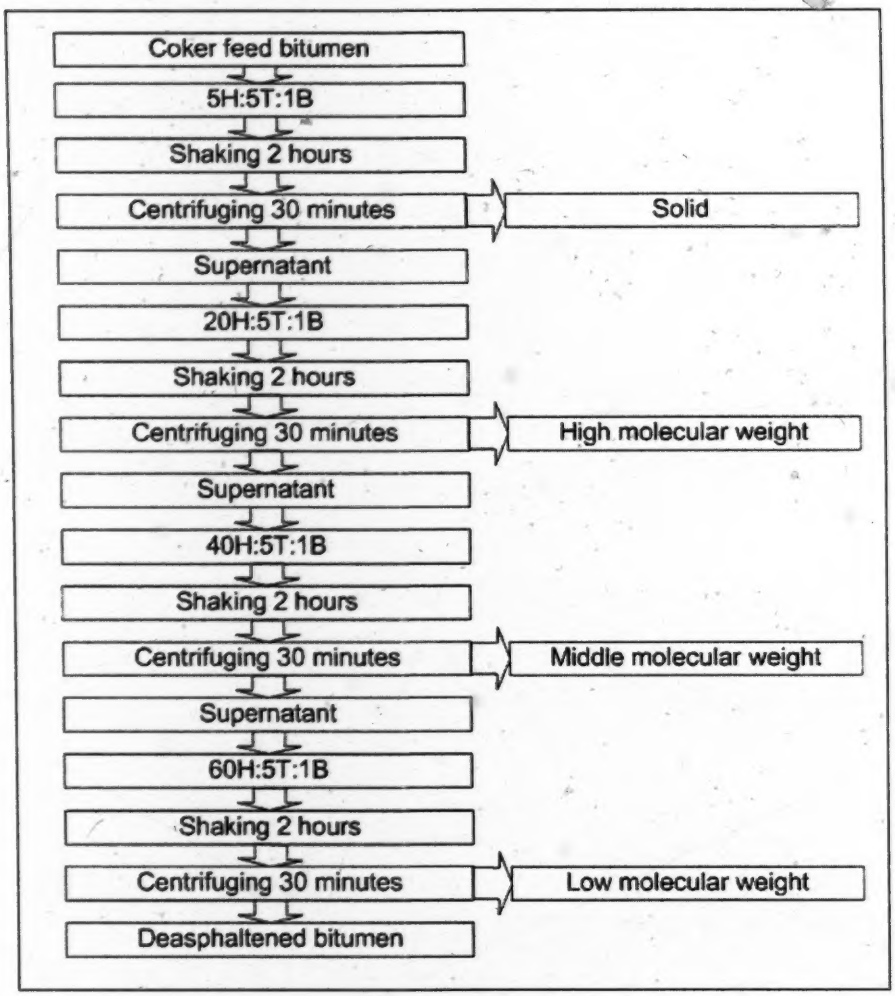

Figure 2.4 Asphaltene fractionation procedure.

2.3.3 Asphaltene Solution Preparation Procedure

Asphaltene solutions in toluene were used in both the Langmuir trough and during density measurements (Section 2.3.5). The solutions were prepared by dissolving asphaltenes in toluene at desired concentration (mg/ml). The solutions were then centrifuged at 20,000 rpm for 30 minutes. Next, the solutions were filtered by pressure

filtration through a Millipore Swinny Stainless 13 mm filter system attached to a Micro-Mate Interchangeable Hypodermic Syringe. An Osmonics nylon disc filter with a pore size of 0.45 μm was used to remove any particulate material insoluble in toluene.

2.3.4 Molecular Weight Analysis by Vapour Pressure Osmometry (VPO)

An analysis of the molecular weights of the asphaltene powders was conducted by the Microanalytical Laboratory, Department of Chemistry at the University of Alberta. The molecular weights were obtained with a Corona Westcan vapour pressure osmometer (VPO) model 232A by dissolving the asphaltenes in toluene at 53°C.

2.3.5 Asphaltene Density Analysis (Vibrating U-Tube)

The density of the asphaltenes dissolved in toluene was measured at 25°C with an Anton Paar DMA 45 densitometer. The asphaltene solutions were prepared following the procedures described in section 2.3.3. The asphaltene density was calculated using (Yarranton & Masliyah, 1996):

$$\rho_a = \frac{x_a}{\left[\rho_t x_a + \left(\frac{1}{\rho_m} - \frac{1}{\rho_t}\right)\right]} \qquad [2.1]$$

where ρ_a, ρ_t, and ρ_m are the densities of the asphaltene, toluene and the mixture, respectively and while x_a is the mass fraction of asphaltene. The densities were measured using 1 and 2 mg/ml solutions to ensure that the densities were independent of solution concentration. Also by conducting the density analysis at more than one concentration, reproducibility could be ensured. For asphaltene concentrations less than

3%, the densities of asphaltenes are independent of solution concentrations (Calemma et al. 1998).

2.3.6 Elemental Analysis

An elemental analysis of the asphaltene powders was conducted by the Microanalytical Laboratory, Department of Chemistry at the University of Alberta. The percentage of carbon, hydrogen, nitrogen and oxygen were independently obtained using a Carlo-Erba EA-1108 Elemental Analyser. The percentage of sulphur was obtained by burning the asphaltene samples in an oxygen flask and titrating $(SO_4)^{2-}$ ions with barium perchlorate.

2.3.7 FTIR Spectral Analysis of Asphaltene Powders

The molecular groups of asphaltene powders were identified using a Bio-Rad FTS 6000 Fourier transform infrared (FTIR) spectrometer. Dry potassium bromide (KBr, FTIR grade) was used to obtain the background spectrum and the mid-IR region from 600 to 4000 cm^{-1} was measured. The asphaltene powders were mixed with KBr at a concentration of 2%. The scan rate was 5 KHz with a resolution of 2 cm^{-1} and a sensitivity factor of 4.

2.3.8 Langmuir Trough (Air-Water Interface)

All experiments were conducted with a barrier compression/expansion speed of 10 mm/min per barrier, a subphase (water) pH of 5.6 to 5.7, and at 20°C unless otherwise indicated. After each experiment the Teflon trough and Derlin barriers were cleaned using ethanol and Tex-Wipe cloths, finally rinsed several times with high purity water.

2.3.8.1 Pressure Area Isotherms

Initially, the cleaned trough was filled with high purity water and the temperature was monitored using a pH/temperature meter (VWR Scientific Products Model 2000) until the water was within +/- 0.1°C of the setpoint. A clean Whatman #5 filter paper strip with a perimeter of 30 mm was used as the Wilhelmy plate and was suspended on the electrobalance. The Wilhelmy plate height was adjusted until the plate was partially immersed in the subphase. To ensure the water surface was contaminant free, the water was further cleaned by removing surface layers with a pipette connected to an aspirator while closing the barriers to achieve a small surface area. This was repeated until the change in surface pressure was less than 0.10 mN/m.

An accurately measured volume of 2 mg/ml asphaltene in toluene solution was added drop-wise onto the water surface using a Hamilton Gastight 10 µl precision syringe (Hamilton Gastight #1810). A waiting period of 15 minutes before compression of the surface allowed the toluene to fully evaporate leaving only the asphaltenes on the water surface. The surface pressure was set to zero and compression was initiated at 10 mm/min per barrier (unless otherwise noted). The surface area and the surface pressure were measured once every second for the duration of the experiment. The barriers approached each other until a collapse in the monolayer was evident from the Π-A isotherm. All the experiments were conducted at least twice and with different volumes of asphaltene solution in order to ensure reproducibility. Volumes of 10-30 µl asphaltene solution were typically used.

2.3.8.2 Compression-Expansion Experiments

All asphaltene monolayers were prepared using the same procedures detailed in section 2.3.8.1. In the compression-expansion tests, compression was performed at 10 mm/min per barrier immediately following expansion of the barriers at the same rate (unless otherwise noted) to a specified low surface pressure (usually 0 mN/m). Both surface pressure and surface area were monitored once every second by the computer connection during the experiment. In the experimental runs with multiple compression-expansion cycles, a five minute waiting time was allowed between each complete compression-expansion cycle.

2.3.8.3 Relaxation

The asphaltene monolayers were initially prepared in the manner detailed in section 2.3.8.1. After a 15 minute wait time that allowed the toluene to evaporate, the asphaltene monolayer was compressed to a specified surface pressure and the barriers were stopped. Surface pressure was then measured as a function of time to monitor the relaxation of the monolayer for a minimum of 30 minutes. For relaxation times less than 60 minutes, surface pressure measurements were recorded once every second. For the longer experiments (1 to 3 hours) measurements were usually recorded once every five seconds to reduce the volume of data produced. Since there are no rapid changes in the surface pressure during relaxation, taking measurements once every five seconds does not reduce the quality of the data obtained. All the experiments were conducted at least twice per given set of conditions to ensure reproducibility.

2.3.8.4 Langmuir Blodgett Deposition

Langmuir monolayers were transferred to silicon wafers and strips of mica using the LB technique. Silicon and mica were chosen for these tests, due to their hydrophilic nature. Due to the hydrophilic nature of the slides, the polar groups of the asphaltenes would readily attach to the substrate during an upstroke LB deposition. Silicon wafers, were initially soaked in a mixture of concentrated sulphuric acid and Nochromix (Fisher Scientific), for several hours, and then rinsed repeatedly with ultra-pure water. The substrates were stored in high purity water until needed for dipping. Immediately before use, the wafers were removed from the water and dried with compressed nitrogen. The wafers were approximately 0.3 mm thick with a width of 10 to12 mm and a length of 20 to 50 mm. The mica strips were prepared by cutting slides of mica 10 to12 mm wide and 20 to 50 mm long. Using a razor blade, both sides of the mica were cleaved off yielding two clean surfaces for LB deposition. The slide was then rinsed with high purity water and dried with compressed nitrogen. The average slide thickness was 0.2 mm. The Langmuir trough was prepared by filling the trough with high purity water and cleaning the surface with a pipette and aspirator. After slide preparation, the substrates were attached to the dipping mechanism and lowered at to least 25 mm below the water surface. Next, the asphaltene solution was added dropwise as detailed in section 2.3.8.1. After a 15 minute wait, the barriers compressed the surface to a specified surface pressure and were programmed to maintain the set pressure by making small changes to the surface area. A control system maintained the surface pressure by increasing and decreasing the surface area as necessary. The maximum speed the barriers could move while maintaining the surface pressure was 3 mm/min per barrier in either direction. The

substrate was then pulled out of the solution using the LB upstroke method (see figure 1.5) at a speed of 5 mm/min. The slide was then dried in air at ambient conditions and stored in a desiccator with anhydrous calcium sulphate as an absorbent material until needed for AFM or contact angle measurements.

At high surface pressures, it was often very difficult to transfer the monolayer to a substrate using the LB method due to the small surface area between the barriers. Instead, the LS method was used (see Figure 1.5), which is useful for the deposition of very rigid films in the solid region of the Π-A isotherm (Ulman, 1991). Microscope glass slides (75 x 25 x 1 mm) were rendered hydrophobic by immersing them overnight in a mixture of toluene and dichlorodimethylsilane (10% by volume). After soaking, the slides were rinsed with pure toluene and air dried in a fume hood. The hydrophobic slides were then stored in airtight glass containers until needed for dipping. In this method, the monolayer was initially compressed to the desired surface pressure and maintained by the control system. The substrate was then horizontally placed on the compressed monolayer then lifted and separated from the surface. The transferred film was then dried in air and stored in a desiccator until needed for further analysis.

2.3.9 Langmuir Trough (Oil-Water Interface)

All experiments in the oil-water trough employed the same conditions detailed in section 2.3.8. After all experiments, the Derlin trough and barriers were cleaned using acetone and Tex-Wipe cloths, finally rinsed several times with high purity water.

2.3.9.1 Pressure Area Isotherms

Initially, the cleaned oil-water trough was filled with high purity water and the temperature was monitored using a VWR Scientific Products Model 2000 ph/temperature meter until the water was within +/- 0.1°C of the setpoint. A platinum strip with a perimeter of 39.24 mm was used as the Wilhelmy plate and was suspended on the electrobalance. The platinum strip was cleaned by flaming with a propane torch for several seconds before each experiment. The Wilhelmy plate height was adjusted until the plate was partially immersed in the subphase. To ensure the water surface was contaminant free, the water was further cleaned by removing the surface layers with a pipette connected to an aspirator and by repeatedly closing the barriers to achieve a small surface area, until the change in surface pressure became less than 0.10 mN/m. The method for adding the asphaltenes to the water surface are detailed in section 2.3.8.1. Approximately 125 ml of the organic phase (usually heptane) was then placed on the surface of the water. The organic phase was added using a transfer pipette and was carefully placed on the lip of the trough surrounding the water phase, as to not excessively disturb the asphaltenes floating on the water surface. A wait time of 10 minutes was given before compression to allow the temperature of the organic phase to stabilise and to allow the asphaltene molecules at the interface to reorganise. The surface pressure was tared to zero and compression was initiated at 10 mm/min per barrier (unless otherwise noted). The surface area and the surface pressure were measured by the system once every second for the duration of the experiment. The barriers were compressed until a collapse in the monolayer was evident from the Π-A isotherm. All experiments were conducted at least twice and with different volumes of asphaltene

solution in order to ensure reproducibility. Volumes of 10 to 25 µl asphaltene solutions were typically used.

2.3.9.2 Compression Expansion Experiments

A monolayer was prepared at the oil-water interface as detailed in section 2.3.9.1. The procedures for compressing and expanding the monolayer are the same as for the air-water trough and are detailed in section 2.3.8.2.

2.3.9.3 Relaxation Experiments

A monolayer was prepared at the oil-water interface as detailed in section 2.3.9.1. The procedure for relaxing a monolayer at the oil-water interface was the same as that for the air-water interface and is detailed in section 2.3.8.3. With some of the more volatile organic phases used, such as heptane, measurements of the monolayer relaxation were not taken for times exceeding 1.5 hours due to the relatively rapid rate of evaporation of the organic phase.

2.3.9.4 Langmuir Blodgett Deposition

Langmuir monolayers were transferred to silicon wafers using the LB technique. The wafers were cleaned in the manner detailed in section 2.3.8.4. The films were transferred using the upstroke method and the substrates were thus immersed in the water phase before the asphaltenes and oil phase had been added to the surface water surface. After the monolayer was compressed and maintained at a set surface pressure, the wafer was drawn up through the interface and oil phase. The wafer was dried in air and stored in a desiccator until needed for further analysis. The LS method was not used on the oil-water trough due to the difficultly of the hydrophobic glass slide being wetted by the

organic phase making it impossible to pick up the material forming the monolayer at the oil-water interface.

2.3.9.5 Demulsifier Addition

Experiments were performed using two demulsifiers provided by Champion Technologies. Two sets of experiments involving demulsifiers were conducted. The first set of experiments examined the effects of the demulsifiers on a heptane-water interface without asphaltene addition. A clean heptane-water interface was created by adding high purity water, waiting until the temperature was stable, and then spreading heptane on the surface of the water. The demulsifiers are heptane soluble and were added dropwise to the heptane located on the water. Changes in surface pressure were measured as a function of time.

The second set of experiments examined the effects the demulsifiers had on a high molecular weight asphaltene monolayer at the heptane-water interface. A monolayer of high molecular weight asphaltene at the heptane-water interface was prepared following the procedure in section 2.3.8.1. The demulsifiers were added dropwise to the heptane and a 40 minute (2400s) wait time was employed to allow the demulsifiers sufficient time to diffuse to the interface and interact with the asphaltene. A pressure-area isotherm was then conducted as per the procedure in section 2.8.8.1. Concentrations of demulsifiers are reported as ppm in heptane.

2.3.10 Contact Angle Measurements

All contact angle measurements were conducted using a Krüss Drop Shape Analysis System (DSA 10-MK2) at room temperature. A sessile drop of water,

controlled by a computerised dosing system, was placed on a single layer of Langmuir-Blodgett asphaltene film deposited on an oxidised silicon wafer. The contact angle was then measured through the water phase at one second intervals for one minute by shape fitting of a digitized video image. The drop shape analysis software reported an average value for the contact angle accompanied by an error distribution. Contact angles were measured at a minimum of four separate locations on each sample and again on at least two independent samples for each set of conditions.

2.3.11 Atomic Force Microscopy (AFM)

Images of the deposited Langmuir-Blodgett films were obtained using a Nano Scope III (Digital Instruments) atomic force microscope (AFM) using a Multimode-Scanning Probe Microscope (MM-SPM) head. A J scanner and silicon nitride tip with a spring constant of 0.38 N/m was used and operated in contact mode under ambient conditions. Images were obtained on at least three separate locations and at least two independent samples were analysed for each set of conditions to ensure reproducibility.

3 Asphaltene Properties

3.1 General Asphaltene Appearance

The whole and low molecular weight asphaltenes appear as dull, dark-brown powders. The high molecular weight fraction is matte and lighter brown in appearance than the other samples. Yarranton et al. (2000) indicated that for accurate determination of the average molecular weight, complete removal of the co-precipitated asphaltenes is necessary. The whole asphaltene was black in appearance before repeated washing with n-heptane but became brown in appearance, indicating the removal of the co-precipitated maltenes which are soluble in n-heptane.

3.2 Asphaltene Molecular Weight Analysis

It is necessary to determine the mean molecular weight of the asphaltenes in order to determine the mean molecular area occupied by an asphaltene molecule at both the air-water and oil-water interface in the Langmuir trough. The molecular weights were determined by the procedure outlined in section 2.3.4 and are shown in Table 3.1.

Table 3.1 Asphaltene Molecular Weights

Sample Name	Molecular Weight (g/mol)
Whole Asphaltene	6870
High Molecular Weight	8310
Low Molecular Weight	6480

The molecular weight results are as expected with the high and low molecular weight fractions yielding the highest and lowest molecular weights respectively, with the

whole asphaltene fraction having an intermediate mean molecular weight. Accurately determining the molecular weight of asphaltenes has been a subject of considerable debate in literature. Vapour pressure osmometry (VPO) and gel permeation chromatography (GPC) are frequently used. Since asphaltenes are a solubility class there are no standard methods for extracting them from crude oils or bitumen. As a result, the physiochemical properties of the asphaltenes in a given study are extremely dependant on the method employed in their extraction. In the literature, the molecular weight of asphaltenes studied has ranged from much less than 1000 to well over 10,000 depending on the extraction method used (Yarranton et al., 2000; Kotlyar et al., 1999; Peramanu et al., 1999; Calemma et al. 1995).

3.3 Density Analysis

Density analysis of the asphaltene powders was conducted by the procedure detailed in section 2.3.5. The asphaltene densities are shown in Table 3.2.

Table 3.2 Asphaltene Density

Sample Name	Density (kg/m^3)
Whole Asphaltene	1140
High Molecular Weight	1180
Low Molecular Weight	1080

These density values are comparable to other literature values ranging from 1100 to 1300 kg/m^3 (Calemma et al., 1998 and Peramanu et al., 1999).

3.4 Elemental Analysis

Elemental analysis was conducted on the asphaltene powders following the procedures described in section 2.3.6. The weight percentages of hydrogen, carbon, nitrogen, and sulphur are shown in Table 3.3.

Table 3.3 Elemental Analysis of Asphaltene Powders

Sample Name	H%	C%	N%	O%	S%
Whole Asphaltene	7.93	79.06	1.14	1.37	7.62
High Molecular Weight	7.66	78.88	1.26	1.26	7.79
Low Molecular Weight	8.16	79.24	1.16	1.43	8.15

3.5 FTIR Spectral Analysis

FTIR spectral analysis was conducted using the procedure detailed in section 2.3.7. The spectra of the asphaltene powders are shown in Figure 3.1 and the assignment of the different bands is given in Table 3.4. The spectra are normalised with the strongest peak at 2924 cm^{-1} (C-H stretching). Strong absorption bands of carbonal (COOH) and carboxylic (COO^-) groups over spectral ranges of 1740 to1680 cm^{-1} and 1650 to1540 cm^{-1} respectively, were not detected, indicating the absence of these groups.

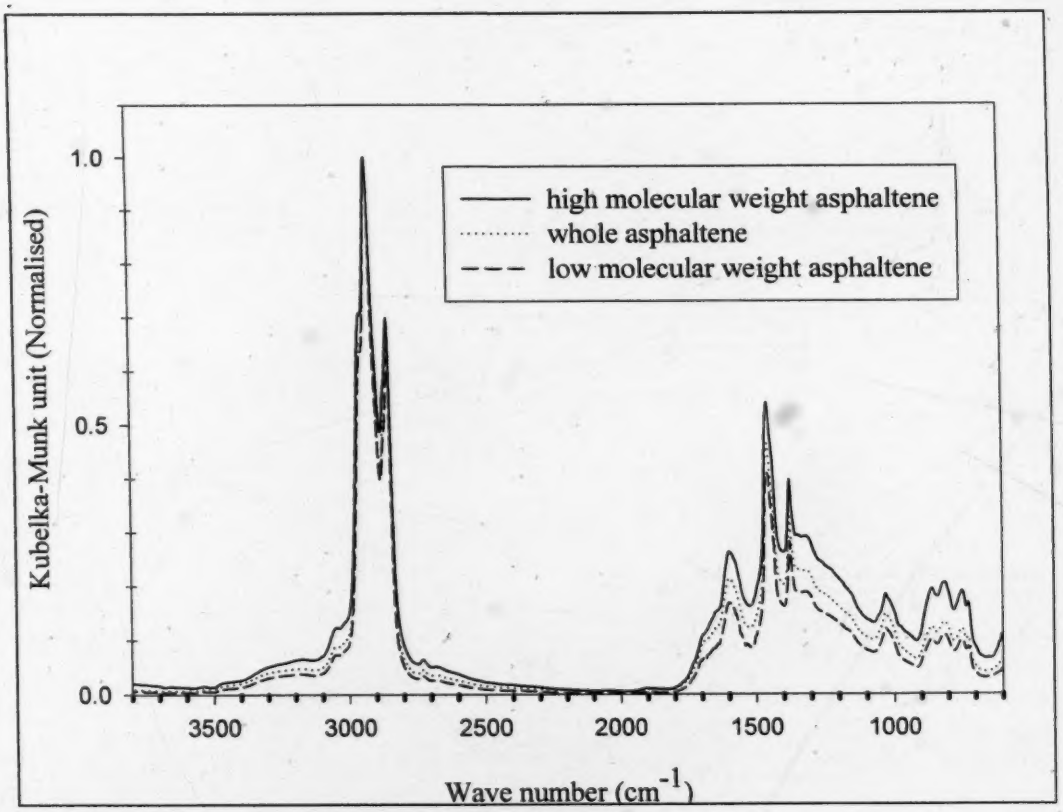

Figure 3.1 FTIR spectral analysis of asphaltene powders.

Table 3.4 Structural Features of Infrared Spectral Bands of Asphaltene Powders

υ , cm^{-1}	Structural Feature (all fractions)
3300 - 3100	N - H stretching
3060	aromatic C - H stretching
2930 - 2855	aliphatic C - H stretching
1606	carbonal C = O stretching
1464, 1378	aliphatic C - H bending
1036, 1028	S - O stretching
862, 813, 747	aromatic C - H bending
720	C - H rocking

4 Air-Water Interface

4.1 Pressure Area Isotherms

In order to confirm the procedure of the Langmuir trough tests at the air-water interface, pressure-area isotherms (Π-A) of arachidic acid on high purity water and on water with $3*10^{-4}$ M $CdCl_2$ at a pH of 6.6 were produced. The tests were conducted at 22°C with a barrier compression speed of 10 mm/min per barrier. The results of these tests are shown in Figure 4.1. The results are comparable to those published previously by Yazdanian et al., 1990 and Claesson and Berg, 1989 (see Figures 4.1b & 4.1c), indicating that the Langmuir trough was operating correctly.

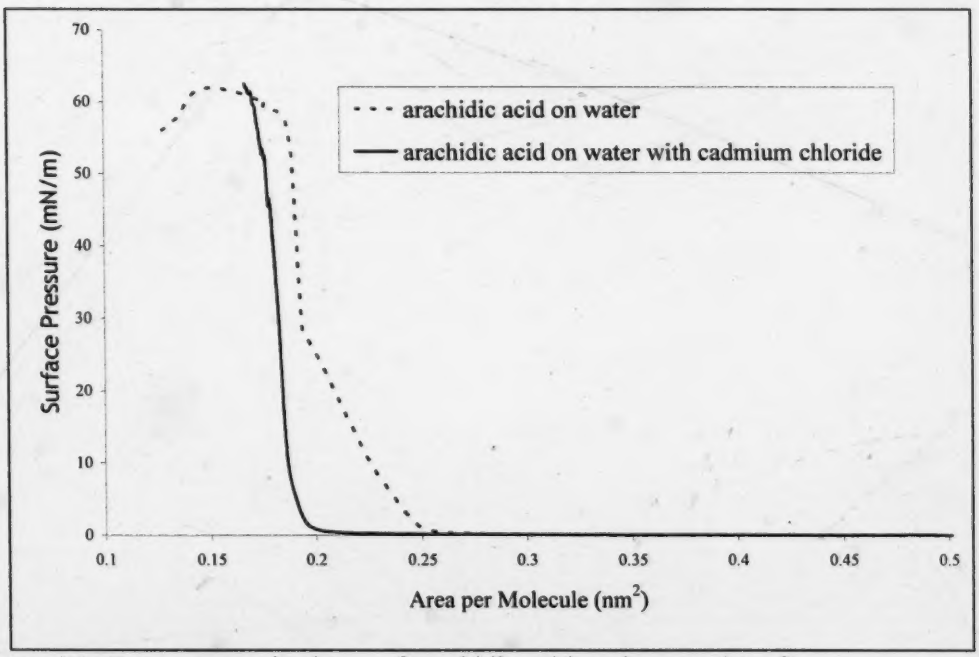

Figure 4.1a Pressure area isotherm of arachidic acid at air-water interface.

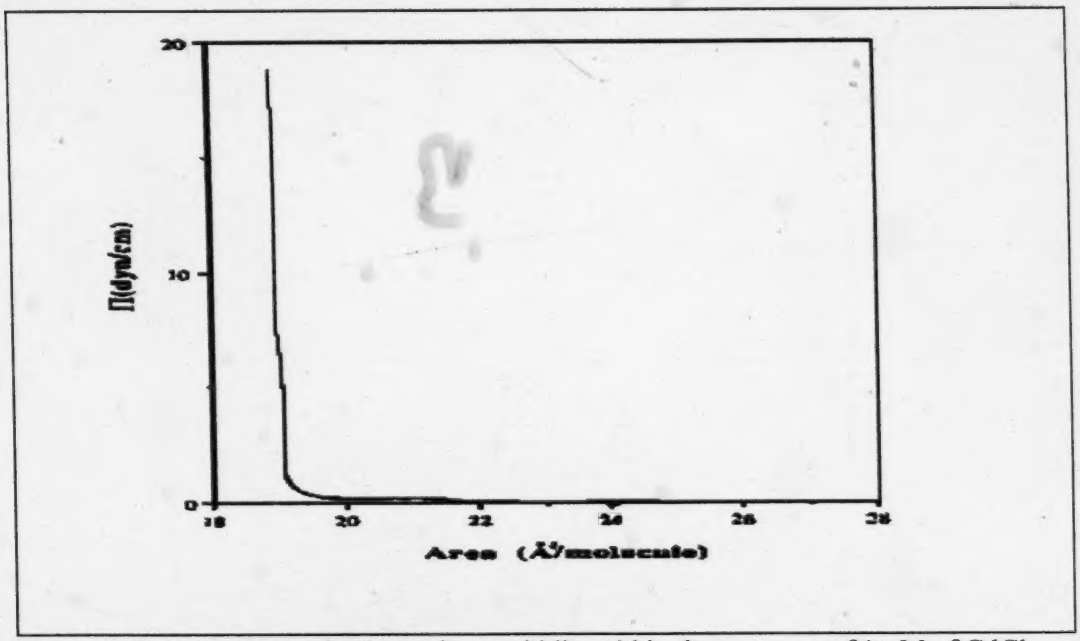

Figure 4.1b Pressure-area isotherm for arachidic acid in the presence of 1mM of $CdCl_2$ at pH 6.0 (modified from Yazdanian et al., 1990).

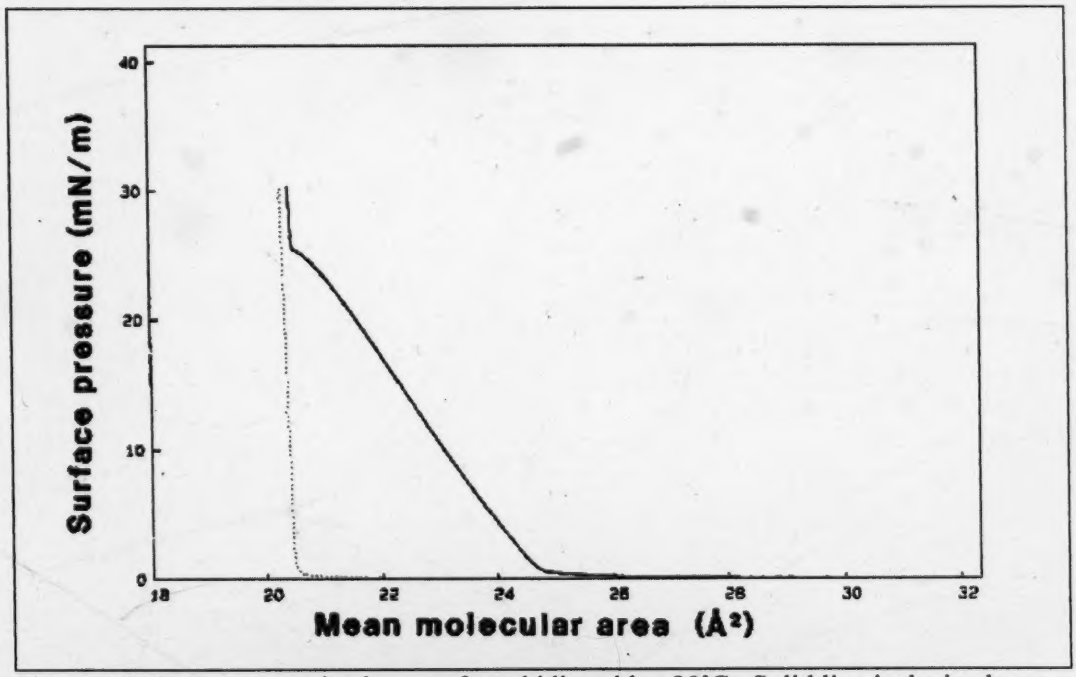

Figure 4.1c Pressure-area isotherms of arachidic acid at 20°C. Solid line is the isotherm on pure water, and the dotted line is on an aqueous subphase containing $3X10^{-4}M$ $CdCl_2$ and $5X10^{-5}M$ $NaHCO_3$ at pH 6.6 (Claesson and Berg, 1989).

For certain systems, barrier compression speed can affect the shape of the isotherm due to the slow rate of re-ordering of the individual molecules during compression. To ensure that compression speed was not a factor in determining the shape of the isotherm, a number of tests were conducted at different compression speeds. A plot of the results of the high molecular weight fraction compressed at various speeds is shown in Figure 4.2. The results clearly indicate that for barrier compression rates ranging from 5 to 100 mm/min per barrier, the shape of the isotherm is not affected and that the isotherm is highly reproducible.

All subsequent isotherms were conducted with a compression speed of 10 mm/min per barrier, with high purity water (pH 5.6 to 5.8) and at 20°C, unless otherwise indicated.

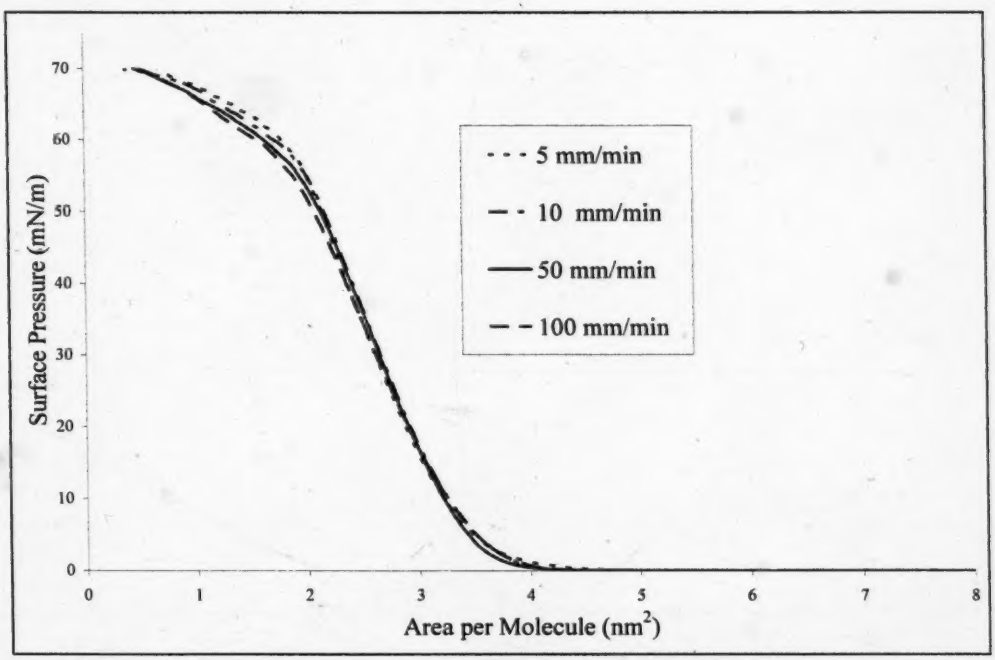

Figure 4.2 Pressure-area isotherms of high molecular weight asphaltene at the air-water interface.

Representative pressure-area isotherms of the three fractions of asphaltenes are shown in Figure 4.3. To ensure that the amount of asphaltene added to the surface did not affect the shape of the pressure-area isotherm, several different volumes ranging from 10 to 30 μl of asphaltene solution (at 2 mg/ml) were spread on the subphase and their isotherms measured. In all cases, the isotherms obtained were identical. For volumes much less than 10 μl, there is insufficient asphaltene material spread on the surface to fully compress the monolayer to a collapsed stage, as the barriers move too close to the Wilhelmy plate. For volumes over approximately 50 μl, there is excess asphaltene on the surface, which is indicated by the fact that as the barriers initially start to move, the surface pressure immediately begins to increase. All asphaltene isotherms were conducted with an asphaltene solution of 2 mg/ml (asphaltene/toluene) and by adding a volume between 15 to 25 μl. The area per molecule is the surface area of the trough divided by the number of molecules added to the surface. The number of asphaltene molecules added to the surface can be calculated from the known asphaltene density, concentration, and volume of the asphaltene solution.

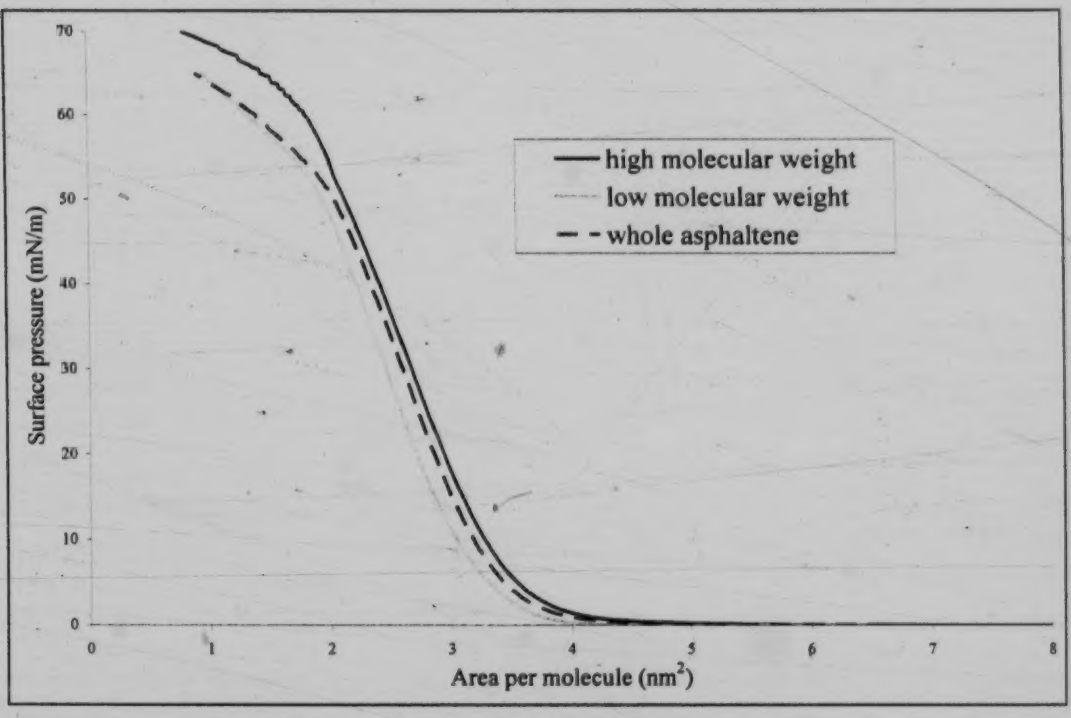

Figure 4.3 Pressure-area isotherms of three fractions of asphaltenes.

The shape of the isotherms is similar to those presented by Mohammed et al., (1993) and LeBlanc and Thyrion, (1989) who also conducted Π-A isotherms of asphaltenes. From the isotherms, it is clear that the high molecular weight fraction occupies the largest molecular area, the low molecular weight the smallest molecular area, and the whole fraction lies in between. This type of relationship between the fractions is anticipated as the high molecular weight fraction has the largest molecules in its mixture, the low molecular weight fraction has the smallest molecules, and the whole fraction is a mixture of the entire range of molecular sizes. As a result, the high molecular weight fraction on average should occupy a larger area per molecule, the low molecular

weight fraction a smaller area per molecule and the whole fraction should have an average somewhere between the two fractions.

No clearly defined phase transitions are visible for all three fractions of asphaltenes, neither from gas to liquid (or liquid expanded) phase nor from liquid to solid phase, indicating that asphaltenes are a complex mixture of molecules of varying molecular weight. For a well defined monolayer, a clear phase transition is normally visible due to the fact that the molecules all behave in a similar manner. In a heterogeneous material however, phase transitions are not visible as all the molecules do not undergo a transition at the same molecular area. The transition is spread out over a range of molecular areas. For a clear example of a phase transition, refer back to Figure 4.1. The arachidic acid monolayer on high purity water undergoes a clear transition at approximately 0.2 nm^2.

Even though the asphaltene pressure-area isotherms shown in Figure 4.3 do not have clearly defined phase transitions, there are still four different phases of the monolayer visible on each isotherm. Figure 4.4 shows the pressure-area isotherm of the whole asphaltene and the four different phases of the monolayer. At very large areas per molecule, the asphaltene molecules are far apart on the surface and do not interact with each other. This region of the isotherm is called the gas (G) phase. As the area per molecule decreases due to barrier compression of the surface, the asphaltene molecules eventually become sufficiently restricted with each other to begin interacting. This phase is called the liquid expanded (LE) phase and is noted by the initial increase of surface pressure as the molecular area decreases. In the next phase, the liquid condensed (LC)

phase, the isotherm behaves in a linear fashion and the asphaltene molecules are assumed to be packed sufficiently close that their side chains are vertically oriented.

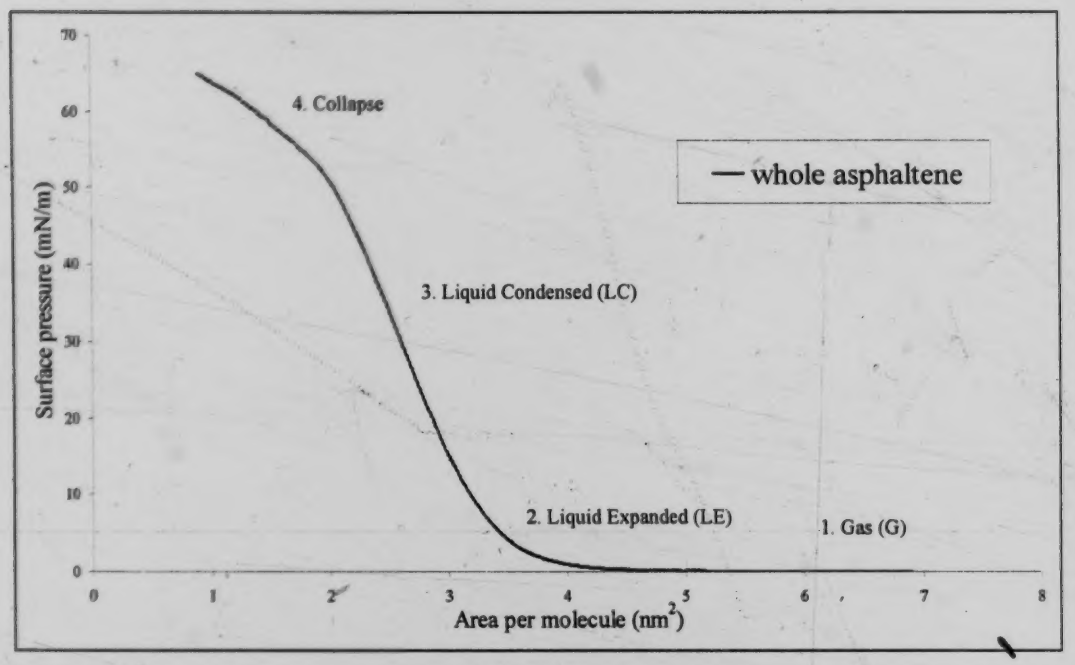

Figure 4.4 Pressure-area isotherm of the whole asphaltene with phases indicated.

The final phase is up to the monolayer collapse which occurs in the region beyond the critical area (A_c). The critical area and the critical pressure (π_c) are the area and surface pressure at which the monolayer begins to fold. With some types of monolayers, there is a solid phase clearly visible after the LE phase and before the collapse. However, with the asphaltene monolayers, no clear solid phase of the monolayer was observed (a solid phase is indicated by a sudden rapid increase in surface pressure just before collapse). Instead, in the region past the critical area, brown streaks became visible on the surface of the water near the inner edges of the compression barriers. This may

indicate that for areas smaller than the critical area, the surface is no longer a monolayer and the molecules begin to fold and slide over each other. This assumption is further evidenced by AFM images that are shown in section 4.6.1. The zero surface area (A_0) is an approximation of the average area per molecule. The critical area, critical pressure and zero surface area are found graphically from the pressure-area isotherms in Figures 4.5a to 4.5c. Table 4.1 shows the zero surface area (A_0), the critical area (A_c) and the critical pressure (π_c) for all three fractions of asphaltene.

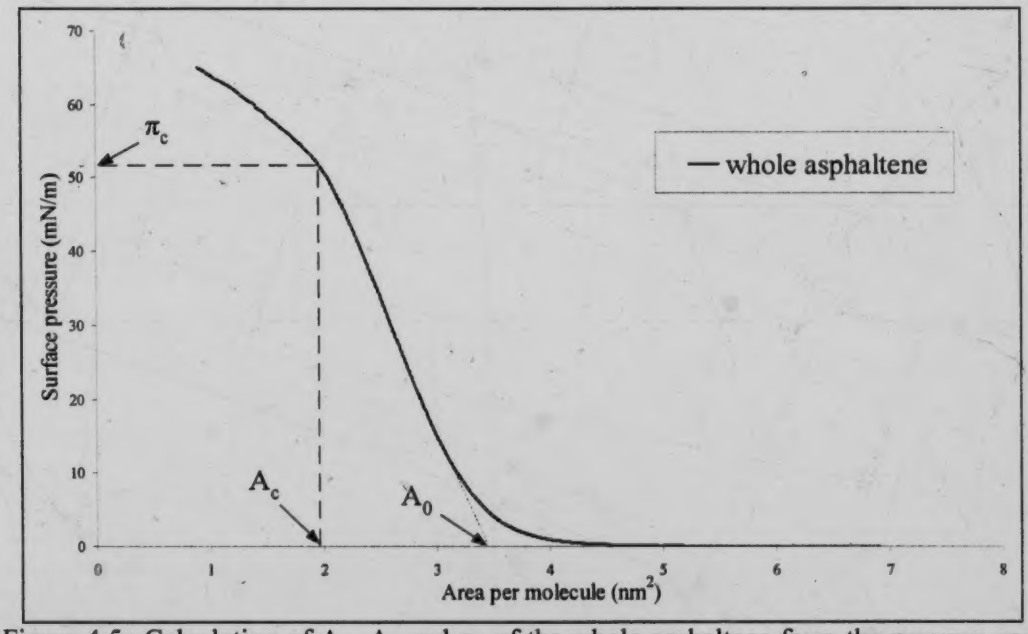

Figure 4.5a Calculation of A_C, A_0 and π_C of the whole asphaltene from the pressure-area isotherm.

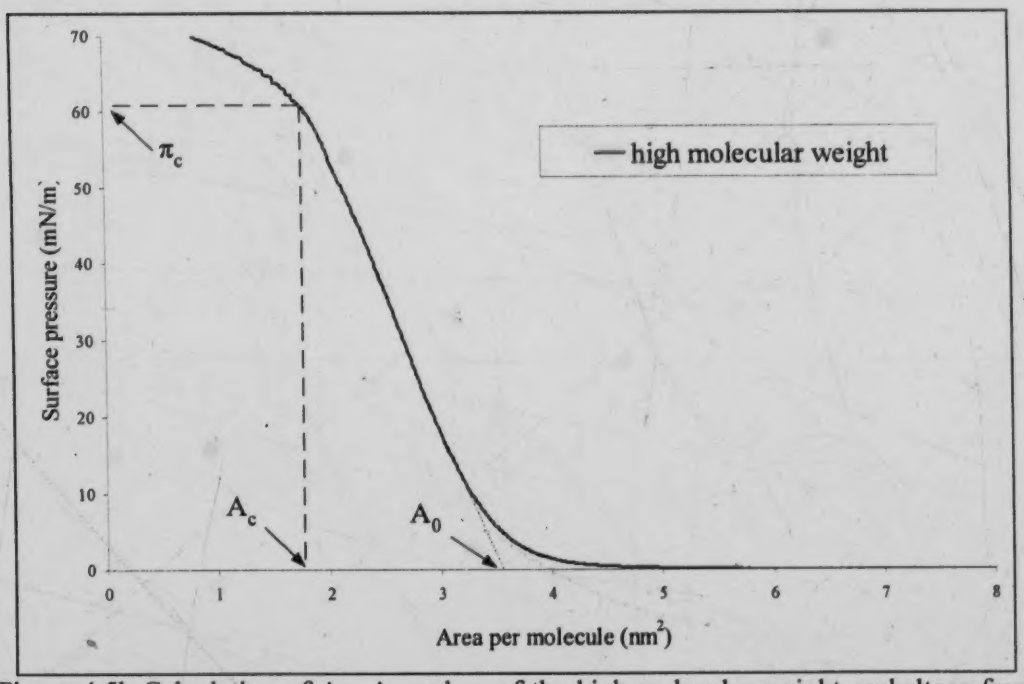

Figure 4.5b Calculation of A_C, A_0 and π_C of the high molecular weight asphaltene from the pressure-area isotherm.

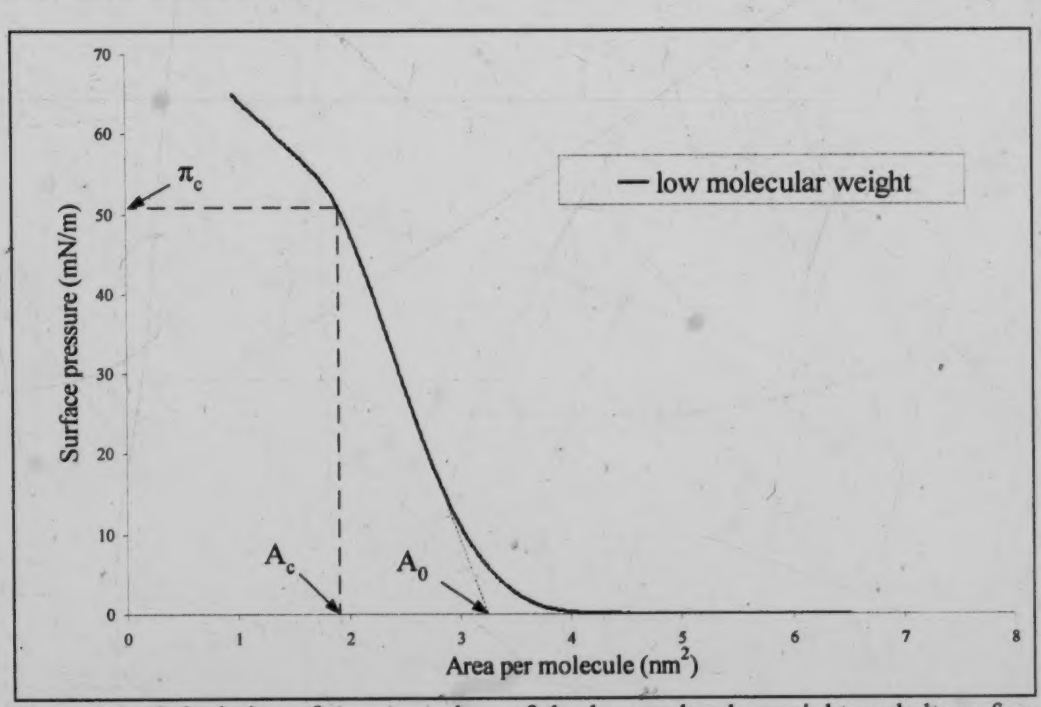

Figure 4.5c Calculation of A_C, A_0 and π_C of the low molecular weight asphaltene from the pressure-area isotherm.

Table 4.1 Extrapolated Critical Area, Critical Surface Pressure and Zero Surface Pressure of Asphaltene Monolayers at Air-Water Interface at 20°C

Sample Name	A_c (nm^2/molecule)	π_c(mN/m)	A_0 (nm^2/molecule)
Whole Asphaltene	1.97	52.47	3.40
High Molecular Weight	1.82	61.76	3.52
Low Molecular Weight	1.88	51.82	3.22

The zero surface pressure and critical surface pressure are both observed to increase with increasing molecular weight of the asphaltene samples (low molecular weight fraction < whole asphaltene < high molecular weight fraction).

4.2 Hysteresis Isotherms

In order to determine the reversibility of the isotherms, the asphaltene monolayers were compressed to various surface pressures and then expanded back to zero for three complete cycles of compression and expansion. For clarity, Figure 4.6 shows only the first and third compression and expansion of the high molecular weight fraction. Arrows have been added to differentiate between the compression and the expansion curves. Figures 4.7a-c show a monolayer of high molecular weight asphaltene, low molecular weight, and whole asphaltene compressed to 20 mN/m and expanded three times.

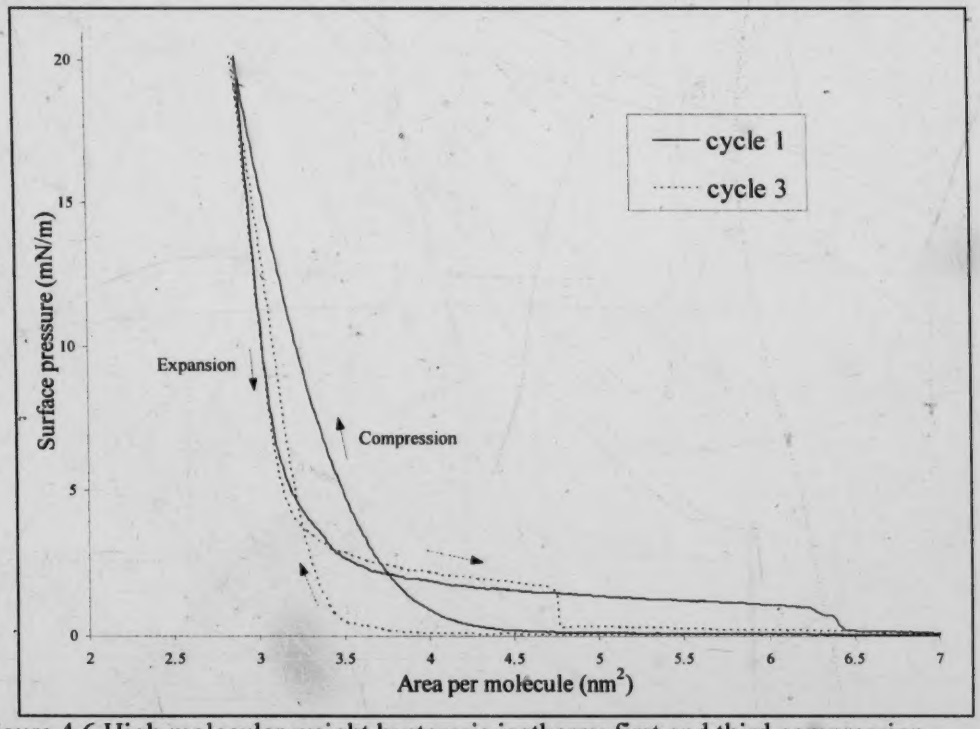

Figure 4.6 High molecular weight hysteresis isotherm; first and third compression-expansion cycles shown.

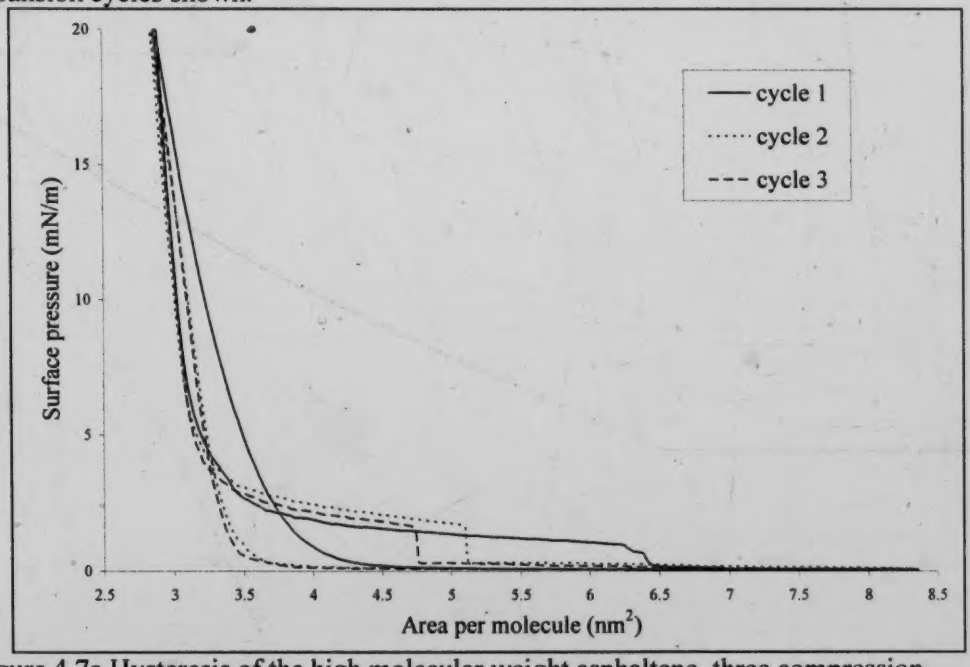

Figure 4.7a Hysteresis of the high molecular weight asphaltene, three compression-expansion cycles shown.

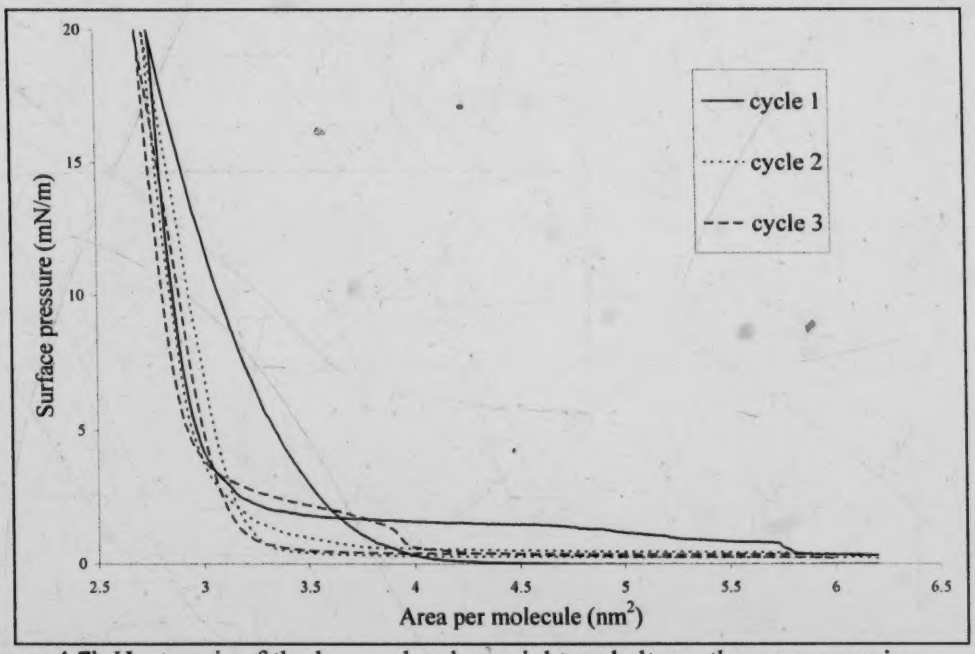

Figure 4.7b Hysteresis of the low molecular weight asphaltene, three compression-expansion cycles shown.

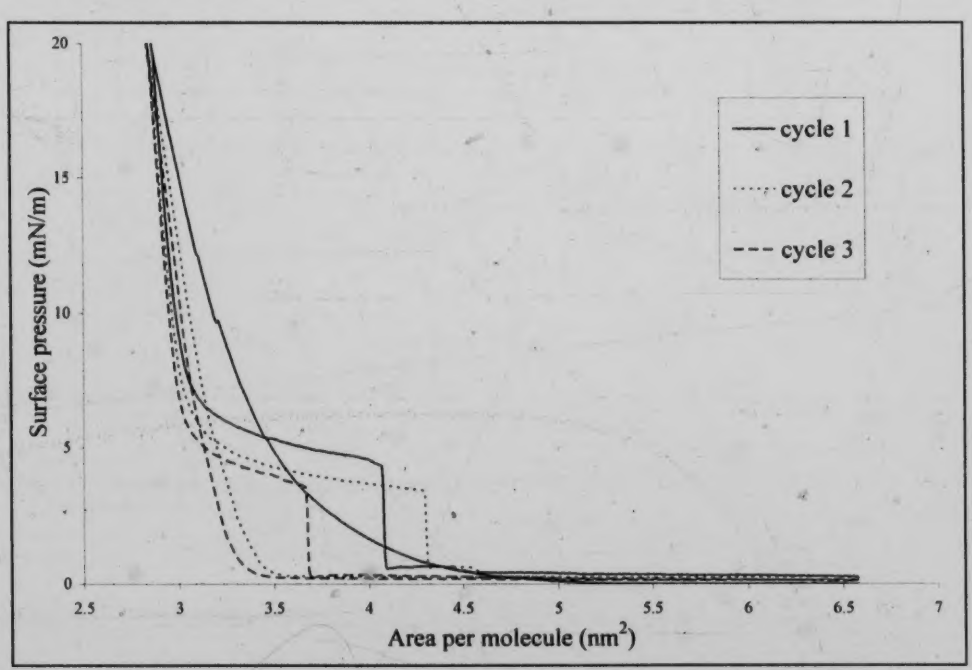

Figure 4.7c Hysteresis of the whole asphaltene, three compression-expansion cycles shown.

It is clear from Figure 4.6 that the expansion deviated significantly from the compression isotherm during the first cycle, indicating a large hysteresis. While relaxation mechanisms could partially account for the hysteresis, movement of the smaller molecules into the subphase during compression is a likely mechanism responsible for the observed hysteresis. The asphaltene molecules do not appear to relax back to their original state after an extended period of time as evidenced by the shifting of the compression curves to the left during subsequent cycles. The movement of smaller molecules into the subphase is further confirmed by the reduction in hysteresis with increasing compression-expansion cycles indicating that less and less material is "squeezed" out with each subsequent compression. Hysteresis is not generally observed with fatty acid monolayers such as arachidic or stearic acid, indicating that the molecular properties of asphaltenes are more complex.

Another interesting phenomenon observed was a sudden drop in surface pressure during the expansion cycle of the monolayer at surface pressures of $\pi < 5$ mN/m. For rigid films, sudden movements of the Wilhelmy plate can sometimes cause abrupt changes in the observed surface pressure (Constantino et al., 1999 and Dynarowicz et al., 2001). However, our observed drop in the pressure was reproducible and therefore cannot be caused by the Wilhelmy plate movement. To ensure that during the expansion cycle of the monolayer, the barriers were not moving too rapidly to disturb the film and the Wilhelmy plate, a number of tests were performed with expansion speeds ranging from 1 to 20 mm/min per barrier. Even at the slowest expansion speed (1 mm/min per barrier), an abrupt drop in surface pressure occurred at $\pi < 5$ mN/m indicating that the barrier speed does not affect this sudden surface pressure drop. A possible explanation

for the abrupt decreases could be a sudden disentanglement of the asphaltene molecules, leading to the rupture of the asphaltene monolayer. During the compression cycle, the asphaltene molecules can become entangled due to their complex structure.

Figure 4.8 compares the hysteresis isotherms for the high molecular weight fraction asphaltene compressed to 20 mN/m and to 60 mN/m.

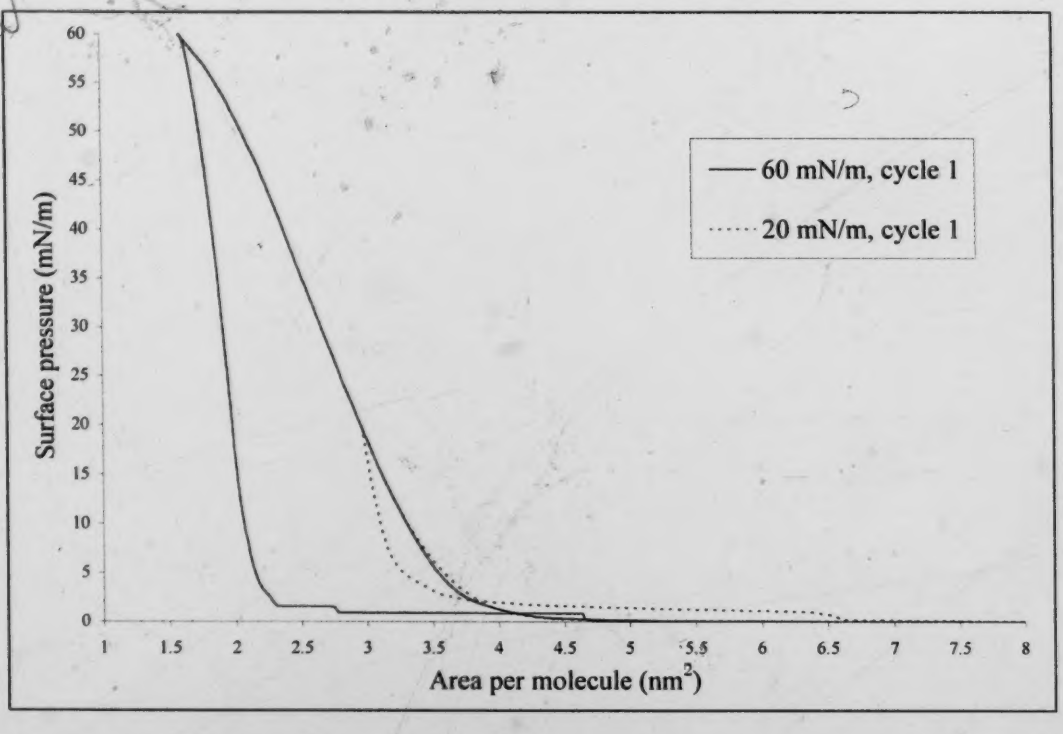

Figure 4.8 High molecular weight asphaltene hysteresis isotherm; comparison of compression to 20 mN/m and 60 mN/m.

It is clear that when the monolayer is compressed to a higher surface pressure, a much larger hysteresis is observed. It is highly likely that with compressions beyond the critical pressure, the surface is no longer a monolayer and the film has started to buckle and fold; brown streaks are visible on the surface of the water in the Langmuir trough.

Further evidence for the buckling of the monolayer will be discussed in Section 4.6.1 using atomic force microscope images of the film at different surface pressures.

4.3 Relaxation Isotherms

To determine the monolayer stability, the relaxation characteristics of the asphaltene monolayers were studied. The monolayers were compressed to a predetermined surface pressure and the barriers were stopped to maintain a constant surface area. Change the in surface pressure was monitored as a function of time. Figures 4.8a to 4.8c show the relaxation isotherms for the low molecular weight, high molecular weight and whole asphaltene compressed to various surface pressures. In order to compare the relaxation curves, the surface pressure is normalised by the compression terminal pressure.

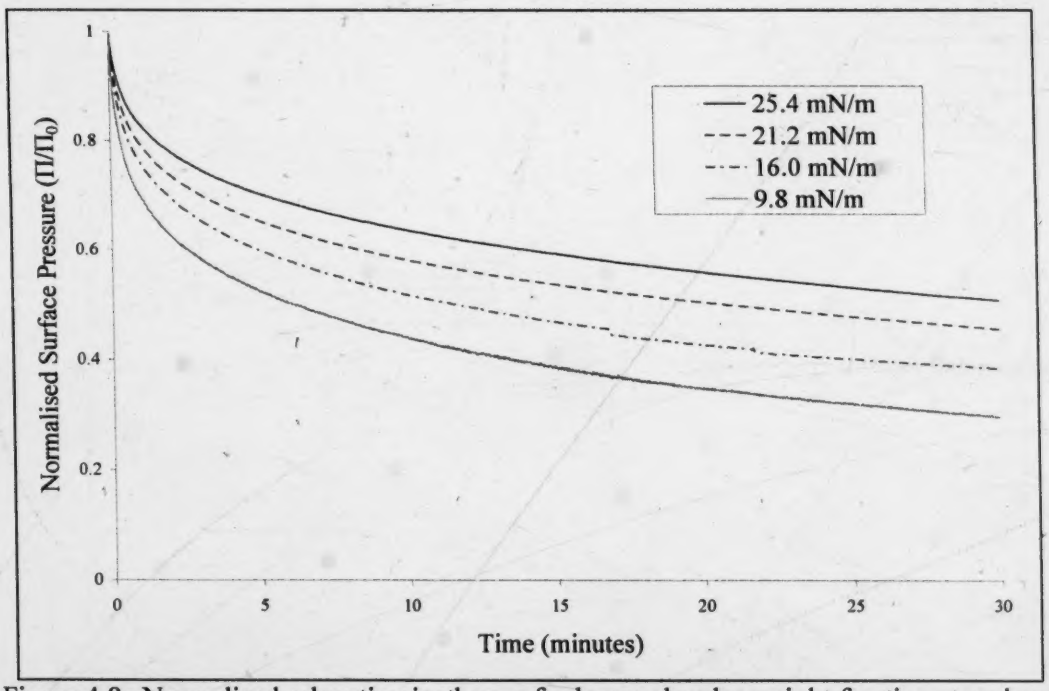

Figure 4.8a Normalised relaxation isotherms for low molecular weight fraction at various compression pressures.

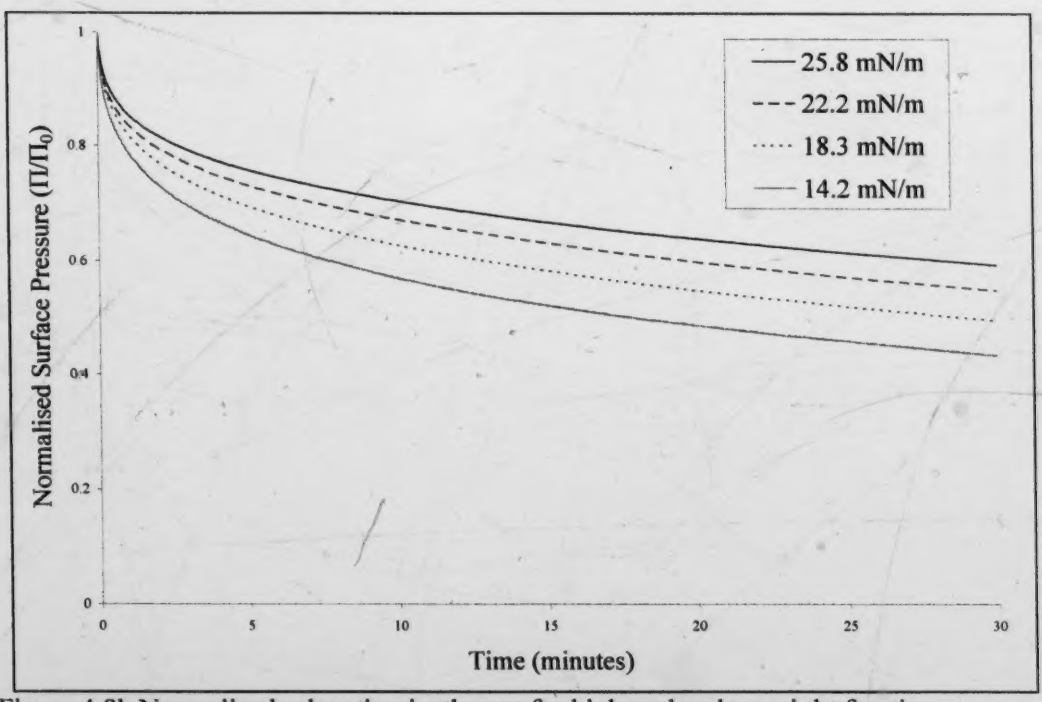

Figure 4.8b Normalised relaxation isotherms for high molecular weight fraction at various compression pressures.

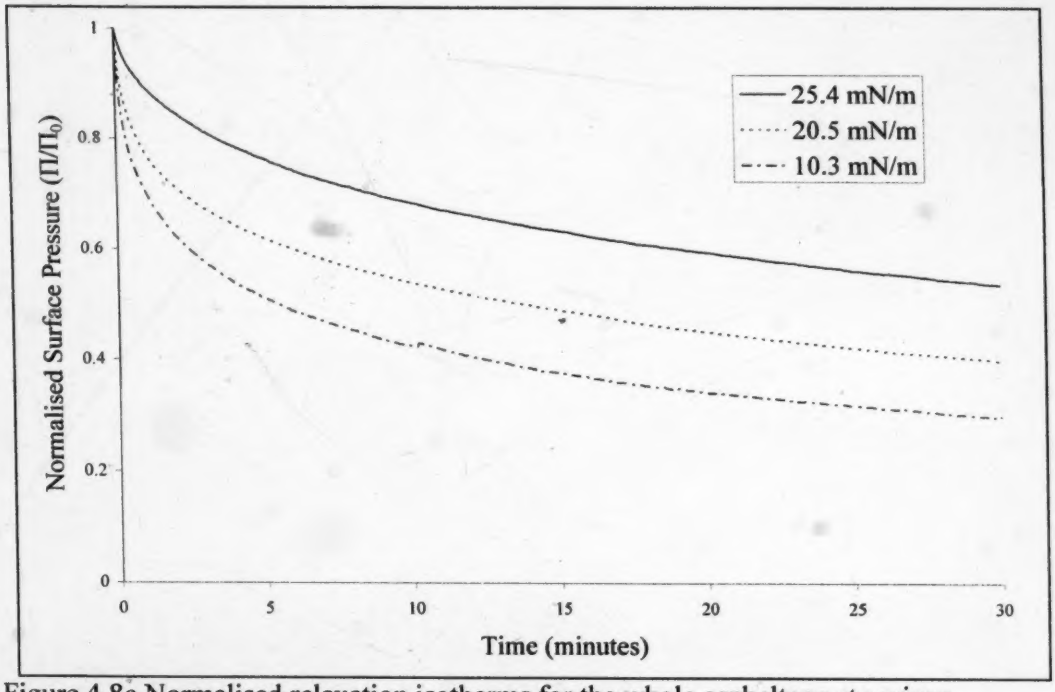

Figure 4.8c Normalised relaxation isotherms for the whole asphaltene at various compression pressures.

The asphaltene monolayers are not in a state of equilibrium during the compression cycle due to their structural complexity. After the initial compression has been stopped, the surface pressure decreases rapidly due to molecular reorientation and possible dissolution of soluble material into the subphase. At lower surface pressures, the rate of decay is more rapid. This trend is true for all three fractions of asphaltene. The higher freedom for the molecules to rearrange at lower surface pressures may account for the faster relaxation rates. At higher surface pressures, the molecules are more densely packed at the interface with some of the smaller molecules and more soluble material already being squeezed out, potentially leading to slower rates of reorientation and dissolution.

Figure 4.9 compares the relaxation rates of the three different fractions of asphaltene when they are compressed to the same surface pressure. The low molecular weight fraction clearly shows a faster rate of relaxation when compared to the higher molecular weight fraction. This is expected as the low molecular weight fraction contains, on average, molecules that are smaller in size, which would produce a higher rate of reordering. In addition, these molecules likely have a higher solubility in water, leading to an increased rate of dissolution in the subphase.

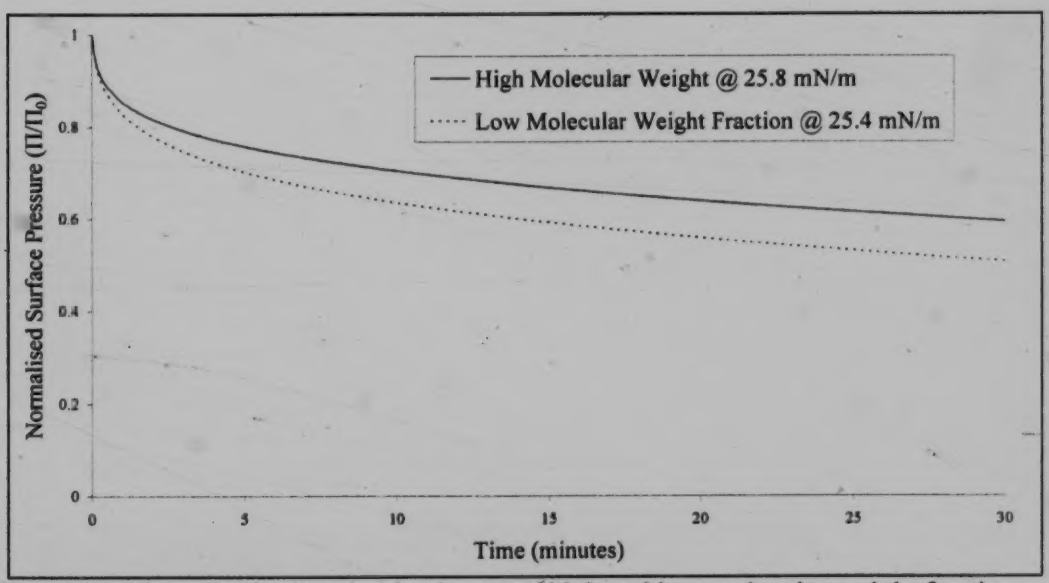

Figure 4.9 Normalised relaxation isotherms of high and low molecular weight fractions initially compressed to 25 mN/m.

4.4 Effect of pH on Π-A Isotherms

Pressure-area isotherms of the high molecular weight fraction were conducted at various pH values of the subphases. Figure 4.10 shows the isotherms obtained at three different pH values: 3.3, 5.8 and 11.2.

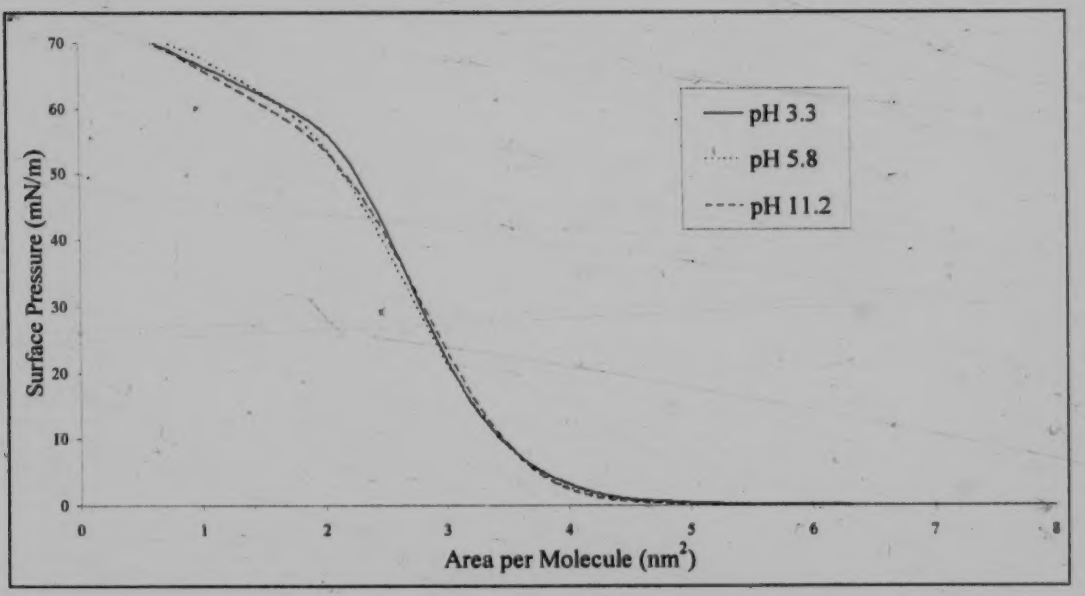

Figure 4.10 High molecular weight asphaltene fraction at different pH values in the aqueous subphase.

It is evident that the pH of the subphase does not affect the Π-A isotherms of asphaltene at the air-water interface. The isotherms shown in Figure 4.10 are essentially identical and within experimental error for the three different pH values. Monolayers of typical fatty acids such as stearic acid or arachidic acid are greatly affected by changes in pH due to variable ionisation of their polar headgroups with pH. However, in a monolayer of asphaltene, the packing of the polyaromatic rings and alkyl sidechains dominates the interactions over the ionised headgroups. As a result, the subphase pH value does not affect the shape of the Π-A isotherm.

4.5 Effect of Temperature on Π-A Isotherms

To determine the effects of temperature on the Π-A isotherms of asphaltene monolayers, isotherms for all three fractions were conducted at approximately 50°C.

Figures 4.11a to 4.11c show a comparison between the original isotherm at 20°C and that at 49°C for the high molecular weight, low molecular weight, and whole asphaltene, respectively.

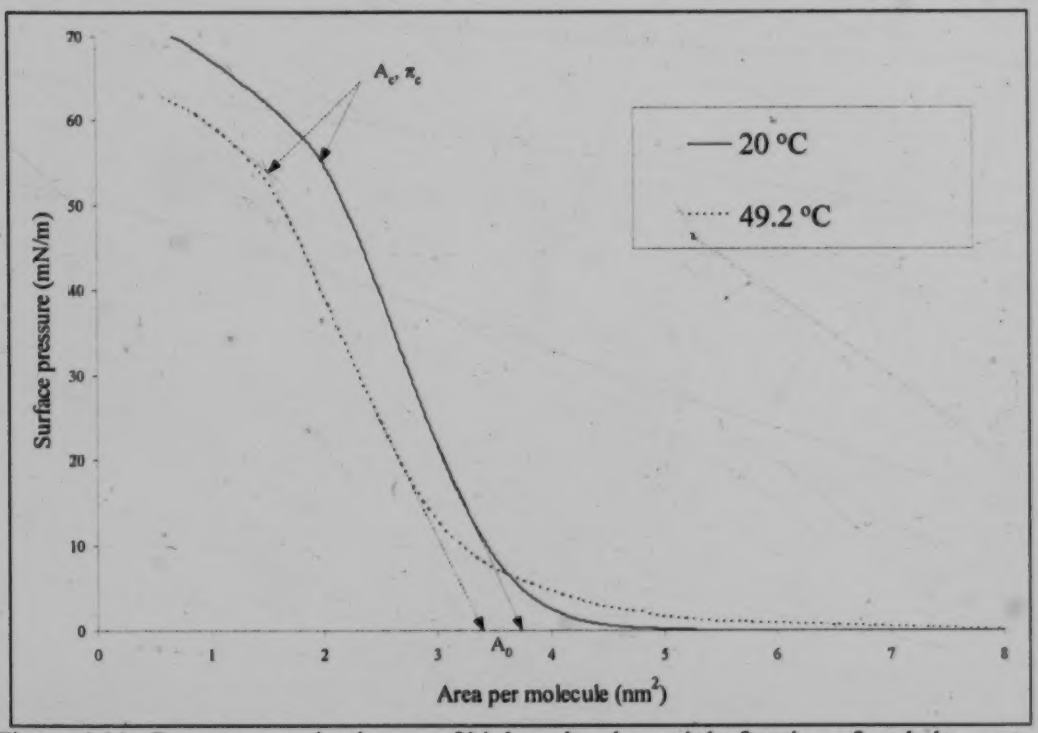

Figure 4.11a Pressure-area isotherms of high molecular weight fraction of asphaltene at 20 and 49.2°C.

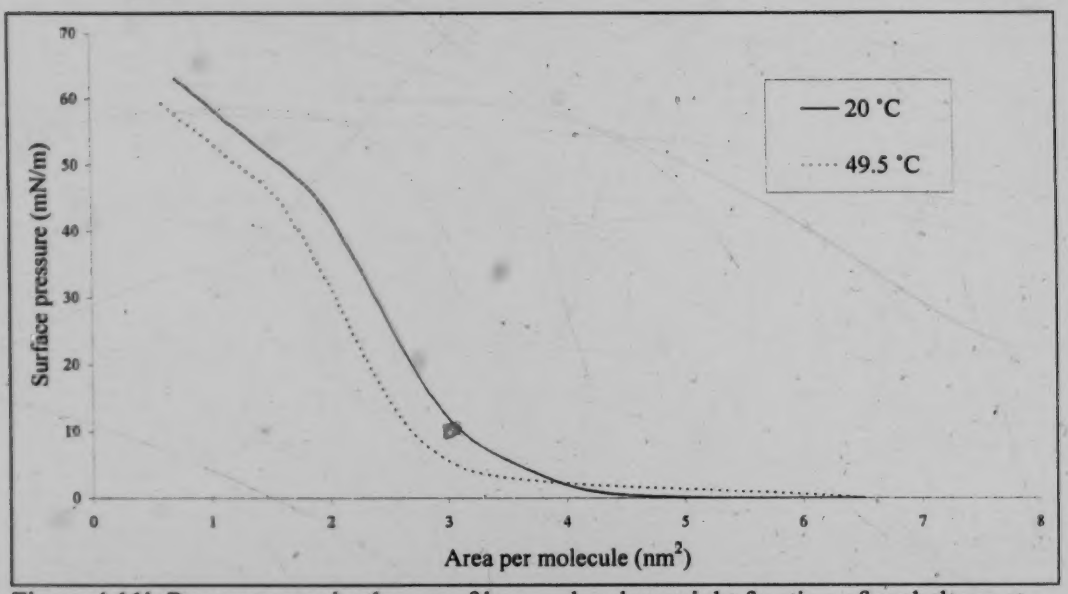

Figure 4.11b Pressure-area isotherms of low molecular weight fraction of asphaltene at 20 and 49.5°C.

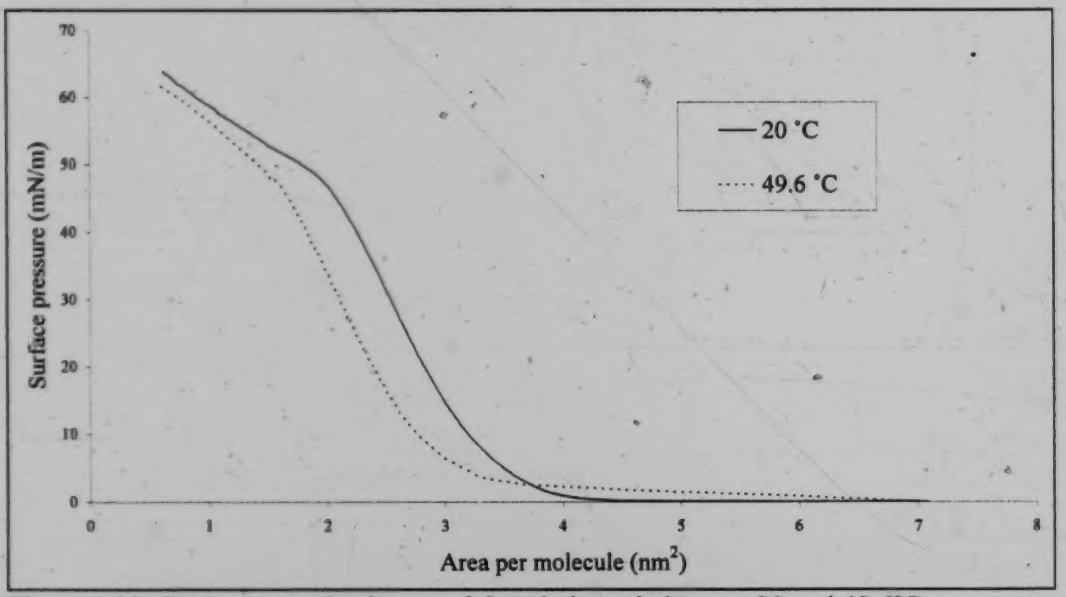

Figure 4.11c Pressure-area isotherms of the whole asphaltene at 20 and 49.6°C.

The general shape of the isotherm at 49°C is similar to the isotherm observed at 20°C. At the higher temperature, critical surface pressure, zero surface area, and critical area are all lower than those values at a lower temperature. This means the asphaltene

monolayer is more contracted and compressible at the higher temperature. Mohammed et al., 1993 reported that monolayers of asphaltenes were more contracted at temperatures of 40°C and 55°C than at 20°C. At the higher temperature condition, the liquid-expanded (LE) phase begins at a much larger surface area than at 20°C. This phenomenon is likely due to increased molecular activity of the asphaltene molecules on the surface at the higher temperature. As a result, the molecules begin to interact with each other at a larger mean molecular area. When comparing the three fractions of asphaltene at the higher temperature, the trends observed are similar to those found at 20°C, with zero surface area and critical surface pressure both increasing with mean molecular weight of the asphaltene samples (see Table 4.2).

Table 4.2 Extrapolated Critical Area, Critical Surface Pressure and Zero Surface Pressure of Asphaltene Monolayers at Air-Water Interface at 49°C

Sample Name	A_c (nm^2/molecule)	π_c (mN/m)	A_0 (nm^2/molecule)
Whole Asphaltene	1.67	46.19	3.09
High Molecular Weight	1.50	55.42	3.47
Low Molecular Weight	1.58	45.69	2.98

4.6 Deposition of Langmuir-Blodgett (LB) Films

A single layer of LB film was deposited on various hydrophilic substrates (oxidized silicon wafer, mica, microscope glass slide) using the LB technique. The transfer ratio is defined as:

$$TR = \frac{Decrease\ in\ area\ of\ Langmuir\ monolayer}{Area\ of\ the\ transferred\ film\ on\ solid\ substrate} \qquad [3.1]$$

This ratio is useful for determining the amount of material that has been transferred to the substrate during deposition. The transfer ratio is easily calculated by comparing the surface area of the solid substrate to the corresponding decrease in area of the Langmuir monolayer at a constant surface pressure. An ideal transfer ratio (TR) has a value of 1 which indicates that a unit area of the Langmuir monolayer has been transferred to the same corresponding area on the solid substrate. A TR of 0 indicates that no material has been transferred to the substrate. Most TR values are between zero and one indicating a partial transfer of material. In this study, transfer ratio was found to be independent of the substrate material used for deposition. Table 4.3 shows typical transfer ratios for single layer of LB films transferred to mica or silicon wafers for all the three fractions of asphaltene.

Table 4.3 Transfer Ratio of Various Samples of Asphaltene at Different Surface Pressures at 20°C

Sample Name	0 mN/m	5 mN/m	30 mN/m
Whole Asphaltene		1.079	1.080
High Molecular Weight	1.056	1.066	0.814
Low Molecular Weight	0.493	0.934	1.018

It was found that a single layer LB film could not be made on a hydrophobic substrate during a downstroke. A TR of 0 was observed. The inability to transfer a monolayer under these conditions is probably due to the complex structure of the asphaltene molecules. Thus, the interactions between the alkyl chains of the asphaltene molecules and the hydrophobic substrate are not sufficiently strong to allow the asphaltene molecules to fold over the substrate (Gaines, 1966). At very high surface pressures (π > 60 mN/m), the trough area became too small for LB deposition to be

conducted. During the upstroke of the substrate, the barriers would approach each other until they were too close to the Wilhelmy plate and the substrate for proper deposition to occur. Under these conditions, the Langmuir-Schaefer (LS) method was used to successfully deposit the film on a hydrophobic substrate. LS depositions are possible at high surface pressures because the alkyl chains are densely packed and the interactions between the hydrocarbon tails of the asphaltene molecules and the hydrophobic substrate are strong.

4.6.1 Atomic Force Microscope (AFM) Images

To study the topography of the LB films, AFM images were produced for monolayers deposited at various surface pressures for each of the three fractions of asphaltene. Figure 4.12 shows an AFM image of a bare mica slide indicating the smooth surface on which the monolayers are deposited.

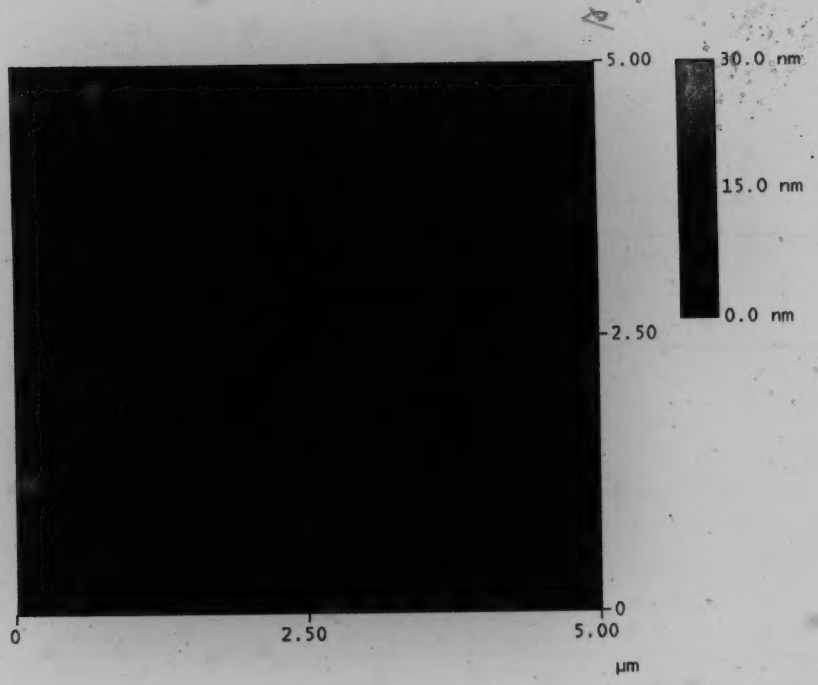

Figure 4.12 Freshly cleaned mica slide with no monolayer on surface.

At a given surface pressure, similar structures were observed in each of the various fractions of asphaltene. A comparison of the three fractions at 30mN/m is shown in Figures 4.13a to 4.13c. Arrows denote film compression direction.

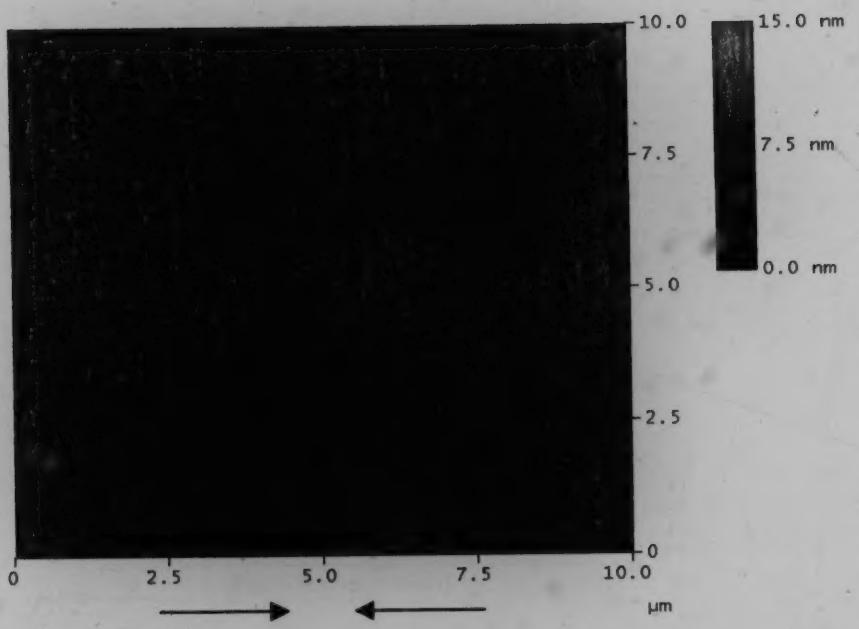

Figure 4.13a AFM image of low molecular weight fraction on mica at 30 mN/m, TR=1.018.

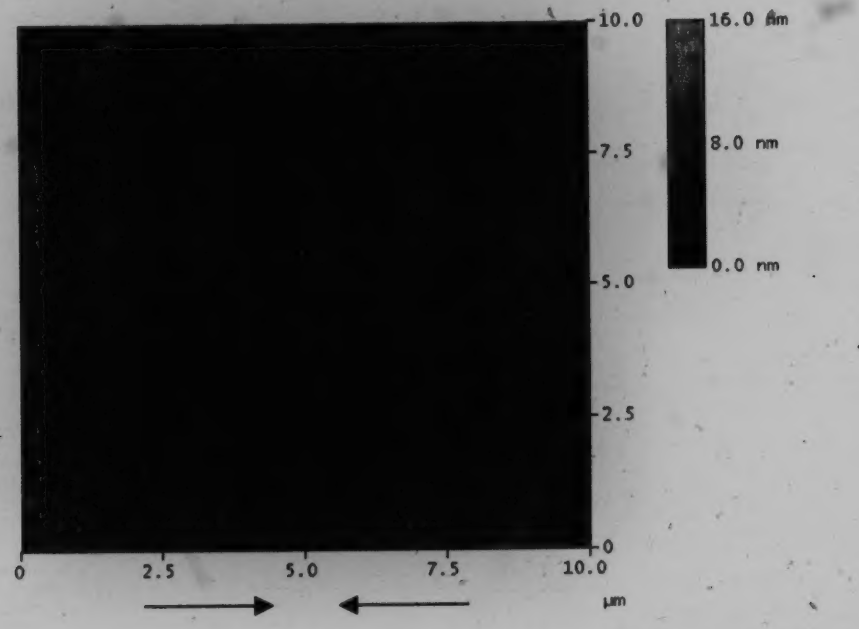

Figure 4.13b AFM image of high molecular weight fraction on mica at 30 mN/m, TR=0.814.

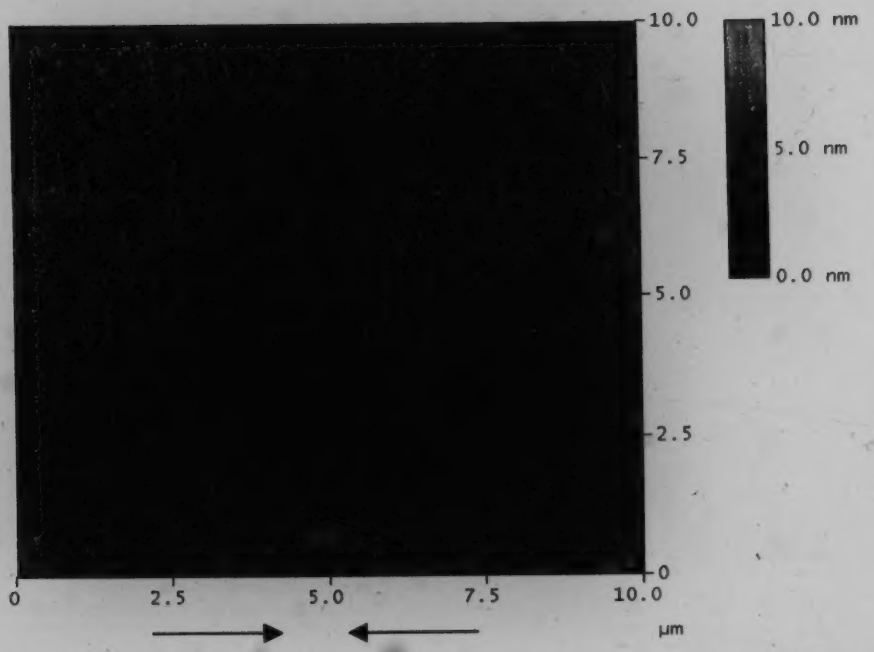

Figure 4.13c AFM image of whole asphaltene on mica at 30 mN/m, TR=0.487.

Figures 4.14a to 4.14d show AFM images of the low molecular weight fraction obtained at 0, 5, 30 and 65 mN/m. Figures 4.15a to 4.15d show the high molecular weight fraction obtained at 0, 5, 30 and 70 mN/m.

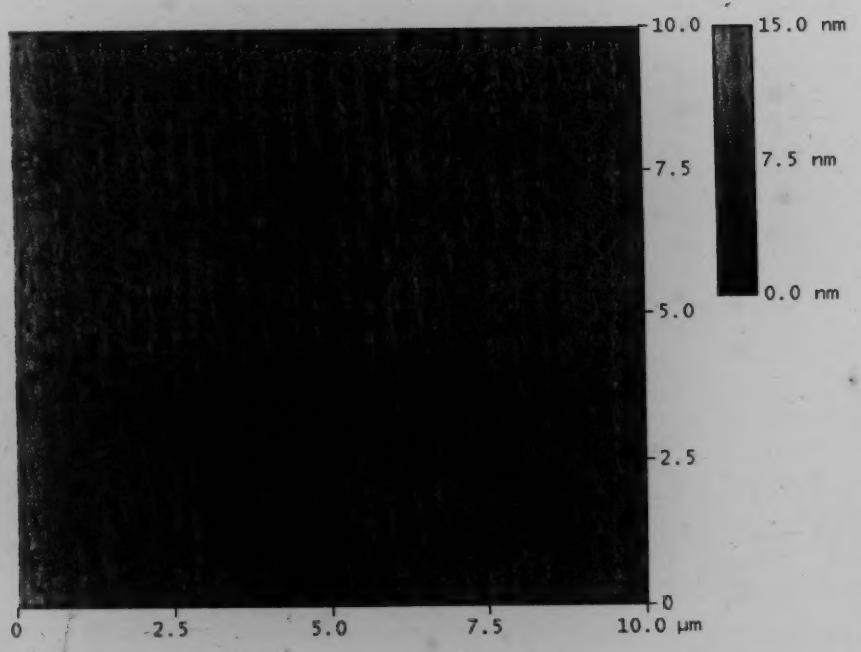

Figure 4.14a AFM image of low molecular weight fraction on mica at 0 mN/m, TR=0.493.

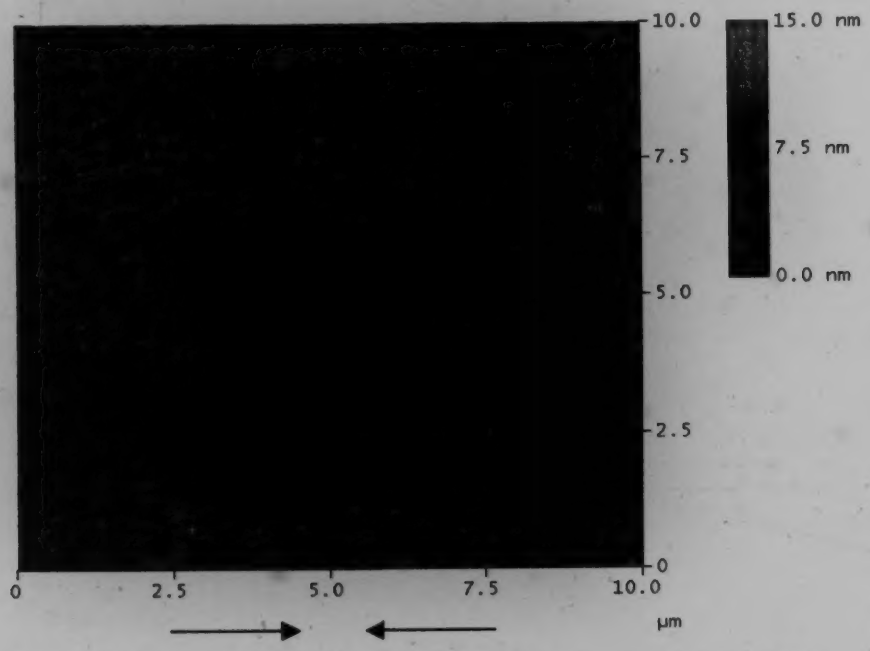

Figure 4.14b AFM image of low molecular weight fraction on mica at 5 mN/m, TR=0.934.

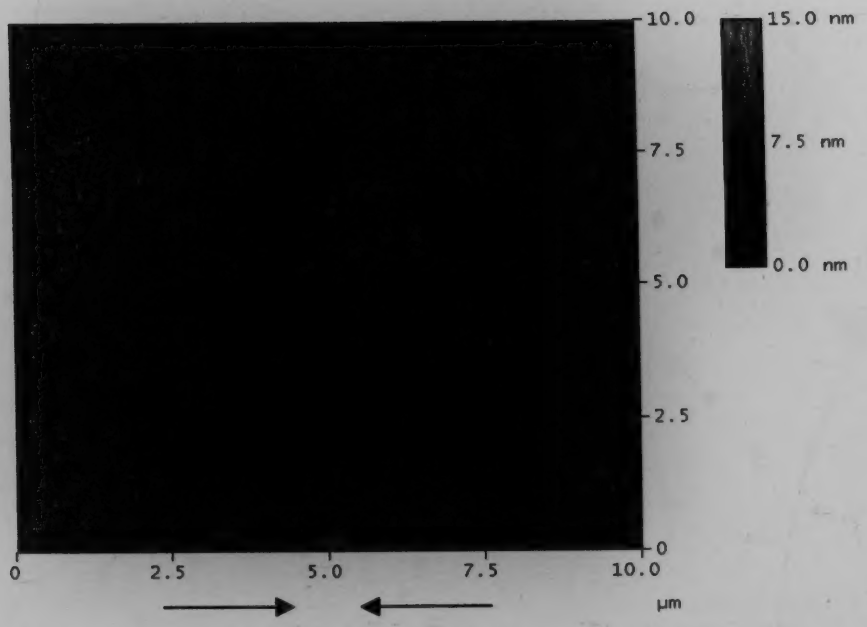

Figure 4.14c AFM image of low molecular weight fraction on mica at 30 mN/m, TR=1.018.

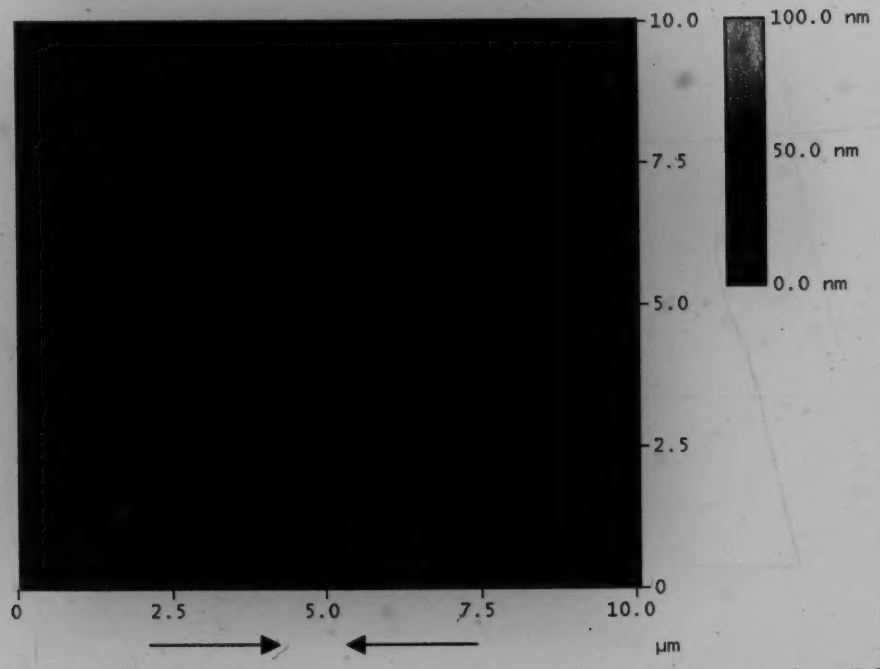

Figure 4.14d AFM image of low molecular weight asphaltene fraction on glass (LS deposition) at 65 mN/m.

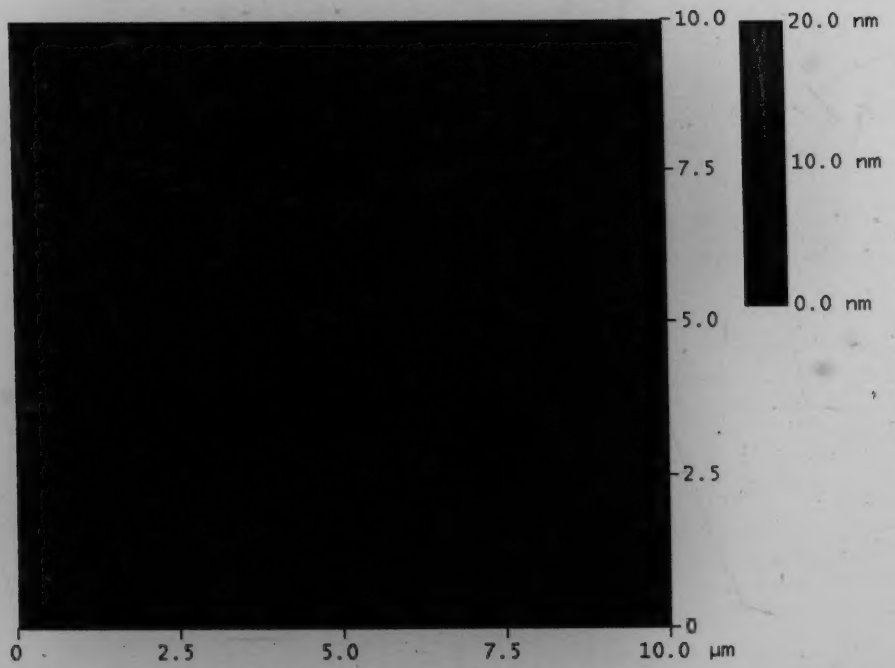

Figure 4.15a AFM image of high molecular weight fraction on mica at 0 mN/m, TR=1.056.

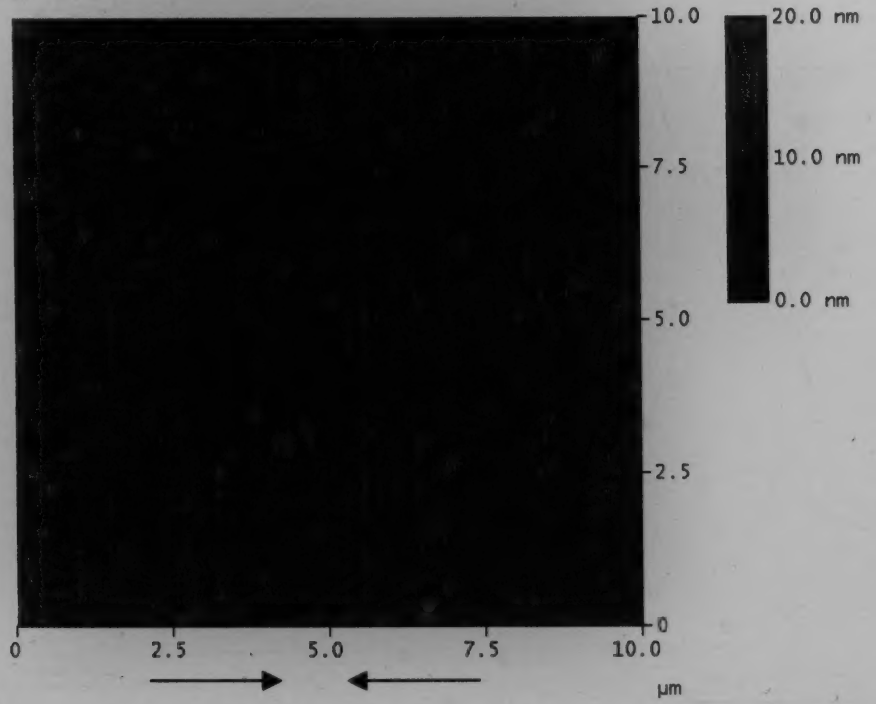

Figure 4.15b AFM image of high molecular weight fraction on mica at 5 mN/m, TR=1.066.

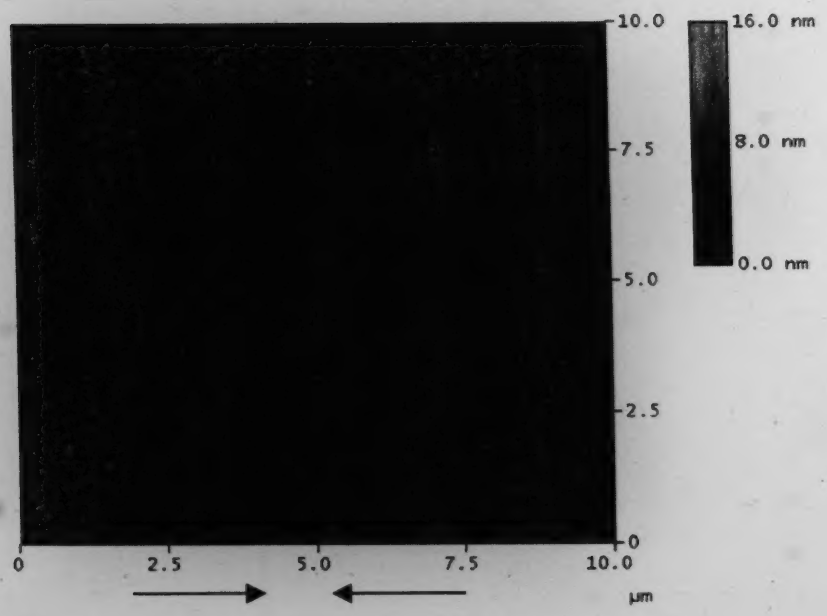

Figure 4.15c AFM image of high molecular weight fraction on mica at 30 mN/m, TR=0.814.

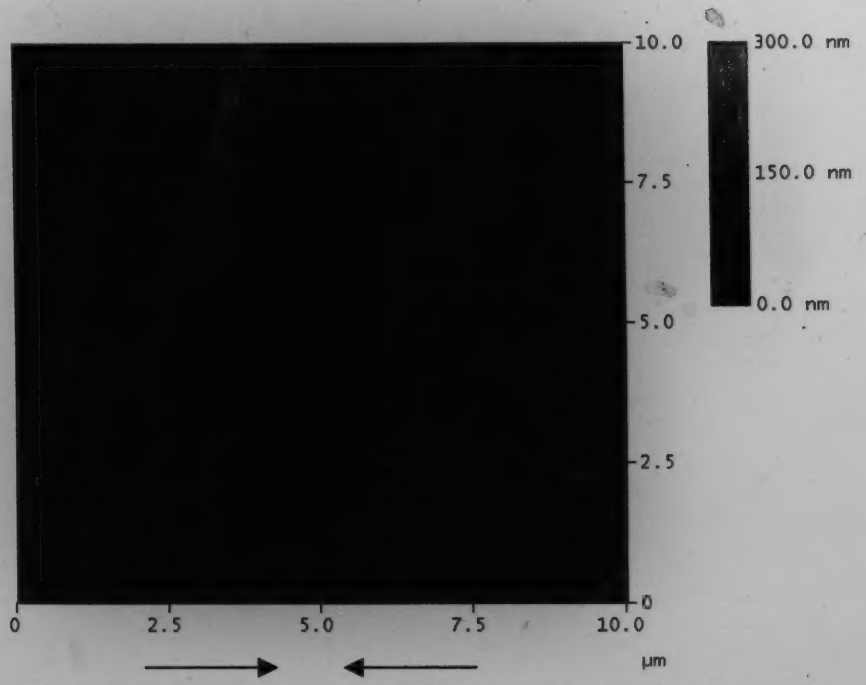

Figure 4.15d AFM image of high molecular weight asphaltene fraction on mica (LS deposition) at 70 mN/m.

Figures 4.14a and 4.15a show that at 0 mN/m discotic aggregates and discs that connect to long rod structures are clearly visible. At this low surface pressure, the structures are loosely packed leaving open areas on the mica surface. At 5 mN/m (Figures 4.14b and 4.15b), the structures have started to deform as they pack together. However, 5 mN/m is still a relatively low surface pressure and there are still many open areas visible on the surface of the mica.

Figures 4.15c and 4.15c show the monolayer compressed to a moderate surface pressure of 30 mN/m. At this surface pressure, the asphaltenes are densely packed on the substrate. The size of the aggregates has also decreased significantly due to the compressible nature of aggregates. Disk shaped structures that connect to long rods are still visible at this pressure.

At surface pressures above the critical pressure, the asphaltene monolayer begins to fold. Figures 4.14d and 4.15d show AFM images of the LB deposited layers using the Langmuir-Schaefer method at a surface pressure of 65 mN/m and 70 mN/m respectively. Folding is clearly visible in the direction normal to the motion of the barriers. The crumpling of the monolayer occurs at a much larger vertical scale (100 nm) than the structures that occur at the lower surface pressures, which have heights in the range of 15 nm. The void space visible in the lower left section of the AFM image is likely due to the non-uniform buckling of the monolayer. At this surface pressure, when conducting dipping experiments, brown streaking is visible on the surface of the water, clearly indicating that the material at the surface is no longer a monolayer.

4.6.2 Contact Angle Measurements

Static contact angles (θ_0) of water on deposited LB films on silicon wafers were measured for the three samples of asphaltenes. Figure 4.16 shows a digital photograph of a water droplet on a solid substrate. The arrows indicate the static contact angle measured.

Figure 4.16 Water droplet on a silicon wafer coated with whole asphaltene at 30 mN/m, TR=0.478.

For clarity Figure 4.17a shows only the contact angles of the deposited films at different surface pressures using high and low molecular weight fractions. For all surface pressures, the contact angle of the whole asphaltene was between the high and low fractions. Figure 4.17b shows a contact angle plot of the whole asphaltene at various surface pressures.

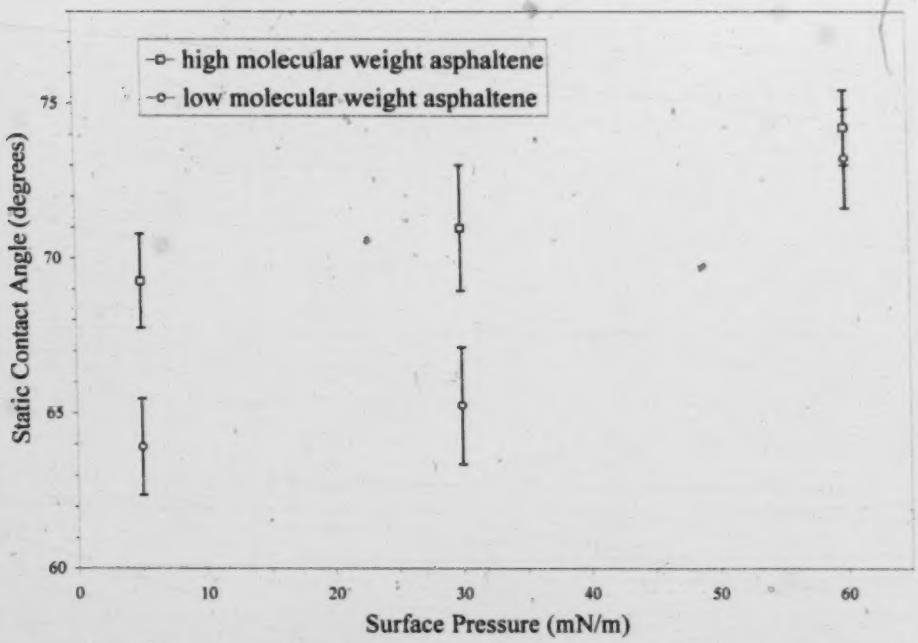

Figure 4.17a Static contact angle of a water droplet on high and low molecular weight fraction LB films at different surface pressures.

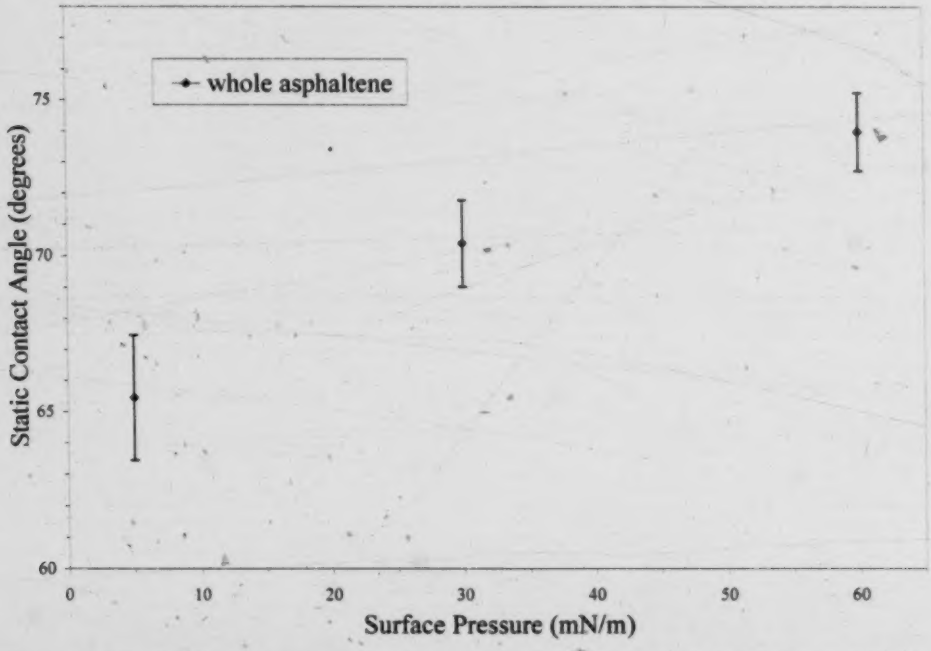

Figure 4.17b Static contact angle of a water droplet on whole asphaltene LB films at different surface pressures.

For all asphaltene fractions, the contact angle slightly increases with increased surface pressure. This effect is caused by the close packing of the hydrocarbon chains when surface pressure increases, making the LB film more hydrophobic. There is a small but statistically significant difference between the asphaltene fractions. The increase in contact angle with increasing mean molecular weight is likely due to the increase in backbone chain length. With increasing surface pressure, all three fractions approach the same contact angle. At 60 mN/m the fractions all have a contact angle of approximately 74 degrees. At this high surface pressure, the monolayers are tightly compressed and differences in backbone length do not affect the molecular packing.

4.7 Summary

The behaviour of asphaltenes at an air-water interface has been studied on the Langmuir trough using a variety of analytical techniques. At the air-water interface, asphaltenes are shown to form rigid monolayers that undergo permanent deformation during compression. The relaxation of a compressed monolayer is due to both molecular reorientation and to the dissolution of asphaltenes into the subphase. The pH does not affect the pressure-area isotherm of asphaltene monolayers as the packing of the polyaromatic rings and alkyl side chains dominates over the ionised headgroups. Asphaltene monolayers are more contracted and compressed at higher temperatures. LB deposition of asphaltenes at the air-water interface show disk shaped structures in all three fractions of asphaltenes at lower surface pressures, and a heavily folded layer at surface pressures above the critical surface pressure. Contact angle measurements indicate that at lower surface pressures, the molecular weight of the asphaltene has an

effect on the contact angle, with lower molecular weight fractions yielding a lower static contact angle. At high surface pressures however, the monolayers are tightly compressed and all three fractions have a contact angle of approximately 74 degrees.

5 n-Heptane-Water Interface

5.1 Π-A Isotherms at n-Heptane-Water Interface

Tests of the oil-water interface trough were conducted to ensure that it was capable of reproducing experimental results that were previously published. A Π-A isotherm of dipalmitoyl phosphatidylcholine (DPPC) was produced at 20°C at a water-hexadecane interface and is shown in Figure 5.1a. The isotherm was reproducible and is comparable to experiments by Thoma and Möhwald (1995) (see Figure 5.1b), indicating that the interfacial trough is operating correctly. Another Π-A isotherm was produced using distearoyl phosphatidylcholine (DSPC) at a heptane-water interface with 0.01M NaCl dissolved in the aqueous phase at 20°C. This isotherm is comparable to experiments by Yue et al. (1976) (see Figure 5.2b), and is shown in Figure 5.2a.

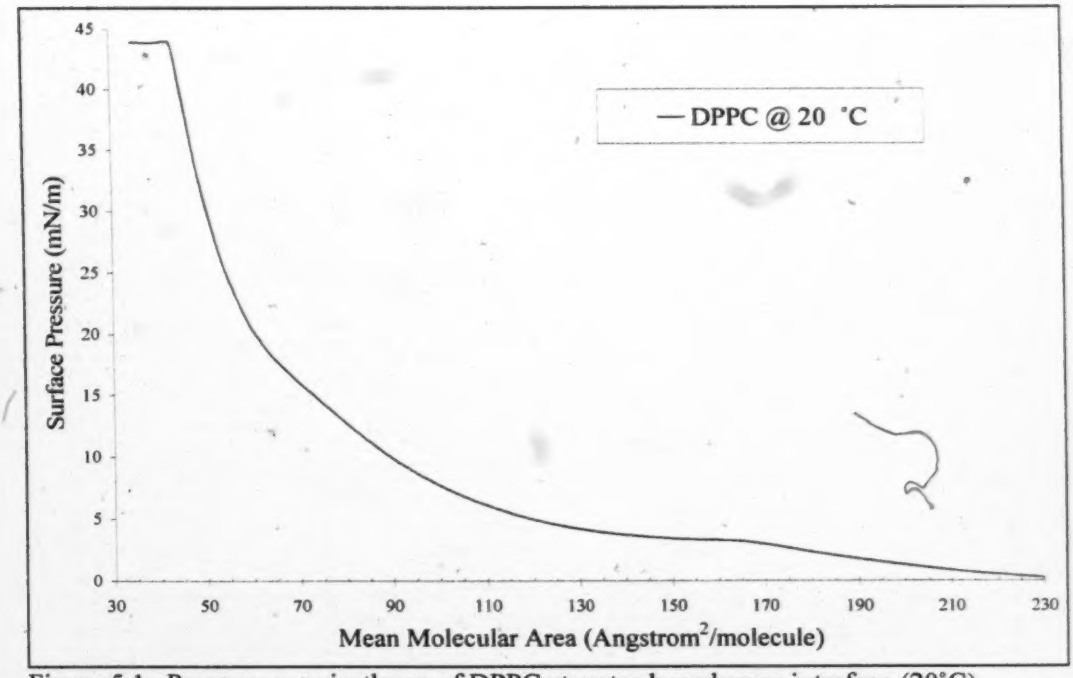

Figure 5.1a Pressure-area isotherm of DPPC at water-hexadecane interface (20°C).

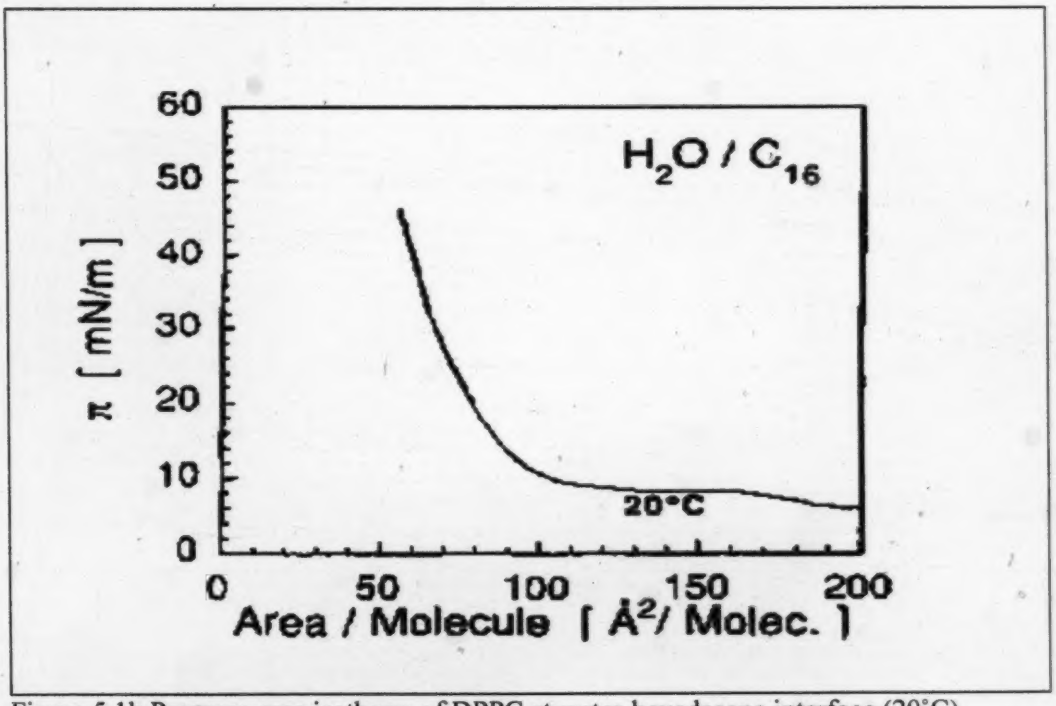

Figure 5.1b Pressure-area isotherm of DPPC at water-hexadecane interface (20°C) (modified from Thoma and Möhwald, 1995).

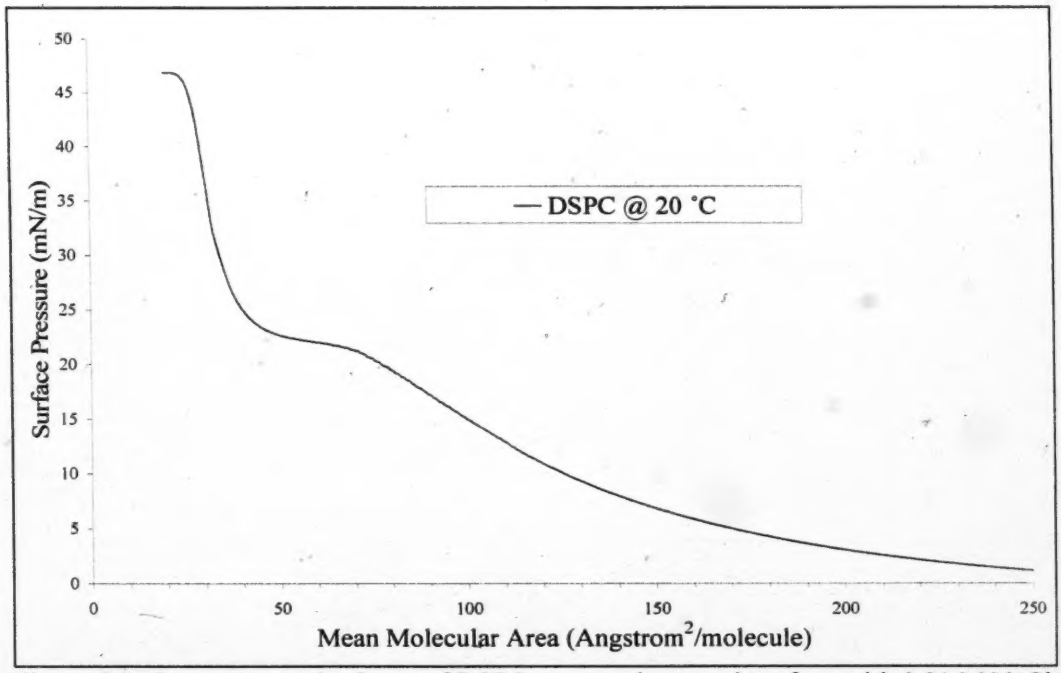

Figure 5.2a Pressure-area isotherm of DSPC at water-heptane interface with 0.01 M NaCl in aqueous phase (20°C).

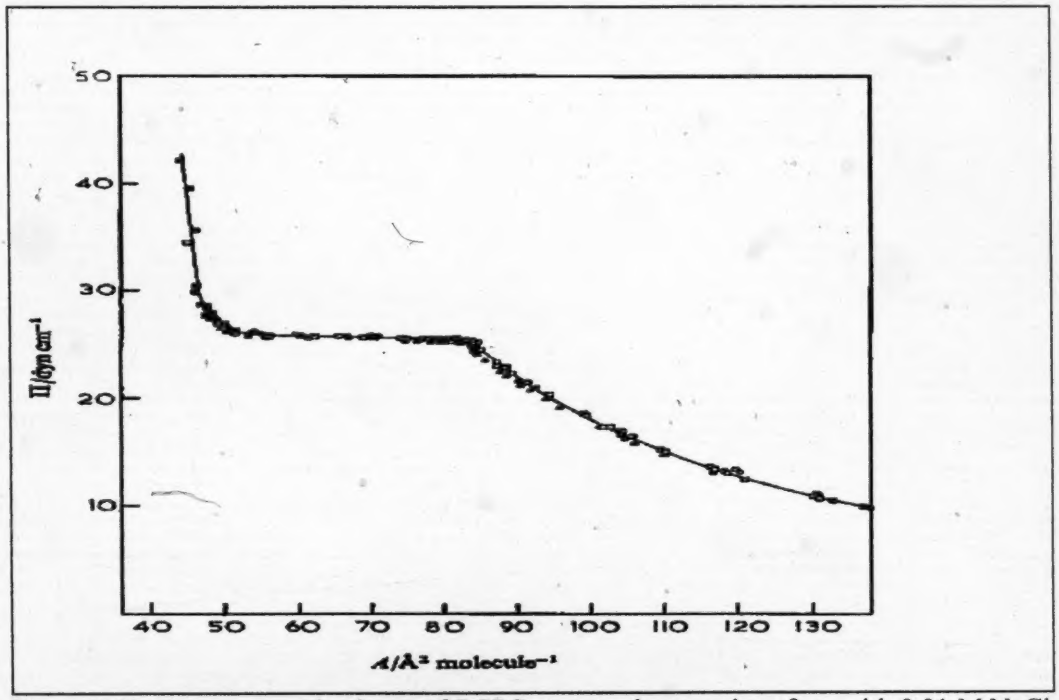

Figure 5.2b Pressure-area isotherm of DSPC at water-heptane interface with 0.01 M NaCl in aqueous phase (20°C) (modified from Yue et al., 1976).

To characterise the behaviour of asphaltenes at an oil-water interface, a series of experiments were conducted at an n-heptane-water interface. Pressure-area isotherms were measured for the low molecular weight, high molecular weight, and whole asphaltene and are shown in Figure 5.3

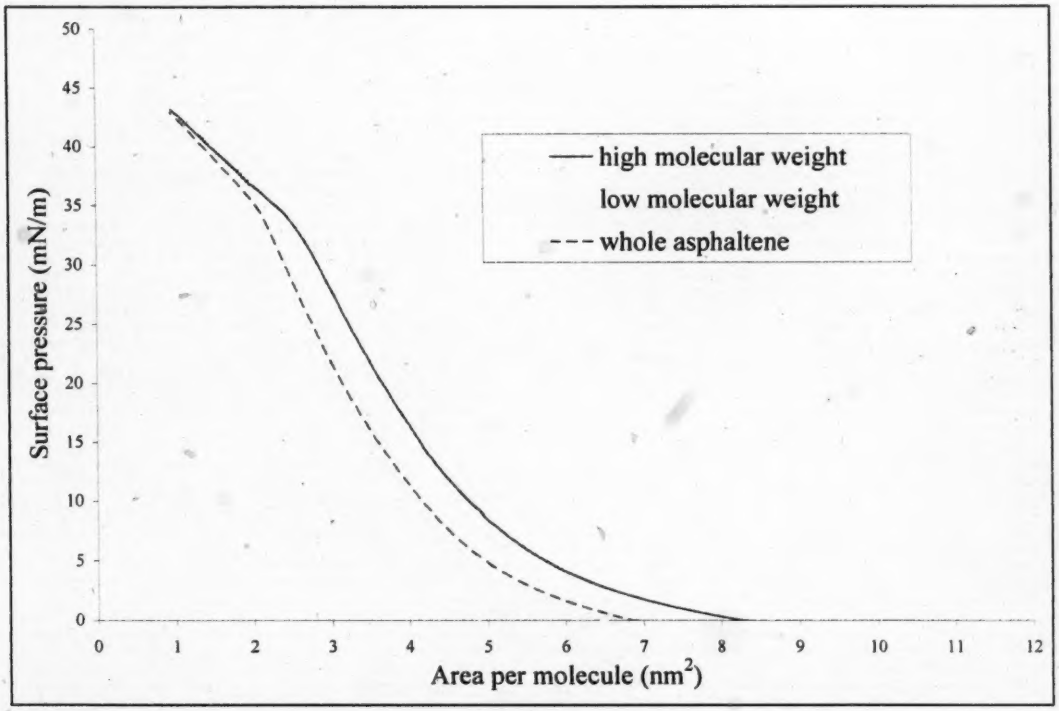

Figure 5.3 Pressure-area isotherms of three asphaltene samples at an n-heptane-water interface at 20°C.

The isotherms of the asphaltenes at the heptane-water interface follow the same trends as observed at the air-water interface, with the high molecular fraction occupying the largest molecular area and the low molecular fraction occupying the smallest. This relationship is anticipated due to the differences in mean molecular weight between the fractions. As at the air-water interface, there are no clearly defined phase transitions visible, due to the heterogeneous nature of the asphaltene samples. Again, at pressures

above the critical surface pressure, there is no abrupt collapse of the monolayer, instead there is a gradual folding and buckling of the surface material. At the heptane-water interface, the maximum attainable surface pressure is much lower than that at the air-water interface; the interfacial tension of heptane and water is 50.2 mN/m at 20°C, while the surface tension of water is 72.8 mN/m at 20° C (Hiemenz and Rajagopalan, 1997). Table 5.1 shows the extrapolated critical area (A_c), critical surface pressure (π_c), and zero area (A_0) for all three fractions of asphaltenes.

Table 5.1 Extrapolated Critical Area, Critical Surface Pressure and Zero Surface Pressure of Asphaltene Monolayers at n-Heptane-Water Interface

Sample Name	A_c (nm^2/molecule)	π_c (mN/m)	A_0 (nm^2/molecule)
Whole Asphaltene	2.21	34.50	4.60
High Molecular Weight	2.29	35.00	5.20
Low Molecular Weight	2.21	33.40	4.45

The critical pressure and zero area are observed to increase with increasing molecular weight of the asphaltene fraction. This is the same trend observed at the air-water interface. At the heptane-water interface, the extrapolated zero area values of the asphaltene samples are greater than those observed at the air-water interface (~4.5 to 5 nm^2 compared with ~3.5 nm^2). This indicates that the asphaltene monolayer is more expanded at the heptane-water interface as compared to the air-water interface. The mechanism causing this expansion is unclear, but is likely due to a stabilising effect of the organic chains in the presence of heptane.

5.2 *Hysteresis Effects at n-Heptane-Water Interface*

In order to determine the reversibility of the isotherms, the monolayers were compressed to a particular surface pressure and then expanded back to 0 mM/m for three complete cycles of compression and expansion. Figure 5.4a shows the compression-expansion isotherms for a monolayer of high molecular weight asphaltene compressed three times to 20 mN/m and expanded back to 0 mN/m. For clarity, only the first and second cycles are shown. Curves for the low molecular weight fraction and whole asphaltene are shown in Figures 5.4b and 5.4c. The whole asphaltene and low molecular weight fraction behaved in a manner similar to the high molecular weight fraction.

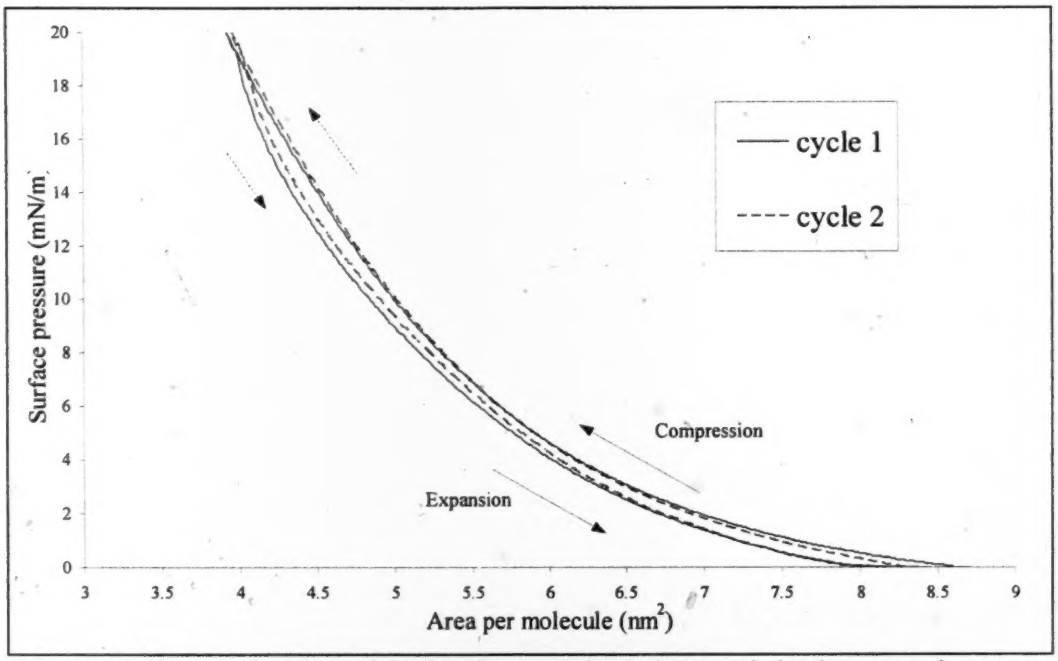

Figure 5.4a High molecular weight fraction asphaltene, hysteresis isotherm at n-heptane-water interface (20°C). First and second compression-expansion cycles are shown.

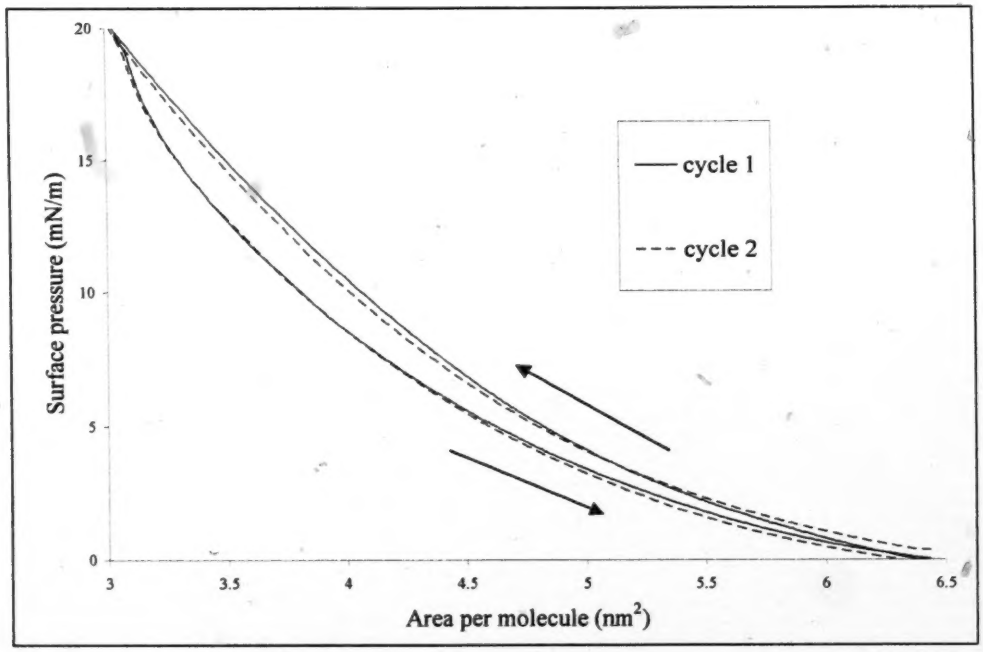

Figure 5.4b Low molecular weight fraction asphaltene, hysteresis isotherm at n-heptane-water interface. First and second compression-expansion cycles are shown.

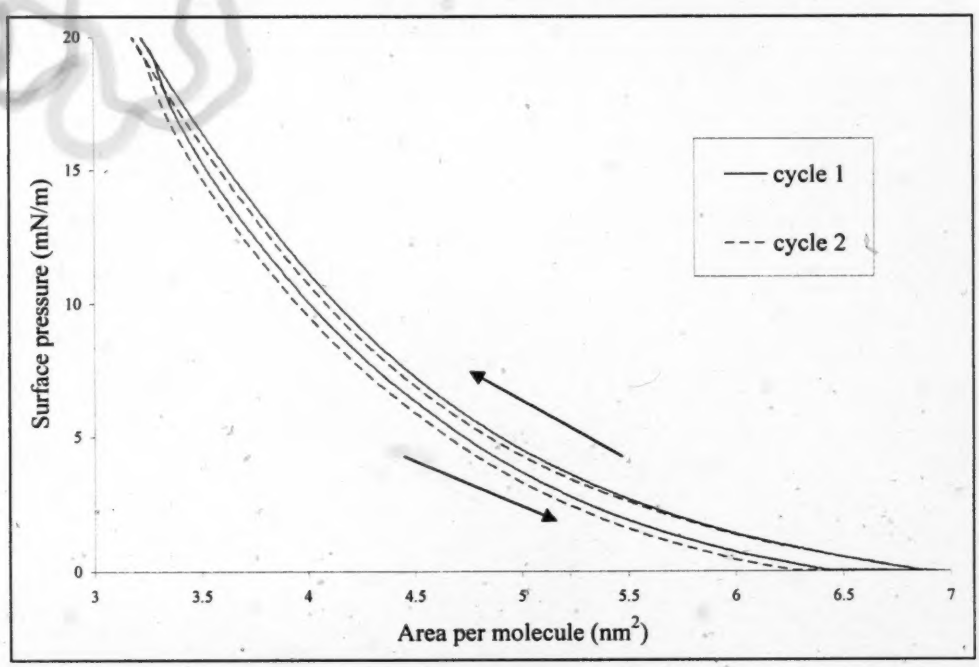

Figure 5.4c Whole asphaltene, hysteresis isotherm at n-heptane-water interface (20°C). First and second compression-expansion cycles are shown.

At the heptane-water interface, the expansion curve did not deviate significantly from its preceding compression isotherm, indicating minimal hysteresis. The slight differences in the compression and expansion curves are probably caused by differences in molecular orientation during compression or expansion. During subsequent compression cycles, there is little, if any difference between the isotherms, indicating that the compression-expansion cycles are reversible and there is no permanent deformation of the monolayer. Minor differences between given cycles are within experimental error. Even after compressing and expanding the monolayer three times, there is no change in the shape of the compression and expansion curves. This reversible behaviour at the n-heptane-water interface is different from the behaviour observed at the air-water interface, where irreversible changes in the monolayer occurred after one compression. During compression at an air-water interface, material is "squeezed out" of the monolayer as the hydrophobic chains of asphaltenes do not have an affinity to water. However, at a heptane-water interface at the same surface pressure, material is not "squeezed out", likely due to the affinity the hydrophobic chains of asphaltene have for the non-polar heptane phase. At an oil-water interface, both the hydrophilic head groups and hydrophobic organic chains can reside in a phase in which they have an affinity. This system is inherently more stable for amphiphilic molecules than for a single liquid phase system such as air and water.

Figure 5.5a shows a compression-expansion isotherm for the high molecular weight fraction, where the monolayer was compressed to 37 mN/m. Cycles 1 and 2 are shown. Compressing the monolayer to this surface pressure exceeds the critical pressure of the high molecular asphaltene which is 35 mN/m. In compression-expansion cycles to

20 mN/m, the process is reversible as shown in Figures 5.4a to 5.4c. However, at surface pressures above the critical pressure, the process is not reversible; the monolayer has been compressed to the point of collapse. In Figure 5.5a, the second compression curve does not follow the path of the first compression curve; it is shifted to the left, indicating that a permanent change has occurred at the interface. It is likely that at surface pressures above the critical pressure, some of the asphaltenes are squeezed out of the interface and the asphaltene at the interface is permanently altered by folding and buckling. Evidence for folding and buckling is discussed in section 5.4. Similar trends are observed with the low molecular weight fraction and the whole asphaltene when the surfaces are compressed beyond their critical pressures; see Figures 5.5b & 5.5c.

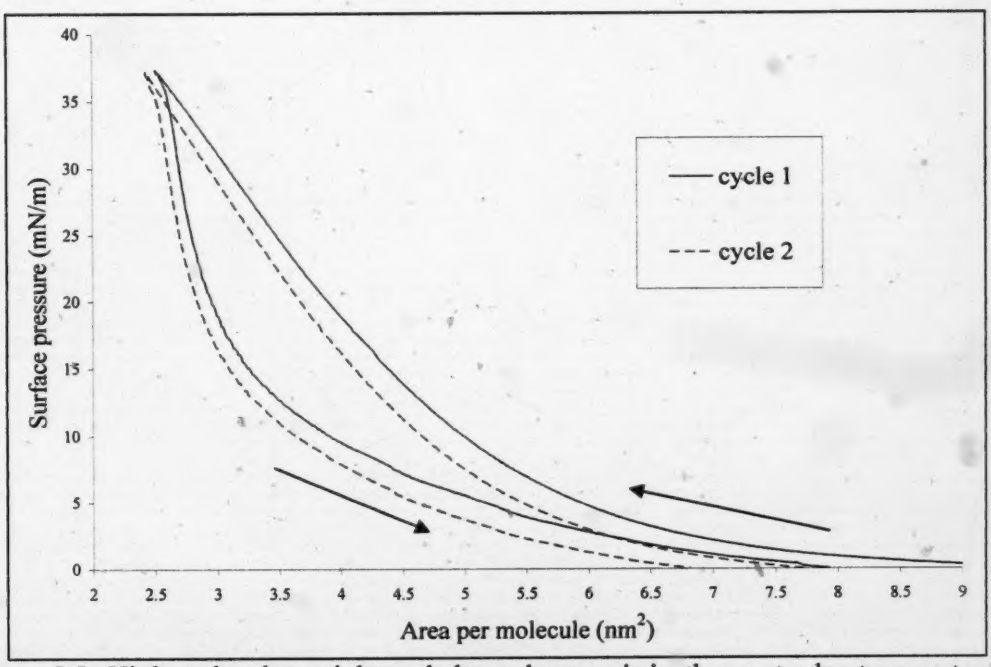

Figure 5.5a High molecular weight asphaltene, hysteresis isotherm at n-heptane-water interface (20°C). First and second cycles are shown.

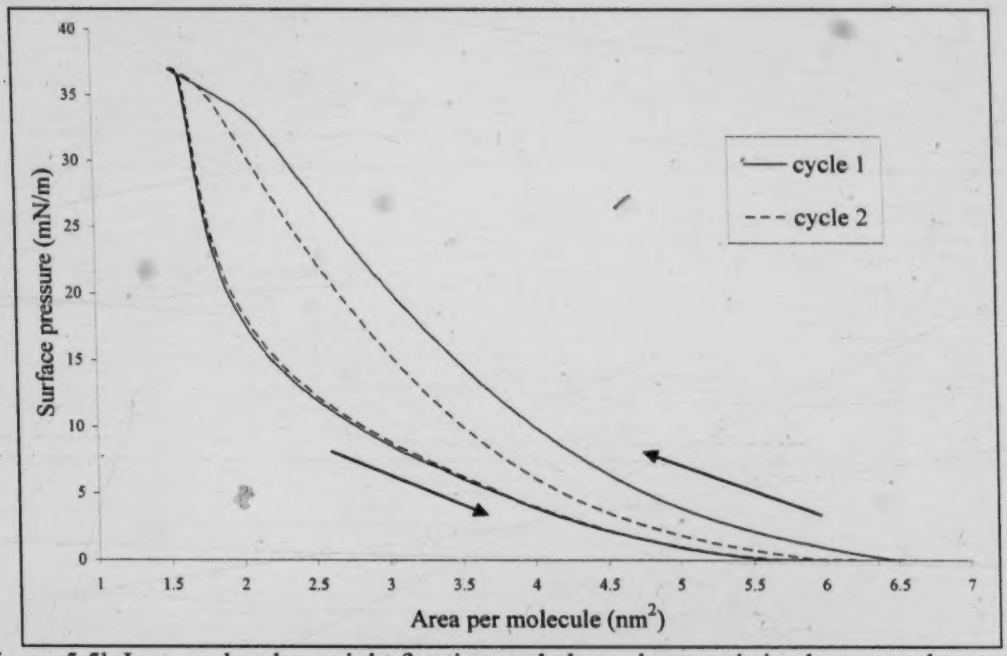

Figure 5.5b Low molecular weight fraction asphaltene, hysteresis isotherm at n-heptane-water interface. First and second compression-expansion cycles are shown.

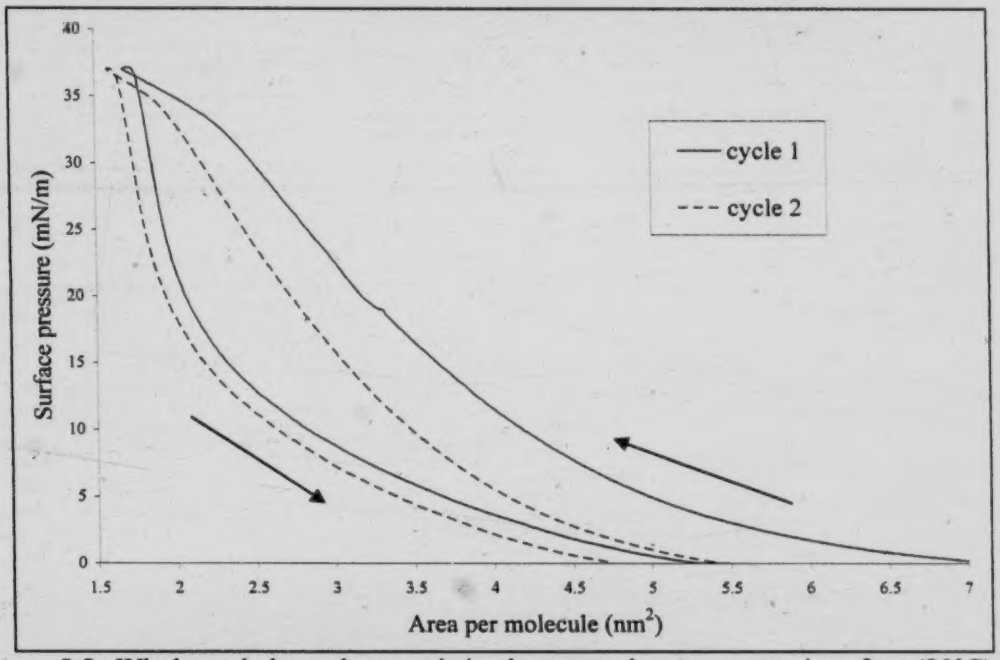

Figure 5.5c Whole asphaltene, hysteresis isotherm at n-heptane-water interface (20°C). First and second compression-expansion cycles are shown.

5.3 *Relaxation Isotherms n-Heptane-Water Interface*

To determine asphaltene monolayer stability at the heptane-water interface, a series of relaxation experiments were performed. Figure 5.6a shows the relaxation curves of the whole asphaltene sample compressed to various surface pressures. The plot has been normalised in order to compare the various curves. The high and low molecular weight fractions exhibited similar behaviour and are shown in Figures 5.6b & 5.6c.

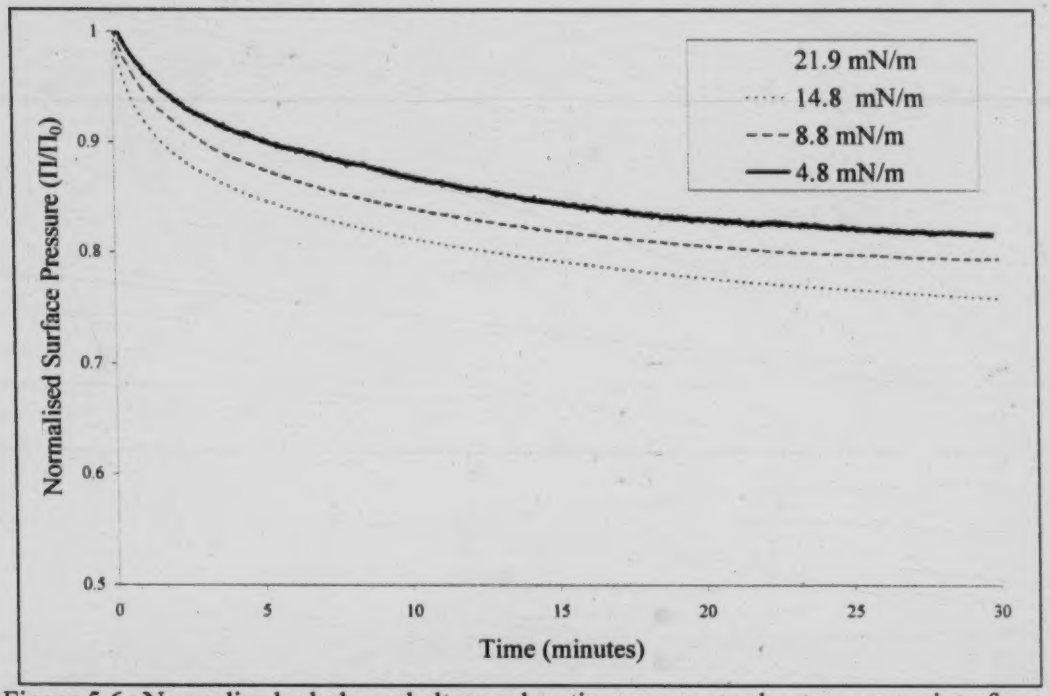

Figure 5.6a Normalised whole asphaltene relaxation curves at n-heptane-water interface, compressed to various surface pressures (20°C).

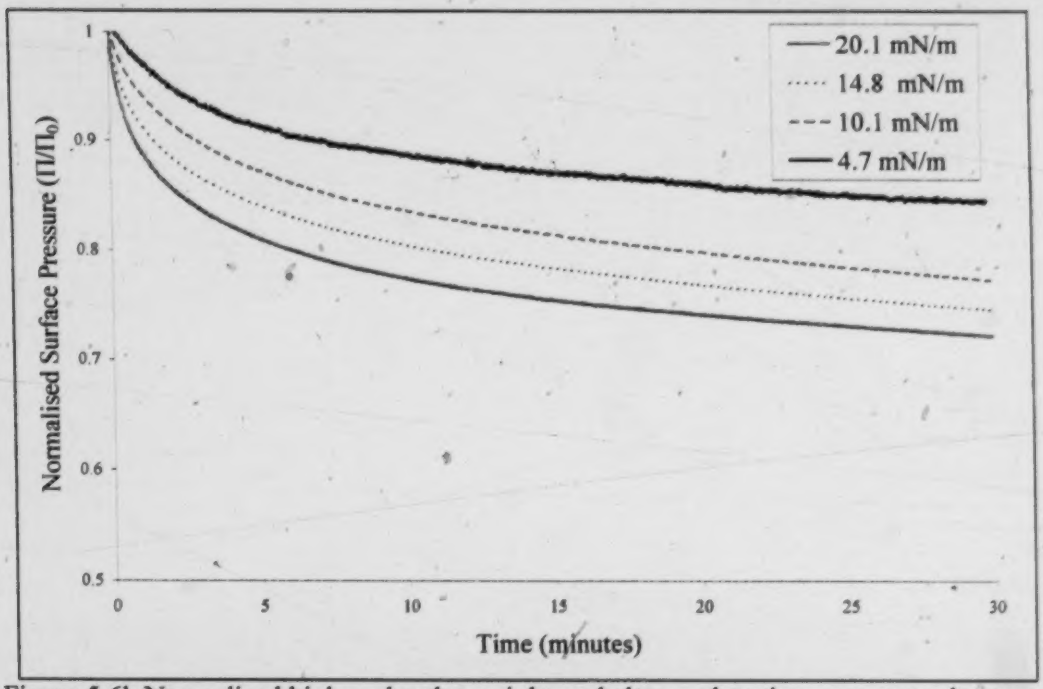

Figure 5.6b Normalised high molecular weight asphaltene relaxation curves at n-heptane-water interface, compressed to various surface pressures (20°C).

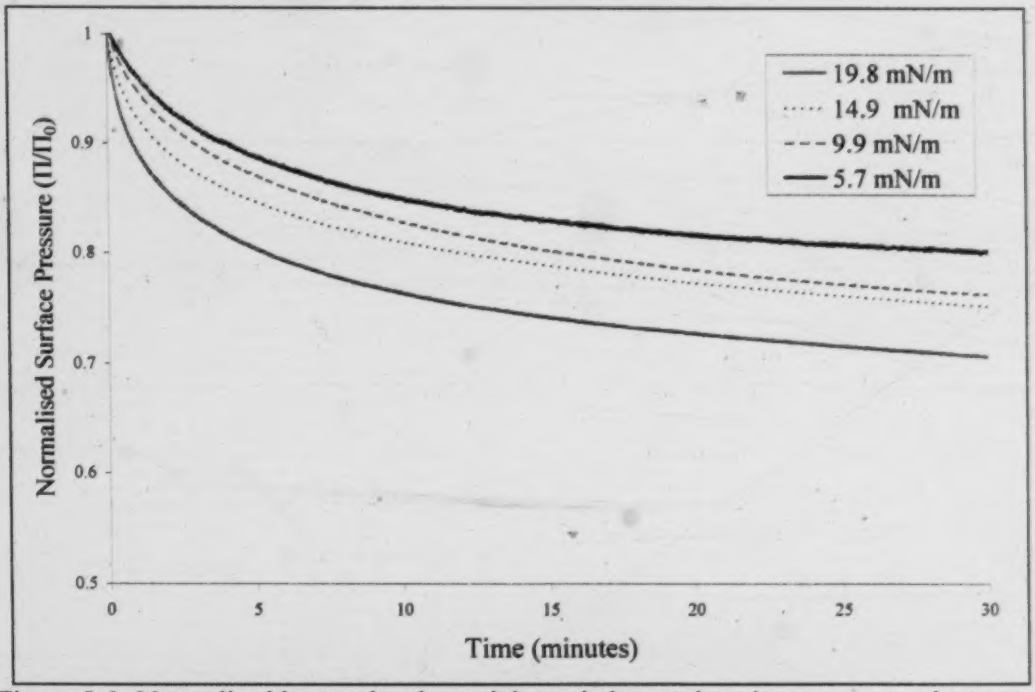

Figure 5.6c Normalised low molecular weight asphaltene relaxation curves at n-heptane-water interface, compressed to various surface pressures (20°C).

At the air-water interface, compressing the monolayer to a higher surface pressure caused the film to relax at a slower rate (see Figures 4.8a to 4.8c). However a completely different trend is observed at the heptane-water interface; the higher the compression surface pressure is, the faster the monolayer relaxes. This significant difference in relaxation rates is likely due to the different mechanisms for relaxation present at the heptane-water interface.

At the air-water interface, the most soluble material in the asphaltenes is squeezed out into the aqueous subphase during compression. The main mechanism of monolayer relaxation is dissolution from the interface. As a result, monolayers compressed to a higher surface pressure, relax at a slower rate, as soluble material is squeezed out with increasing surface pressure. At the heptane-water interface however, compression-expansion curves are reversible, as material does not leave the interface during compressions for surface pressures less than the critical pressure. In this environment, the main type of relaxation is molecular reorientation. The lower pressure compressions relax at a slower rate. This is because the forces driving relaxation are smaller in a monolayer that is compressed only by a small amount as opposed to a monolayer that is compressed by a larger amount.

Figure 5.7 compares the normalised relaxation curves of the three fractions of asphaltene compressed to the same surface pressure.

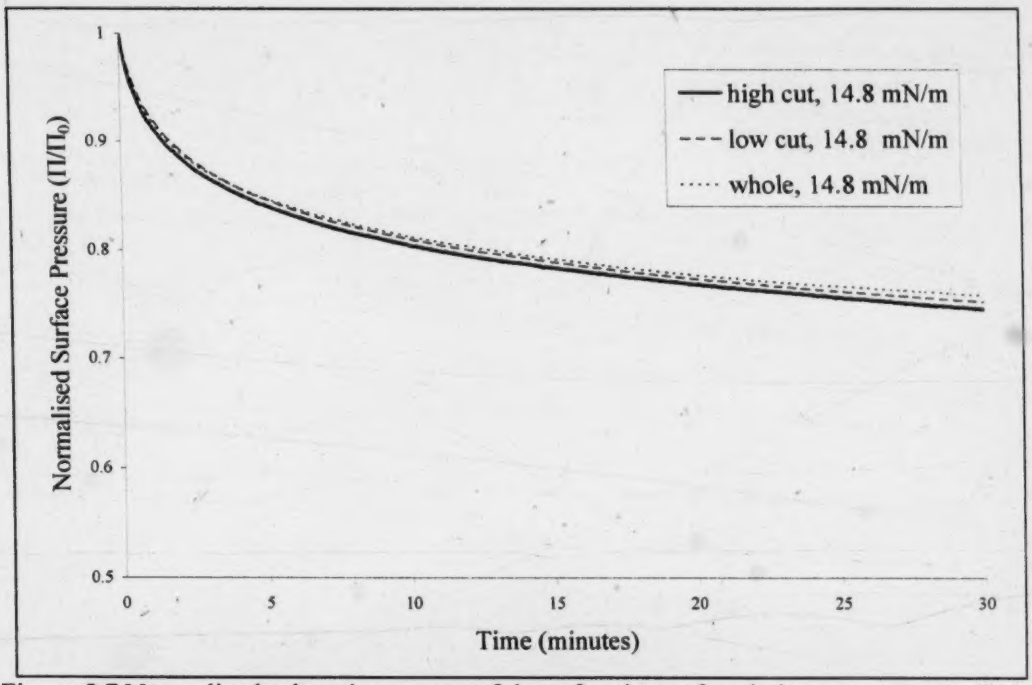

Figure 5.7 Normalised relaxation curves of three fractions of asphaltenes compressed to similar surface pressures at n-heptane-water interface (20°C).

At the heptane-water interface, the molecular weight of the fraction does not affect the rate of monolayer relaxation. All three fractions compressed to similar surface pressures relaxed at the same rate. At the air-water interface, dissolution of slightly soluble material into the subphase caused the low molecular weight asphaltene to relax at a faster rate than the high molecular weight fraction. However, at the heptane-water interface, movement of the asphaltene molecules away from the interface does not occur as the asphaltenes are stabilised by the presence of the heptane. As a result, the three asphaltene fractions give the same relaxation rate.

Figures 5.8a & 5.8b compare the rate of relaxation for the high and low molecular weight asphaltene fractions, respectively, at the air-water and heptane-water interface.

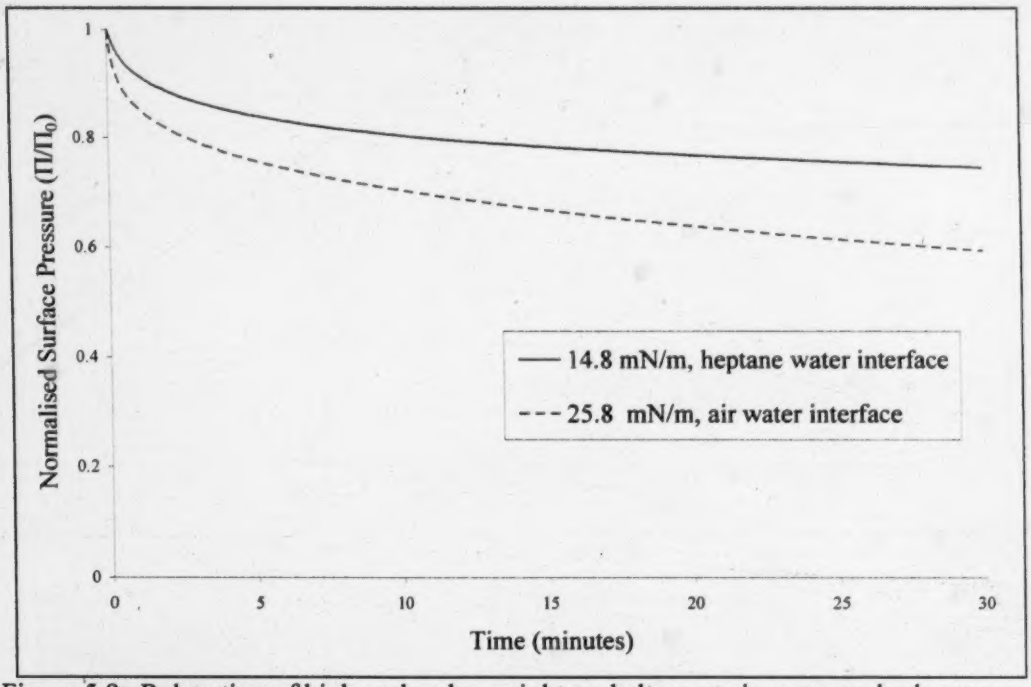

Figure 5.8a Relaxation of high molecular weight asphaltene at air-water and n-heptane-water interfaces (20°C).

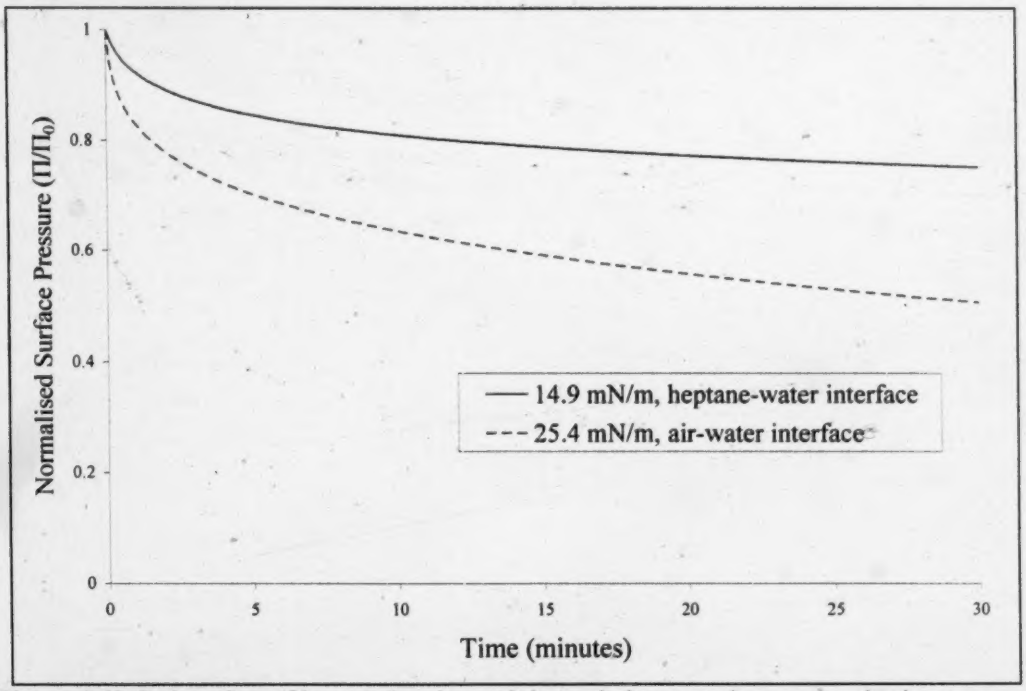

Figure 5.8b Relaxation of low molecular weight asphaltene at air-water and n-heptane-water interfaces (20°C).

It is difficult to compare the relaxation rates for a specific surface pressure in different interfacial environments, because of the differences in interfacial tension. A film compressed to a particular pressure at an air-water interface would not be compressed to the same degree if compressed to the same surface pressure at a heptane-water interface. However, Figures 5.8a & 5.8b compare asphaltene monolayers that have been compressed approximately to the same degree in their respective interfacial environments. Each monolayer was compressed to the same mean molecular area in the middle of the liquid expanded phase. As a result, a general idea of the relaxation rates can be compared between the two systems. It is clear from Figures 5.8a & 5.8b, that when the asphaltene monolayers are compressed to approximately the same degree, the monolayer relaxes at a faster rate at the air-water interface. A slower rate of relaxation is anticipated at the heptane-water interface as the only mechanism of relaxation is molecular reorientation. At the air-water interface, dissolution and molecular reorientation occur leading to a faster rate of relaxation. This effect is even more pronounced with the low molecular weight asphaltene at the air-water interface (see Figure 5.8b). The low molecular weight fraction contains material that is more likely to dissolve into the aqueous subphase; as a result, relaxation of the low molecular weight asphaltene at the air-water interface is accelerated.

5.4 AFM Images of LB Films (n-Heptane-Water Interface)

To study the monolayers at heptane-water interfaces, LB films were deposited on silicon wafers and glass slides at a variety of surface pressures. Images of the films were obtained using an AFM. Figure 5.9 shows an AFM image of a bare silicon wafer. The image indicates that the surface was smooth and free of defects.

AFM images of the low molecular weight, high molecular weight, and whole asphaltene fractions at 5 mN/m are shown in Figures 5.10a to 5.10c. These figures indicated that at the same surface pressure, similar structures were observed in each of the various fractions of asphaltene. At the heptane-water interface, LB depositions show a transfer ratio greater than one in all situations. The high TR values are not caused by dissolution into the subphase (as shown in Figures 5.4a-c). Therefore, the transfer ratios above unity are likely caused by a denser packing of the asphaltene molecules on the silicon surface than at the heptane-water interface (Bassereau & Pincet, 1997).

Figures 5.11a to 5.11c show AFM images of the high molecular fraction compressed to 5, 20 and 40 mN/m, respectively.

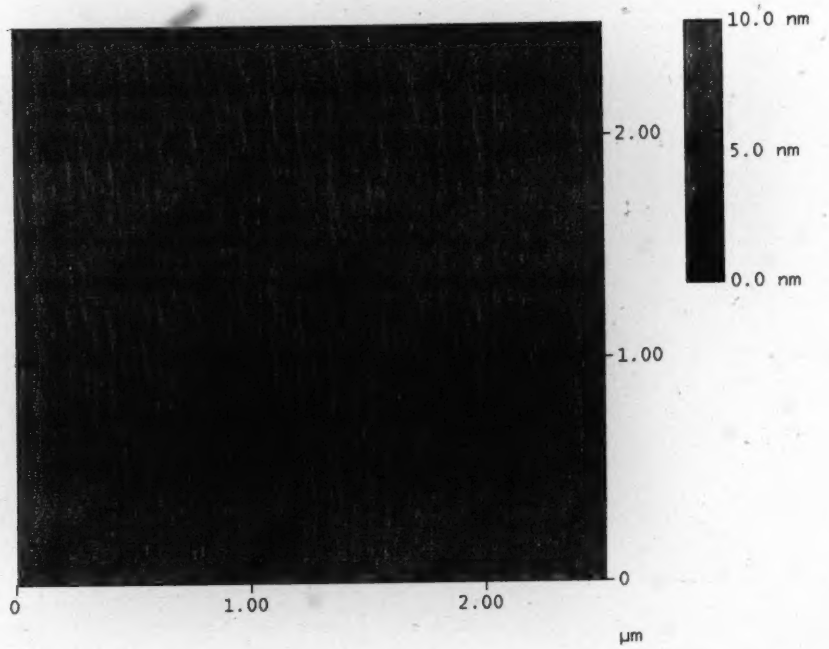

Figure 5.9 AFM image of bare silicon wafer with no monolayer on the surface.

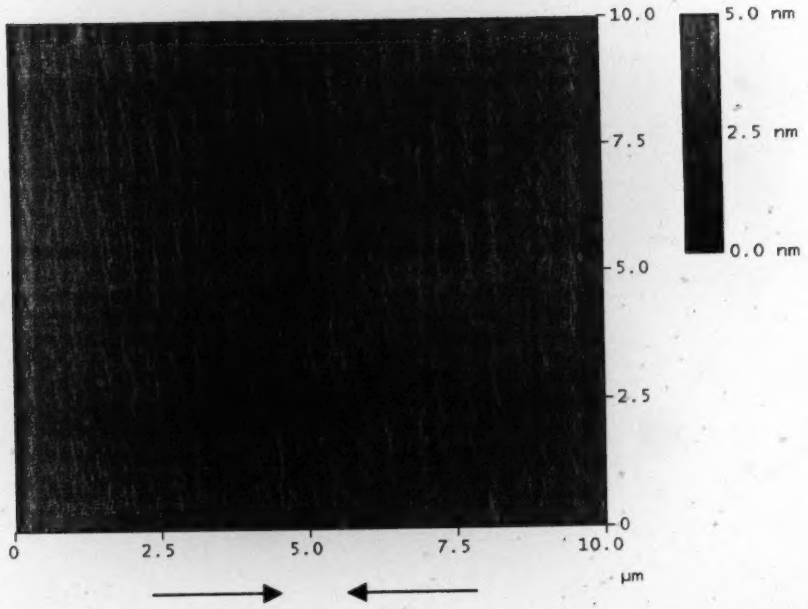

Figure 5.10a AFM image of low molecular weight asphaltene LB film on silicon wafer compressed to 5 mN/m, transfer ratio 1.404, at an n-heptane-water interface (20°C).

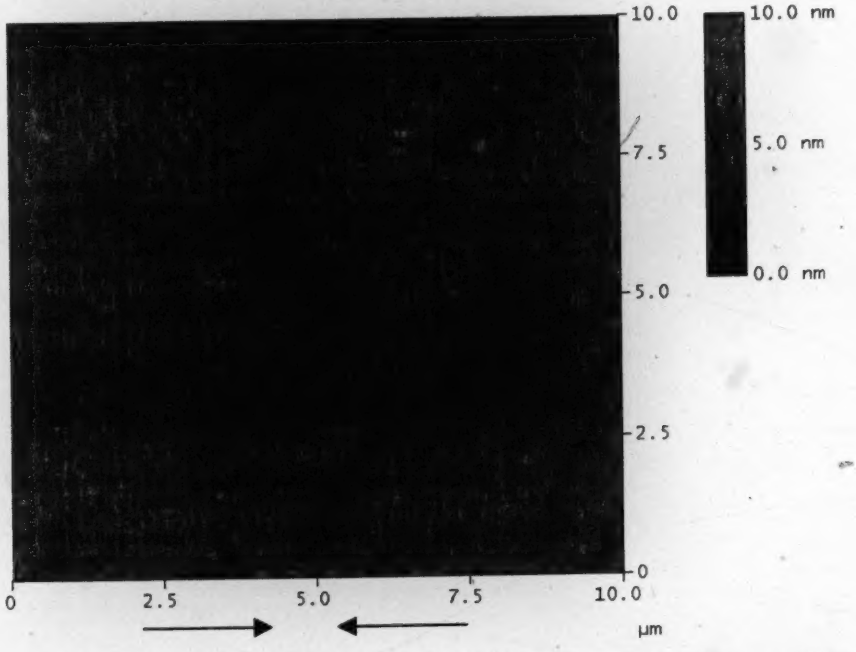

Figure 5.10b AFM image of high molecular weight asphaltene LB film on a silicon wafer compressed to 5 mN/m (transfer ratio 1.331) at the n-heptane-water interface (20°C).

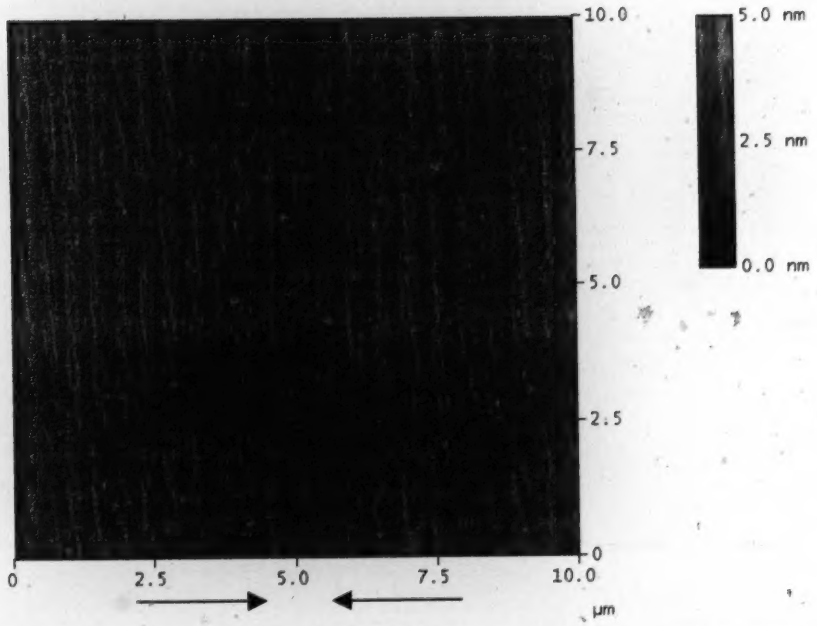

Figure 5.10c AFM image of whole asphaltene LB film on silicon wafer compressed to 5 mN/m, transfer ratio 1.259 at n-heptane-water interface (20°C).

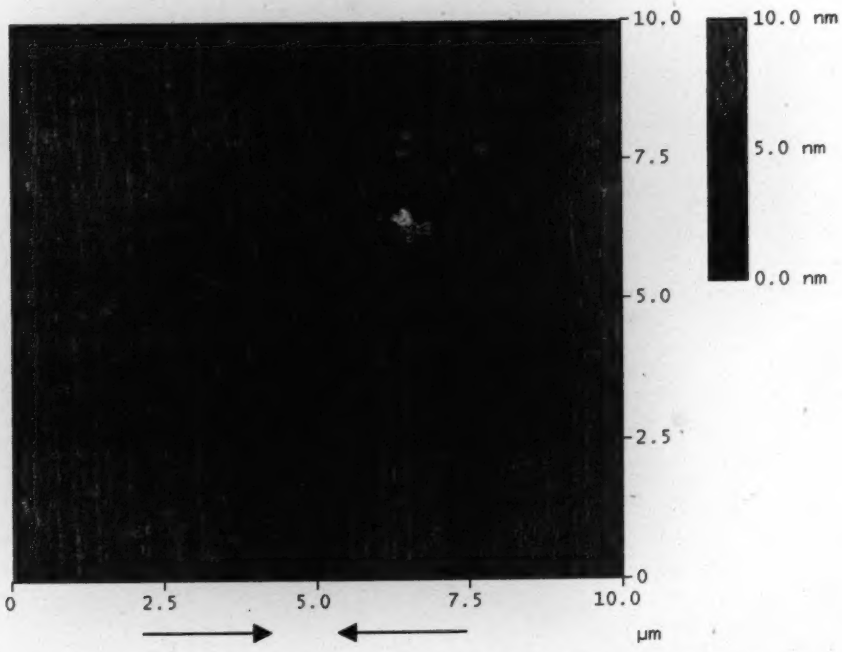

Figure 5.11a AFM image of high molecular weight asphaltene LB film on silicon wafer compressed to 5 mN/m, transfer ratio 1.331 at n-heptane-water interface (20°C).

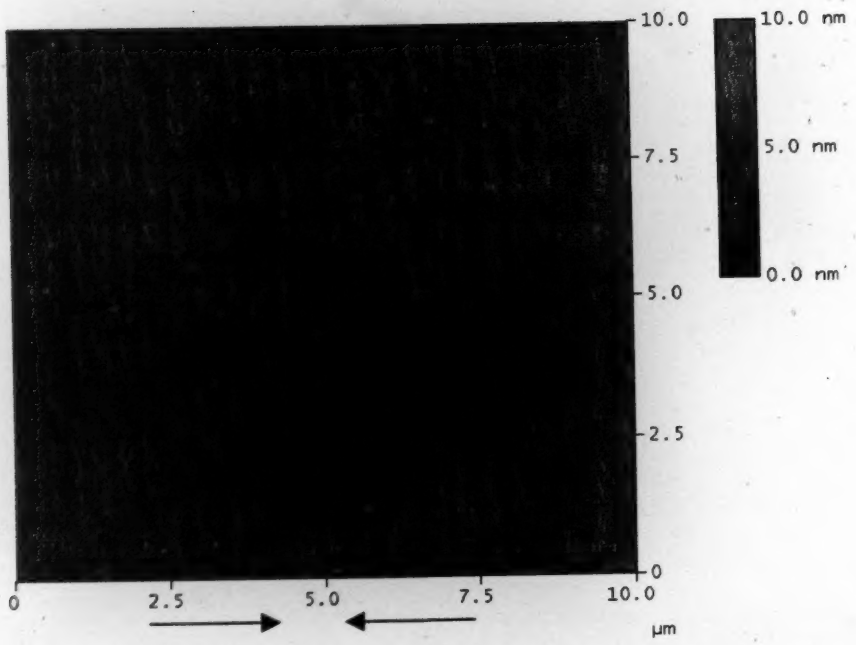

Figure 5.11b AFM image of high molecular weight asphaltene LB film on silicon wafer compressed to 20 mN/m, transfer ratio 1.176 at n-heptane-water interface (20°C).

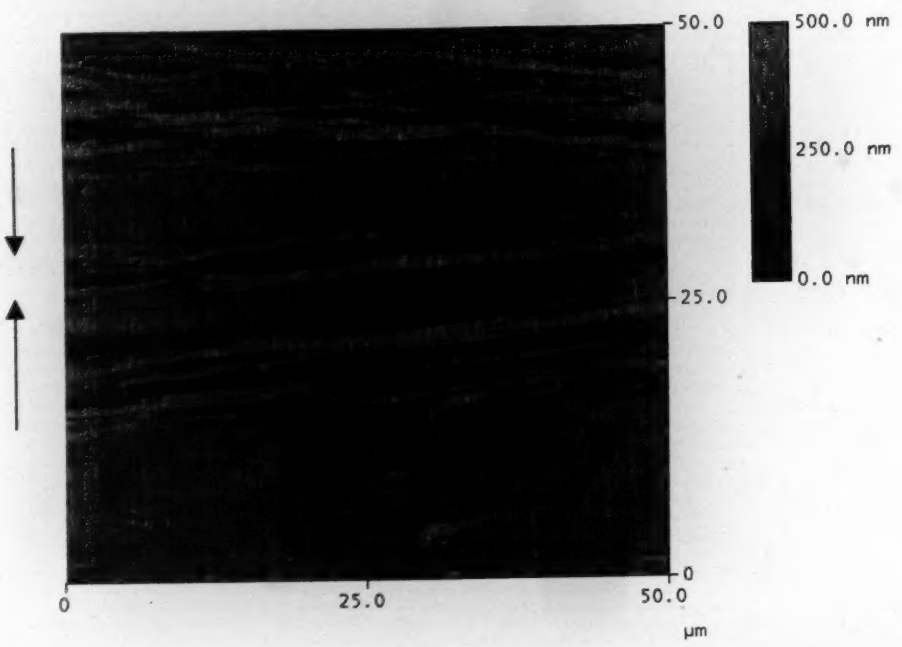

Figure 5.11c AFM image of high molecular weight asphaltene compressed to 40 mN/m, transferred by LS method onto hydrophobic glass slide at n-heptane-water interface.

Figure 5.11a (5mN/m) shows an evenly distributed monolayer punctuated by small raised areas. This distribution is significantly different from that of the air-water interface in which disc and rod structures were clearly visible. At the heptane-water interface, the presence of heptane stabilises the asphaltenes and enables them to spread out over the interface in a much more uniform pattern than at the air-water interface.

With increasing surface pressure, as seen in Figure 5.11b, the monolayer is further compressed and the raised structures that are visible at 5 mN/m are now smaller in size, indicating they have been compacted. At 20 mN/m, the asphaltenes are evenly distributed over the interface compared to the air-water interface, showing an absence of significant structures up to the point of monolayer collapse.

Figure 5.11c shows the asphaltene film compressed to 40 mN/m. This surface pressure exceeds the critical pressure of the high molecular weight asphaltene (35 mN/m) at which the film begins to collapse. Buckling occurs in the direction normal to the motion of the barriers, as anticipated. Comparing the height scales of Figures 5.11b and 5.11c, one can observe that the height of the buckled film greatly exceeds the height of any structural features present in a non-collapsed film. The fact that the film is able to buckle to such significant heights rather than collapsing as observed in a typical fatty acid monolayer, indicates that the material present at the interface forms a very rigid film.

5.5 Contact Angle Measurements

Static contact angles (θ_0) of water on deposited LB films from the n-heptane-water interface were measured for the three fractions of asphaltenes. The LB films were either transferred to silicon wafers (by the LB technique) or to hydrophobic glass slides

(by the LS method). Figure 5.12 shows the high molecular weight fraction contact angles at different surface pressures. The image of the water droplet at each surface pressure is shown as well. A clean silicon wafer that has passed through a heptane-water interface without any asphaltenes present is still extremely hydrophobic after drying, and has a low static contact angle. This indicates that the heptane alone does not affect the static contact angle of the wafer.

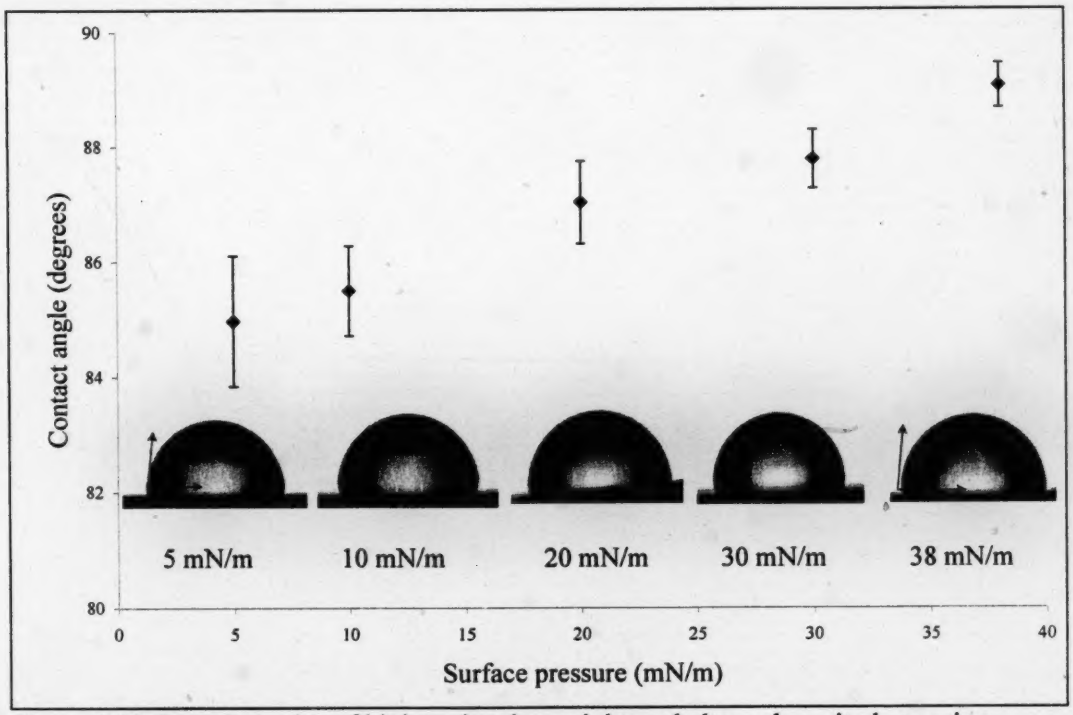

Figure 5.12 Contact angles of high molecular weight asphaltene deposited at various surface pressures from an n-heptane-water interface at 20°C.

At the heptane-water interface, the static contact angle is observed to increase with increasing surface pressure. This is expected with increased compression as the hydrophobic organic chains are packed closer together. The trend is similar to that observed for the material deposited from an air-water interface. However, with the asphaltenes from the heptane-water interface, the contact angle is 25 to 30 degrees

higher. This increase in contact angle is likely due to closer packing of the molecules at the heptane-water interface as opposed to the air-water interface. This observation is consistent with the AFM images which indicate a more uniform film at the heptane-water interface. The presence of the heptane stabilises the organic chains of the asphaltenes and leads to a closer packing structure.

Figure 5.13 compares the high and low fraction of asphaltene at various surface pressures. For a given surface pressure, the whole molecular weight fraction lies in between the two fractions at each surface pressure, but it is not displayed for clarity. See Table 5.2 for a listing of all the contact angles of the asphaltene layers deposited at various surface pressures.

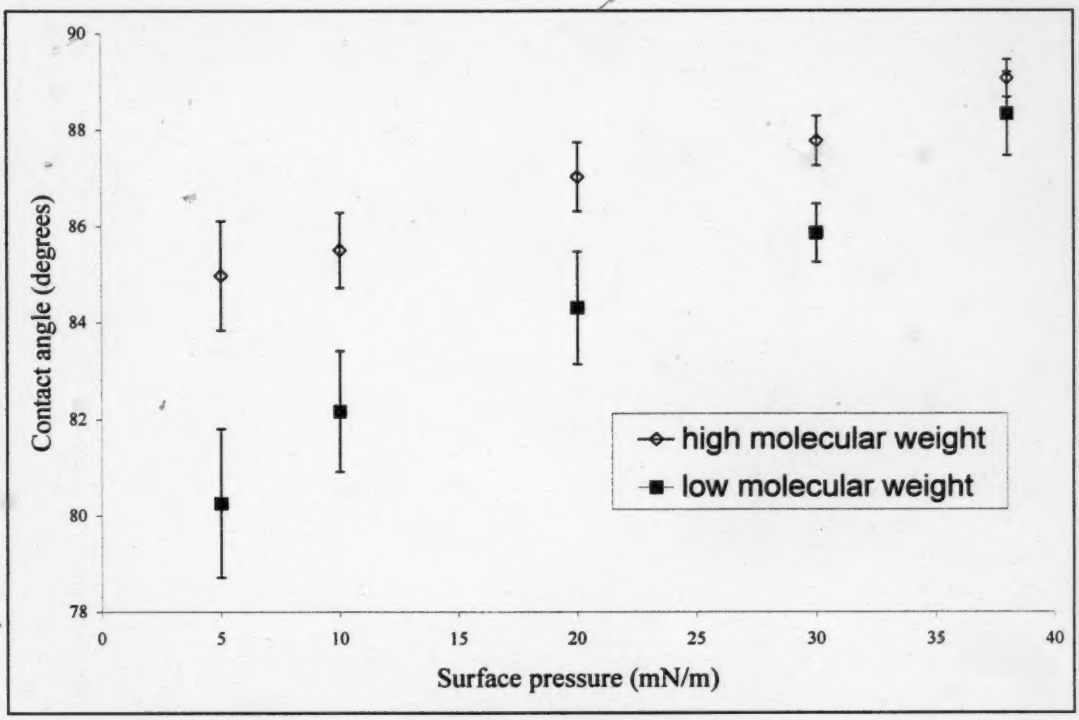

Figure 5.13 Contact angles of high and low molecular weight asphaltenes deposited at various surface pressures from an n-heptane-water interface at 20°C.

Table 5.2 Static Contact Angle and Error for Asphaltene Fractions at Different Surface Pressures

Sample Name	Surface Pressure (mN/m) 5	10	20	30	38	40
Low Molecular Weight	80.26	82.16	84.30	85.86	88.33	
Error (+/-) degrees	1.54	1.25	1.66	0.61	0.86	
Whole Asphaltene	81.9		85.7			
Error (+/-) degrees	1.23		0.56			
High Molecular Weight	84.97	85.5	87.03	87.77	89.06	90.75
Error (+/-) degrees	1.13	0.78	0.72	0.51	0.39	0.89

The contact angle of asphaltene layers deposited at low surface pressures is proportional to the mean molecular weight of the asphaltene sample. This observation is valid for films deposited at both the heptane-water and air-water interfaces. As previously mentioned, at lower surface pressures, the higher molecular weight fraction has a higher static contact angle due to increased length in backbone chain length. The contact angle is highest for all asphaltene fractions when the film is compressed to a high surface pressure. At high surface pressures, the films are highly compressed, as a result, the compression of the monolayer causes the increase in contact angle and the backbone length of asphaltene molecules is not a significant contributor.

5.6 Summary

The behaviour of asphaltenes at an n-heptane-water interface has been studied on a Langmuir trough using a variety of analytical techniques. At the heptane-water interface, asphaltenes are shown to form stable monolayers that do not permanently deform during compression at surface pressures below the critical surface pressure. Compression-

expansion curves are reversible indicating that material does not dissolve from the interface. The relaxation of a compressed monolayer is due to molecular reorientation and occurs at a slower rate than at the air-water interface. LB depositions of asphaltenes at the heptane-water interface show an evenly distributed monolayer at surface pressures below the critical surface pressure, indicating that the heptane has a stabilising effect on the asphaltenes at the interface. At surface pressures above the critical surface pressure, a heavily folded layer is visible indicating that compression of the monolayer has caused the film to buckle. Contact angle measurements indicate that at lower surface pressures, the molecular weight of the asphaltene has an effect on the contact angle, with lower molecular weight fractions yielding a lower static contact angle. At high surface pressures however, the monolayers are tightly compressed and all three fractions have a contact angle of approximately 89 degrees. The contact angle is larger at the heptane-water interface compared to the air-water interface, indicating a closer packing of the asphaltene molecules at the heptane-water interface.

6 Effects of Demulsifiers at n-Heptane-Water Interfaces

The effects of two commercial demulsifiers (obtained from Champion Technologies Inc.) on asphaltene monolayers at the n-heptane-water interface were studied. For simplicity, the demulsifiers will be referred to as demulsifier A and B.

6.1 Demulsifier Properties

A short description of the demulsifier properties is shown in Table 6.1.

Table 6.1 Properties of Commercial Demulsifiers from Champion Technologies Inc.

Demulsifier A	
Reference Name:	Emulsion Breaker Intermediate BOH2-32A
Generic Description:	n-alkylamine neutralised polyalkylated napthalene sulphonic acid
Class of Chemical:	Hydrotrope
Molecular Weight:	< 500 AMU
Demulsifier B	
Reference Name:	Emulsion Breaker Intermediate BOH2-32B
Generic Description:	Mixed alkylphenol formaldehyde resin oxyalkylate
Class of Chemical:	Calixarene oxyalklated emulsion breaker intermediate
Molecular Weight:	< 2000 AMU

6.2 Demulsifiers at n-Heptane-Water Interface

The effects of demulsifiers on the surface pressure of a pure heptane-water interface were first investigated by adding different concentrations of a demulsifier to a system containing a clean heptane-water interface. For demulsifier A, concentrations in the order of magnitude of 50 PPM are found to affect the interfacial surface pressure. Figure 6.1 shows the change in surface pressure as a function of time for a heptane-water interface with 50 PPM of demulsifier A added to the heptane phase.

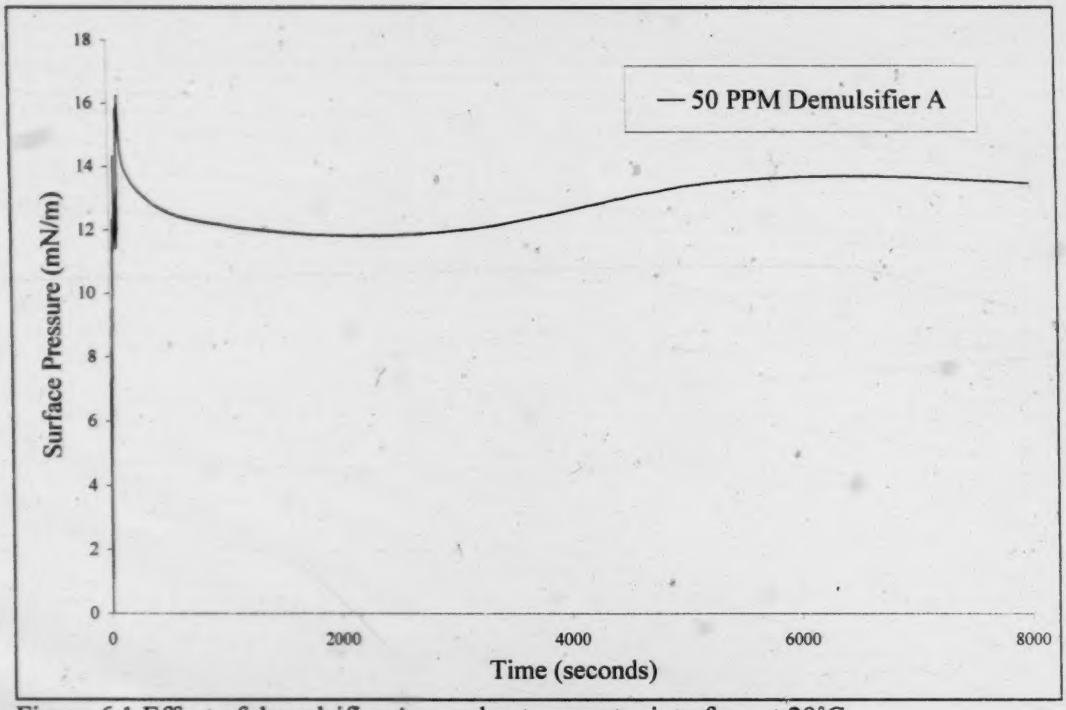

Figure 6.1 Effect of demulsifier A on n-heptane-water interface at 20°C.

At this concentration, the demulsifier diffused to the interface and increased the surface pressure by approximately 13 mN/m. At concentrations less than 10 PPM, demulsifier A did not significantly affect the surface pressure of the interface.

For demulsifier B, concentrations as low as 0.25 PPM are found to affect the surface pressure for a pure heptane-water interface. Figure 6.2 shows the change in surface pressure as a function of time of a heptane-water interface with 1 PPM of demulsifier B added to the heptane phase.

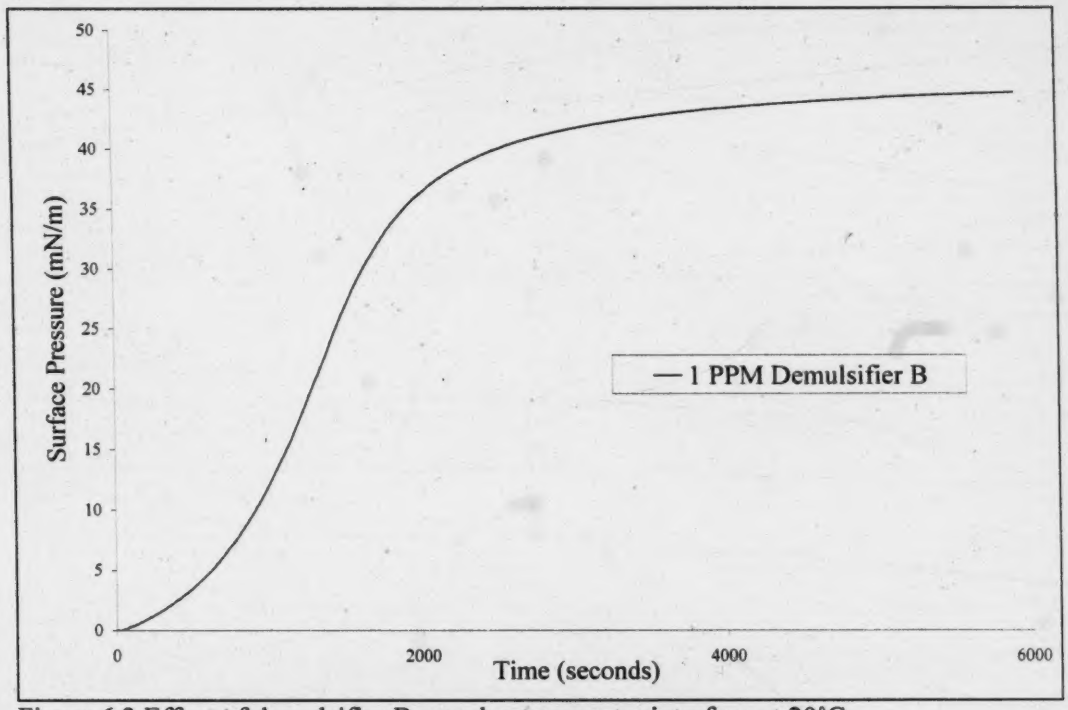

Figure 6.2 Effect of demulsifier B on n-heptane-water interface at 20°C.

A gradual increase in surface pressure was observed over approximately 2000 seconds. Demulsifier B induced a much larger net change in surface pressure, with a surface pressure increase of approximately 45 mN/m.

The difference in the rate at which the demulsifiers affected the interface is related to the concentration of their dosage. If demulsifier B is added to the heptane at a concentration of 50 PPM, the change in surface pressure is very rapid as a function of time. However, demulsifier B is capable of increasing the surface pressure at much lower concentrations than demulsifier A, and the changes induced by demulsifier B are much greater than demulsifier A (13 to 45 mN/m respectively).

A demulsifier that can reduce film rigidity will generally decrease the stability of an emulsion. If the rigidity of a film surrounding a droplet of an emulsion is reduced, the

likelihood of droplet coalescence is increased when two droplets encounter each other (Sharma, 1995). It is clear that demulsifier B is more effective than demulsifier A as it can affect the surface pressure at much lower dosages and it affects the surface pressure to a much greater degree.

6.3 Demulsifier Effect on Asphaltenes at n-Heptane-Water Interface

Figures 6.3 and 6.4 compare the effects of demulsifiers A and B at various concentrations for the high molecular weight asphaltene. With both demulsifiers, a clear reduction in film rigidity is observed as a function of demulsifier addition. Polar molecules in the surfactants reduce film rigidity by penetrating the asphaltene film (Singh, 1994) and displacing the asphaltene molecules (Sharma, 1995). During the initial compression of the monolayer, the film is observed to be more expanded with the addition of demulsifier. This is anticipated as more material is likely to be present at the interface with the addition of demulsifier.

Demulsifier B is clearly more effective at affecting the asphaltene monolayer than demulsifier A. With concentrations as low as 0.5 PPM, demulsifier B can significantly reduce the rigidity of the asphaltene monolayer. Demulsifier A does not start to affect the asphaltene film until concentrations greater than 10 PPM are added to the heptane. The effectiveness of demulsifier B may be related to its molecular weight. Demulsifier B has a mean molecular weight around 2000 while demulsifier A has a mean molecular weight around 500. There may be a higher tendency for the larger demulsifier B molecules to migrate to the interface and displace or interact with the asphaltene molecules present.

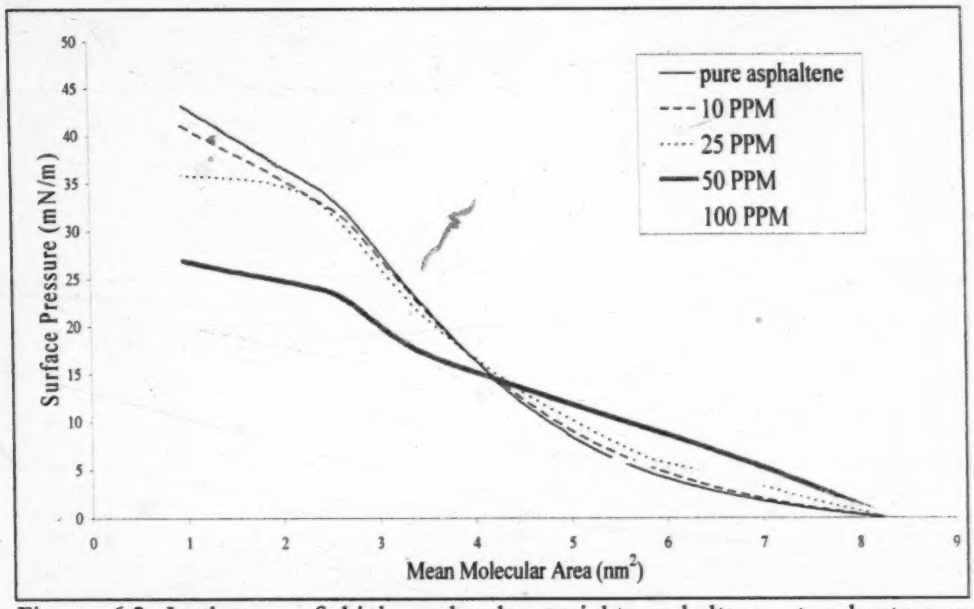

Figure 6.3 Isotherms of high molecular weight asphaltene at n-heptane-water interface with varying concentrations of demulsifier A.

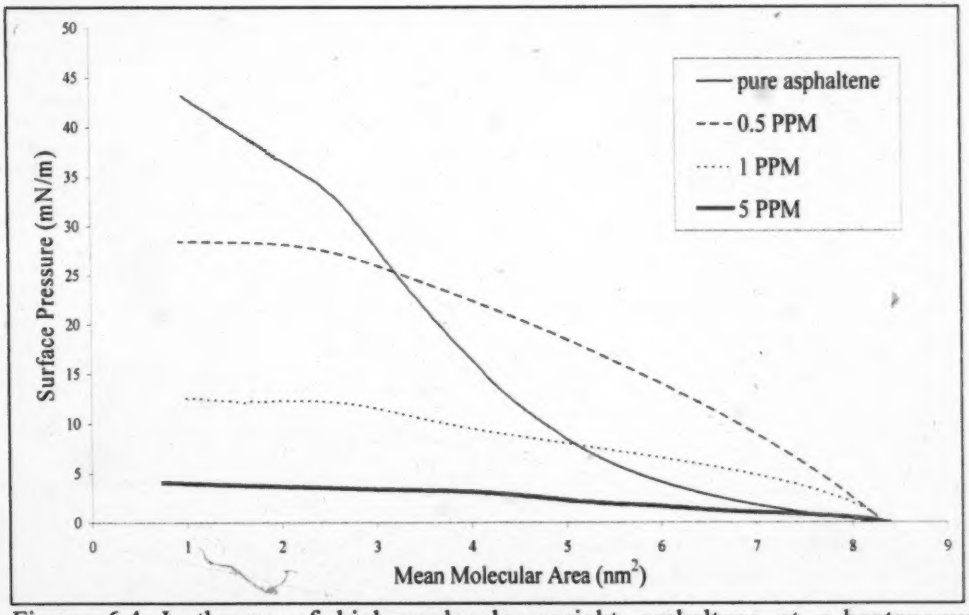

Figure 6.4 Isotherms of high molecular weight asphaltene at n-heptane-water interface with varying concentrations of demulsifier B.

6.4 Summary

The effects of demulsifier A and B at n-heptane-water interfaces and on asphaltene monolayers at n-heptane-water interfaces were compared. Demulsifier B has a higher molecular weight and was found to affect the surface pressure of an n-heptane-water interface to a greater degree than demulsifier A. Demulsifier B also affected the surface pressure of an n-heptane-water interface at much lower concentrations than demulsifier A.

7 Conclusions and Recommendations for Future Work

7.1 General Summary

Asphaltenes play an important role at interfaces in the formation of water-in-oil emulsions relevant to crude oil and bitumen production. Study of asphaltene behaviour at interfaces provides important insights to understanding their interfacial interactions and helps develop potential methods of destabilising emulsions.

The behaviour of asphaltenes at interfaces was investigated using a Langmuir trough to produce asphaltene monolayers, from which various mechanical properties were investigated. Asphaltene films were transferred to solid substrates to investigate other relevant properties such as surface topography and film hydrophobicity.

In the past, the Langmuir trough has been extensively used to study fatty acids at interfaces, particularly at air-water interfaces. However, little work has been done to investigate asphaltenes using a Langmuir trough. Recent developments in Langmuir trough technology have also led to the development of an interfacial trough enabling the study molecular behaviour at the interface of two immiscible liquids. Studying the behaviour of asphaltenes at an oil-water interface can lead to a more realistic environment in which asphaltenes play a role in forming and stabilising emulsions.

7.2 Summary of Experimental Results

7.2.1 Asphaltene Properties

The asphaltenes were fractionated into three solubility classes (low molecular weight, high molecular weight and whole asphaltene) with average molecular weights of

6480, 8310, 6870, respectively. The FTIR characterisation showed negligible differences in the functional groups in the three fractions. However, FTIR did find a number of hydrophilic functional groups within the asphaltenes indicating that the asphaltenes are amphiphilic in nature. Elemental analysis found only negligible differences between the three fractions. Densitometer tests found the asphaltenes were slightly denser than water and their density increases with increasing molecular weight. The densities for the low, whole and high fractions are 1080, 1140, 1180 kg/m^3, respectively.

7.2.2 Air-Water Interface

All classes of asphaltenes are found to be capable of forming a rigid film at an air-water interface due to their amphiphilic nature. However, at an air-water interface, the asphaltene monolayer was found to deform plastically as evidenced by its irreversible behaviour during monolayer compression. AFM images of the asphaltenes indicate that the asphaltenes tend to form in a relatively heterogeneous and loosely packed manner at the air-water interface. Contact angle values for the deposited asphaltene monolayers indicate a relatively loose packing of molecules at the surface. While the three fractions of asphaltenes are relatively similar in density, elemental composition and contain similar functional groups, there are differences in the contact angle of the deposited films. There is a small but significant increase in contact angle with increasing asphaltene molecular weight. The increase in contact angle is likely due to an increase in backbone chain length with increasing molecular weight of asphaltene fraction. For all three fractions of asphaltenes, differences in the pH of the aqueous subphase did not affect the Π-A isotherms at the air-water interface. This is likely due to the fact than in a monolayer of

asphaltenes, the packing of the polyaromatic rings and alkyl sidechains dominates the interactions over the ionised headgroups.

7.2.3 n-Heptane-Water Interface

At the n-heptane-water interface, asphaltenes form a rigid and stable film. Compared with the air-water interface, the presence of heptane stabilises the asphaltene molecules at the interface, even during compression the molecules do not leave the interface. AFM images of deposited asphaltene films from the n-heptane-water interface indicate a closely packed, homogeneous film. Contact angle measurements also indicate a much higher degree of hydrophobicity for asphaltenes deposited from an n-heptane-water interface, indicating a closer molecular packing than at the air-water interface.

Two commercial demulsifiers were tested for their effects on asphaltene monolayers at n-heptane-water interfaces. Both demulsifiers were found to destabilise the asphaltene monolayer and reduce film rigidity. The higher molecular weight Demulsifier B is significantly more effective at destabilising the asphaltene interfacial layer than Demulsifier A, and at much lower concentrations.

7.3 Summary of Contributions

This research represents a systematic study of asphaltene monolayers at air-water and n-heptane-water interfaces using a Langmuir trough. The study provides valuable information on the behaviour of asphaltenes at air-water and n-heptane-water interfaces. The fundamental information extracted from this study can be related to the role asphaltenes may have in the formation and stabilisation of water-in-oil emulsions.

7.4 Recommendations for Future Work

There are a number of areas in which this research can be continued. In this thesis, the water subphase did not contain any suspended solids. The presence of suspended solids or ions may have a significant effect on the packing of asphaltene molecules at both air-water and oil-water interfaces.

It is possible to study the effects of asphaltenes at a variety of oil-water interfaces using the oil-water Langmuir trough. Heptane was used in this thesis as the oil phase, but any number of water-immiscible solvents could be used instead. It is also possible to precipitate asphaltenes from bitumen or crude oil using a different solvent such as pentane; leading to a slightly different asphaltene composition.

There is a potential for more research to be conducted studying the effect demulsifiers has on molecular behaviour of asphaltenes at oil-water interfaces using a Langmuir trough. Extensive research in this area can be conducted relating demulsifier effectiveness to demulsifier structure and composition.

A limitation of Langmuir-Blodgett depositions is the fact that a monolayer deposited onto a solid substrate is not the same as a monolayer at a gas-liquid or liquid-liquid interface. During deposition the monolayer can be stretched, compressed, torn, or the molecular orientation can be altered. As a result, the study of an LB film on a solid substrate can only approximate the behaviour of a film at an interface. Ellipsometry however, is an optical technique that can probe the dielectric properties of a sample through the use of polarised light. Ellipsometry has been used extensively in the past to analyse thin films, and could be used to analyse the layer thickness and morphology of a Langmuir monolayer without the need to transfer the material onto a solid substrate.

On one final note, it is important to realise that the use of a Langmuir trough only approximates some of the mechanisms responsible for the stabilisation of emulsions. However, with the improved understanding of how asphaltenes interact at interfaces, one can extend this knowledge and combine it with research in other areas, to larger scale applications.

Bibliography

Andersen, S. I.; Speight, J. G. "Petroleum Resins: Separation, Character, and Role in Petroleum" *Petroleum Science and Technology*, **2001**, Vol. 19, No. 1&2, 1-34.

Arslanov, V. V. "Monolayers and Langmuir-Blodgett Films of Monomers and Polymers Polyreactions, Structural Transformations, Properties and Applications" *Advances in Colloid and Interface Science*, **1992**, Vol. 40, 307-370.

Aveyard, R.; Clint, J. H.; Nees, D.; Paunov, V. N. "Compression and Structure of Monolayers of Charged Latex Particles at Air/Water and Octane/Water Interfaces" *Langmuir*, **2000**, Vol. 16, 1969-1979.

Baker, S.; Petty, M. C.; Roberts, G. G.; Twigg, M. V. "The Preparation and Properties of Stable Metal-Free Phthalocyanine Langmuir-Blodgett Films" *Thin Solid Films*, **1983**, Vol. 99, 53-59.

Balashev, K.; Jensen, T. R.; Kjaer, K.; Björnholm, T. "Novel methods for studying lipids and lipases and their mutual interactions at interfaces. Part I. Atomic force microscopy" *Biochimie*, **2001**, Vol. 83, 387-397.

Banerjee, R.; Bellare, J. R. "In vitro evaluation of surfactants with eucalyptus oil for respiratory distress syndrome" *Respiration Physiology*, **2001**, Vol. 126, 141-151.

Bassereau, P; Frédéric, P. "Quantitative Analysis of Holes in Supported Bilayers Providing the Adsorption Energy of Surfactants on Solid Substrate" *Langmuir*, **1997**, Vol. 13, No. 26, 7003-7007.

Bouhadda, Y.; Bendedouch, D.; Sheu, E.; Krallafa, A. "Some Preliminary Results on a Physico-Chemical Characterization of a Hassi Messaoud Petroleum Asphaltene" *Energy & Fuels*, **2000**, Vol. 14, No.4, 845-853.

Calemma, V.; Rausa, R.; D'Antona, P.; Montanari, L. "Characterization of Asphaltenes Molecular Structure" *Energy & Fuels*, **1998**, Vol. 12, No. 2, 422-428.

Claesson, P. M.; Berg, J. M. "The Stability of Carboxylic Acid Langmuir-Blodgett Films as Studied by the Surface Force Technique" *Thin Solid Films*, **1989**, Vol. 176, 157-164.

Constantino, C. J. L.; Dhanabalan, A; Oliveira Jr., O. N. "Experimental artifacts in the surface pressure measurement for lignin monolayers in Langmuir troughs" *Review of Scientific Instruments*, **1999**, Vol. 70, No. 9, 3674-3680.

Cyr, N.; McIntyre, D. D.; Toth, G.; Strausz, O. P. "Hydrocarbon structural group analysis of Athabasca asphaltene and it g.p.c. fractions by ^{13}C n.m.r." *Fuel*, **1987**, Vol. 66, December, 1709-1714.

Dynarowicz-Latka, P.; Dhanabalan, A.; Oliveira Jr., O. N. "Modern physiochemical research on Langmuir monolayers" *Advances in Colloid and Interface Science*, **2001**, Vol. 91, 221-293.

Dickie, J. P.; Yen, T. F. "Macrostructures of the Asphaltic Fractions by Various Instramental Methods" *Analytical Chemistry*, **1967**, Vol. 39, No. 11, 1847-1852.

Ese, M. –H. "An atomic force microscopy study of asphaltenes on mica surfaces. Influence of added resins and demulsifiers" *Colloid and Polymer Science*, **2000**, Vol. 278, 532-538.

Ese, M. –H. "Langmuir Film Properties of Indigenous Crude Oil Components. Influence of Demulsifiers". PhD Thesis, University of Bergen, **1999a**.

Ese, M. –H. "Compressibilities and excess surface areas of mixed asphaltene/resin monolayers. Influence of demulsifiers". *Journal of Dispersion Science and Technology*, **1999b**, Vol. 20, No. 7, 18-49-1859.

Ese, M. –H.; Galet, L.; Clausse, D.; Sjöblom, J. "Properties of Langmuir Surface and Interfacial Films Built up by Asphaltenes and Resins: Influence of Chemical Demulsifiers" *Journal of Colloid and Interface Science*, **1999**, Vol. 220, 293-301.

Ese, M. –H.; Yang, X.; Sjöblom, J. "Film forming properties of asphaltenes and resins. A comparative Langmuir-Blodgett study of crude oils from North Sea, European continent and Venezuela" *Colloid & Polymer Science*, **1998**, Vol. 276, 800-809.

Fingas, M. "Water-in-Oil Emulsion Formation: A Review of Physics and Mathematical Modelling" *Spill Science & Technology Bulletin*, **1995**, Vol. 2, No. 1, 55-59.

Galet, L.; Pezron, I.; Kunz, W.; Larpent, C.; Zhu, J.; Lheveder, C. "Selective complexation of copper ions in monolayers of a new amphiphilic cage molecule at the liquid/air and liquid/liquid interfaces" *Colloids and Surfaces A: Physicochemical and Engineering Aspects*, **1999**, Vol. 151, 85-96.

Gaines, G. L.; "On the history of Langmuir-Blodgett films" *Thin Solid Films*, **1983**, Vol. 99, 9-13.

Gaines, G. L "Insoluble monolayers at liquid-gas interfaces" Wiley-Interscience, **1966**, New York.

Ghaicha, L.; Leblanc, R. M.; Villamagna, F.; Chattopadhyay, A. K. "Monolayers of Mixed Surfactants at the Oil/Water Interface, Hydrophobic Interactions, and Stability of Water-in-Oil Emulsions" *Langmuir*, **1995**, Vol. 11, No. 2, 585-590.

Grandell, D.; Murtomäki, L. "Surface Pressure Control of Phospholipid Monolayers at the Water/1,2-Dicholoethane Interface" *Langmuir*, **1998**, Vol. 14, 556-559.

Hiemenz, P. C.; Rajagopalan, R. "Principles of Colloid and Surface Chemistry" Marcel Dekker, Inc., **1997**, 3rd Edition, Revised and Expanded, ISBN 0-8247-9397-8, New York.

Hollars, C. W.; Dunn, R. C. "Submicron Structure in L-α-Dipalmitoylphosphatidylcholine Monolayers and Bilayers with Confocal, Atomic Force, and Near-Field Miscroscopy" *Biophysical Journal*, **1998**, Vol. 75, 342-352.

Izumi, M.; Ohnuki, H.; Kato, R.; Imakubo, T.; Nagata, M.; Noda, T.; Kojima, K. "Recent progress in metallic Langmuir-Blodgett films based on TTF derivatives" *Thin Solid Films*, **1998**, Vol. 327-329, 14-18.

Kotlyar, L. S.; Sparks, B. D.; Woods, J. R.; Chung, K. H. "Solids Associated with the Asphaltene Fraction of Oil Sands Bitumen" *Energy and Fuels*, **1999**, Vol. 13, No. 2, 346-350.

Kotlyar, L. S.; Sparks, B. D.; Woods, J. R.; Raymond, S.; Le Page, Y.; Shelfantook, W. "Distribution and Types of Solids Associated with Bitumen" *Petroleum Science & Technology*, **1998**, Vol 16, No. 1&2, 1-19.

KSV Instruments Ltd. "KSV Minitrough: Instruction Manual for Windows 95/98/NT/2000" Helsinki, Finland.

Kuhn, H. "Present Status of Future Prospects of Langmuir-Blodgett Film Research" *Thin Solid Films*, **1989**, Vol. 178, 1-16.

Kurnaz, M. L.; Schwartz, D. K. "Morphology of Microphase Separation in Arachidic Acid/Cadmium Arachidate Langmuir-Blodgett Multilayers" *Journal of Physical Chemistry*, **1996**, Vol. 100, No. 26, 11113-11119.

Kurihara, K. "Direct measurement of surface forces as a novel means of investigating supramolecular assemblies" *Advances in Colloid and Interface Science*, **1997**, Vol. 71-72, 243-258.

Leblanc, R. M.; Thyrion, F. C. "A study of monolayers of asphalts at the air/water interface" *Fuel*, **1989**, Vol. 68, 260-262.

Lee R. F. "Agents Which Promote and Stabilize Water-in-Oil Emulsions" *Spill Science & Technology Bulletin*, **1999**, Vol. 5, No. 2, 117-126.

Lucassen-Reynders, E. H. "Competitive adsorption of emulsifiers 1. Theory for adsorption of small and large molecules" *Colloids and Surfaces A*, **1994**, Vol. 91, 79-88.

MaKay, D. "Formulation and stability of water-in-oil emulsions" *Environment Canada Manuscript Report EE-93*, **1987**, Ottawa, Ontario, 97-99.

McLean, J. D.; Kilpatrick, P. K. "Effects of Asphaltene Solvency on Stability of Water-in-Crude-Oil Emulsions" *Journal of Colloid and Interface Science*, **1998**, Vol. 189, 242-253.

Menon, V. B.; Nilolov, A. D.; Wasan, D. T. "Interfacial effects in solids-stabilized emulsions: effect of surfactant and pH on film tension and particle interaction energy" *Journal of Dispersion Science and Technology*, **1988**, Vol. 9, 575-593.

Miller, J. D.; Veeramasuneni, S.; Drelich, J.; Yalamanchili, M. R.; Yamauchi, G. "Effect of Roughness as Determined by Atomic Force Microscopy on the Wetting Properties of PTFE Thin Films" *Polymer Engineering and Science*, **1996**, Vol. 36, No. 14, 1849-1855.

Mohammed, R. A.; Bailey, A. I.; Luckham, P. F.; Taylor, S. E. "Dewatering of crude oil emulsions 2. Interfacial properties of the asphaltic constituents of crude oil" *Colloids & Surfaces A*, **1993**, Vol. 80, No. 2-3, 237-242.

Müller, D. J.; Engel, A.; Amrein, M. "Preparation techniques for the observation of native biological systems with the atomic force microscope" *Biosensors & Biometrics*, **1997**, Vol. 12, No. 8, 867-877.

Mullins, O. C.; Sheu, E. Y.; "Structures and Dynamics of Asphaltenes" Plenum Press, **1998**, New York and London.

Murray, B. S.; Nelson, P. V. "A Novel Langmuir Trough for Equilibrium and Dynamic Measurements on Air-Water and Oil-Water Monolayers" *Langmuir*, **1996**, Vol. 12, No. 25, 5973-5976.

Nordli, K. G.;Sjöblom, J.; Kizling, J.; Stenius, P. "Water-in-crude oil emulsions from the Norwegian continental shelf 4. Monolayer properties of the interfacially active crude oil fraction" *Colloids and Surfaces*, **1991**, Vol. 57, 83-98.

Peng, J. B.; Barnes, G. T.; Gentle, I. R. "The Structures of Langmuir-Blodgett films of fatty acids and their salts" *Advances in Colloid and Interface Science*, **2001**, Vol 91, 163-219.

Peng, P.; Morales-Izquierdo, A.; Hogg, A., Strausz, O. P. "Molecular Structure of Athabasca Asphaltene: Sulfide, Ether and Ester Linkages" *American Chemical Society*, **1997**, Vol. 11, No. 6, 1171-1187.

Peramanu, S.; Pruden, B. B.; Rahimi, P. "Molecular Weight and Specific Gravity Distributions for Athabasca and Cold Lake Bitumens and Their Saturate, Aromatic, Resin, and Asphaltene Fractions" *Ind. Eng. Chem. Res.*, **1999**, Vol. 38, 3121-3130.

Possmayer, F.; Nag, K.; Rodriguez, K.; Qanbar, R; Schürch, S. "Surface activity in vitro: role of surfactant proteins" *Comparative Biochemistry and Physiology Part A*, **2001**, Vol. 129, 209-220.

Puskás, S.; Balázs, J.; Farkas, A.; Regdon, I.; Berkesi, O.; Dékány, I. "The significance of colloidal hydrocarbons in crude oil production Part 1. New aspects of the stability and rhological properties of water-crude oil emulsions" *Colloids and Surfaces A*, **1996**, Vol. 113, 279-293.

Sharma, R. "Surfactant Adsorption and Surface Solubilization" *ACS Symposium 616*, **1995**, Washington, D.C., ISBN 0-8412-3333-0.

Sigiyama, N.; Shimizu, A.; Nakamura, M.; Nakagawa, Y.; Nagasawa, Y.; Ishida, H. "Molecular-scale structures of Langmuir-Blodgett films of fatty acids observed by atomic for microscopy (II) – cation dependence" *Thin Solid Films*, **1998**, Vol. 331, 170-175.

Singh, B. P. "Performance of Demulsifiers: Prediction Based on Film Pressure-Area Isotherms and Solvent Properties" *Energy Sources*, **1994**, Vol. 16, 377-385.

Stokes, R. J.; Evans, D. F. "Fundamentals of Interfacial Engineering" **1996**, John Wiley & Sons Inc., ISBN: 0471186473.

Strauz, Otto P.; Mojelsky, Thomas W.; Faraji, Farhad; Lown, Elizabeth M.; Peng, Ping'an "Additional Structural Details on Athabasca Asphaltene and Their Ramifications" *Energy and Fuels*, **1999**, Vol. 13, No. 2, 207-227.

Su, Y.; Artok, L.; Murata, A.; Nomura, M. "Structural Analysis of the Asphaltene Fraction of an Arabian Mixture by Ruthenium-Ion-Catalyzed Oxidation Reaction" *Energy & Fuels*, **1998**, Vol. 12, No. 6, 1265-1271.

Thoma, M.; Möhwald, H. "Monolayers of dipalmitoylphosphatidylcholine at the oil-water interface" *Colloids and Surfaces A: Physicochemical and Engineering Aspects*, **1995**, Vol. 95, 193-200.

Thoma, M.; Möhwald, H. "Phospholipid Monolayers at Hydrocarbon/Water Interfaces" *Journal of Colloid and Interface Science*, **1994**, Vol. 162, 340-349.

Toulhoat, H.; Prayer, C.; Rouquet, G. "Characterization by atomic force microscopy of adsorbed asphaltenes" *Colloids and Surfaces A: Physicochemical and Engineering Aspects*, **1994**, Vol. 91, 267-283.

Tsukruk, V. V. "Assembly of Supramolecular Polymers in Ultrathin Films" *Prog. Polymer Science*, **1997**, Vol. 22, 247-311.

Ulman, A. "An introduction to ultra-thin organic films-from Langmuir-Blodgett films to self-assembly" Academic Press, **1991**, Boston.

Vickery, S. A.; Dunn, R. C. "Direct Observation of Structural Evolution in Palmitic Acid Monolayers following Langmuir-Blodgett Deposition" *Langmuir*, **2001**, Vol. 17, No. 26, 8204-8209.

Viseu, M. I.; Gonçalves da Silva, A. M.; Costa, S. M. B. "Reorganisation and Desorption of Catanionic Monolayers. Kinetics of π-t and A-t Relaxation" *Langmuir*, **2001**, Vol.17, No. 5, 1529-1537.

Watanabe, T.; Matsumura, H.; Inokuma, S.; Kuwamura, T.; Furusawa, K. "Effects of Ion Binding and Oily Conditions on the Adsorbed Monolayer of Crown Ether Compound at the Oil/Water Interface" *Langmuir*, **1990**, Vol. 6, No. 5, 987-991.

Yarranton, Y. W.; Alboudwarej, H.; Jakher, R. "Investigation of asphaltene association with vapor pressure osmometry and interfacial tension measurements" *Ind. Eng. Chem. Res.*, **2000**, Vol. 39, No. 8, 2916-2924.

Yarranton, H. W.; Masliyah, J. H. "Molar Mass Distribution and Solubility Modeling of Asphaltenes" *AICHE Journal*, **1996**, Vol. 42, No. 12, 3533-3543.

Yang, X.; Lu, W.; Ese, M.; Sjöblom, J "Film Properties of Asphaltenes and Resins" *Encyclopaedic Handbook of Emulsion Technology*, **2001**, Marcel Dekker Inc., New York.

Yazdanian, M.; Yu, H.; Zografi, G. "Ionic Interactions of Fatty Acid Monolayers at the Air/Water Interface" *Langmuir*, **1990**, Vol. 6, No. 6, 1093-1098.

Yue, B. Y.; Jackson, C. M.; Taylor, J. A. G.; Mingins, J.; Pethica, B. A. "Phospholipid Monolayers at Non-polar Oil/Water Interfaces Part 1.-Phase Transitions in Distearoyl-lecithin Films at the n-Heptane Aqueous Sodium Chloride Interface" *J. Chem. Soc. Faraday I*, **1976**, Vol. 72, 2685-2693.

Zasadzinski, J. A.; Viswanathan, R.; Madsen, L.; Garnaes, J.; Schwartz, D. K. "Langmuir-Blodgett Films" *Science*, **1994**, Vol. 263, 1726-1733.